UCLouvain

epl

École polytechnique de Louvain

Need analysis and technical study of an open-source sequential compression device towards an appropriable hospital

Authors: **Thalie Sarafidis Thiriar, Arthur Van Geersdaele**
Supervisors: **David Bol, Benoît Herman**
Readers: **Renaud Ronsse, Rémi Dekimpe**
Academic year 2022–2023
Master [120] in Biomedical Engineering

Acknowledgements

First and foremost, we would like to thank our supervisors, David Bol and Benoît Herman, for their guidance and support during this academic year. Without their assistance and suggestions this work would not have been the same. Thank you for all the feed-backs, your ideas and critiques always helped us to progress.

This thesis could not have existed without the financing by the donations made during a fundraiser launched by the Louvain Foundation in the first months of the COVID-19 pandemic for the development and distribution of open-source medical devices. We want to thank the Fondation Louvain and its generous donors. Their donations allowed us to work on a exciting project with meaning in our eyes. We hope they will be proud of the work we accomplished.

We extend our appreciation to Rémi Dekimpe that answered present to help us when we felt blocked and could not resolve some problems. We are also very grateful to Simon De Jaeger for his support at the CREDEM platform.

Thank you to Frank Hesbois and Regis Lomba for their advice respectively on the testing and fabrication phases.

Our gratitude also goes to our proofreaders for their time, attention and suggestions.

Thalie Sarafidis Thiriar and Arthur Van Geersdaele

A special word is addressed to Jean-François Van Geersdaele for his support. Thank you for putting electronics in my hands.

Arthur

I want to thank my parents, Gilles and Louise for their support. Their confidence helps me to find mine.

Thalie

Contents

Abstract

The recent COVID-19 pandemic triggered a general effort to produce technologies with a different mindset. It put light on the importance of having access to affordable, modular and open devices. This is why the stakes and the need for open-source appropriable medical devices was studied. The research was financed by donations made during a fundraiser launched by the Louvain Foundation in the first months of the COVID-19 pandemic for the development and distribution of open-source medical devices. It led to create a selection method to identify the devices to prioritize for development in this frame. Then the sequential compression device, a device attached around the legs that creates compression and help blood flow, was chosen and studied. A first open-source version has been published by Schara et al. in November 2022. In this thesis, it was updated and adapted to be even more appropriable. A new geometrical model, the truncated pyramid model, was developed to assess the behavior of the hand-made pneumatic bands. The final open-source prototype is economic (average price of 71.20€), can be fabricated with basic laboratory tools, is carefully documented and modular. The results of the study put on light inaccuracies in the testing protocol and a leak that skewed our pressure estimations. Therefore further analysis should validate the model and prototype.

All material and resources useful to the prototype production and testing has been made available freely, on Forge UCLouvain in the OpenMedTech group:

`https://forge.uclouvain.be/openmedtech/sequential-compression-device.git`

Introduction

During the year of 2020, the world faced a health crisis that affected multiple aspects of society. The SARS-CoV2 pandemic impacted severely the number of people needing urgent treatment and so for several months. The pandemic highlighted the immediate need for critical medical equipment, including ventilators, to support patients with severe respiratory illness [1]. The outbreak quickly overwhelmed healthcare systems and strained the availability of medical resources, resulting in a shortage of critical equipment necessary to treat patients suffering from the novel coronavirus [2].

Therefore, this situation underscored the importance of having a strong and resilient healthcare system [3], from the supply chain to the end-users [4], that can quickly adapt to emerging crises and meet the evolving needs of patients. The COVID-19 pandemic also triggered a global effort to develop new technologies and strategies to combat the virus. Researchers and engineers worldwide worked tirelessly to develop innovative solutions that can help mitigate the spread of the virus [5]. For example, engineers and other volunteers joined forces with members of the healthcare sector, industries and investors to develop low-cost medical ventilators in an initiative called "Breath4Life", which is a non-profit and open-source effort catalysed by UCLouvain [6].

This work is inspired by these events and intends to make a step forward towards open-source and appropriable hospitals. Open-source research on devices allows to speed up the fabrication process in case of urgent need. It also reduces research cost and thus possibly the prices on the market. The initial goal of the thesis was to better the way crisis situations are handled from the medical device aspect. However, during this year, it slightly shifted to any help that open-source can bring for medical devices. A prime example of how open-source research can ameliorate the healthcare system in general, is the potential it has to treat overflow, prepare the future medical trends, make the most used devices more affordable and accessible. The sequential compression device is a perfect fit for that objective.

The thesis you are about to read focuses on this specific device. Sequential Compression Device (SCD) produces repeated compression from the bottom to the top of the leg in order to facilitate blood circulation in the veins and prevent blood clot formation. It is used for patients bedridden for long periods of time, that are at high risk of blood clot formation. Those patients require constant medical assistance and therefore could easily lead to an overflow of the hospital resources if numerous patients are in that situation. If the number of long term bedridden patients increases, at once because of a major incident or over time with aging population, an appropriable open-source version of the sequential compression device would be very useful.

One open-source prototype of this device was released in November 2022, under a

Creative Commons CC-BY licence, by Schara et al. from Rice University, Houston [7]. This paper explains the basic mechanism and the mathematical model, describes the fabrication process, and some results. Nevertheless, a review and update could bring enhancements and make it fit the appropriable open-source states more. In this manuscript you will find a reproduction of the Rice University prototype with a more detailed approach, as well as identification of shortcomings, development of a new geometric model, updates and improvements in the open-source spirit and the testing of the prototype[1]. Prospects for improvement are listed at the end for future open-source coworkers the continue the research. The work was financed by donations made during a fundraiser launched by the Louvain Foundation in the first months of the Covid-19 pandemic for the development and distribution of open-source medical devices.

The objectives of the thesis are the following :

- Summarize the stakes and the meaning of an open-source appropriable medical device.
- Identify the need for an open-source appropriable medical device.
- Develop a selection method for appropriate devices.
- Expand on the sequential compression device, its operation and the existing devices on the market.
- Develop a functioning prototype, including modeling and fabrication, by aiming to improve the open-source proposition of Schara et al.. Enhancements regarding the open-source appropriable aspect should be brought and all the material for future update provided.
- Test the prototype, compare the results to those expected by the original model and discuss them.
- Suggest future prospects for consecutive research.

The manuscript is arranged in 4 main parts. It will guide the reader through the process of analyzing the context for an open-source hardware hospital during the first part. It includes research about the open-source status, our definition of an appropriable medical device and clarifications about situations where open-source devices are useful. This section prepares the choice of the medical device. Consequently, part II details the medical device that was worked on. Its first chapter presents the selection protocol used to choose an appropriate device. This part can serve as methodology for future selection of other relevant devices. Afterwards the sequential compression device is described and the existing devices are presented with their specifications. The third part relates to the development of the Sequential Compression Device (SCD) prototype with a presentation of the prototype released by Rice University. It dives into its model, the hardware and results with all the given material. The dimensioning and fabrication of the updated version of the device are explained subsequently. The open-source appropriable frame was taken into account and choices were made to create a modular and documented prototype. Furthermore it is thought to be affordable and has a mean cost of 71.2€. Finally, part

[1] It is hereby announced that ChatGPT, was employed to assist some of the research conducted for this thesis.

IV is about the study of the produced device. Testing was conducted on qualitative and quantitative aspects and future prospects are suggested. The thesis ends with a conclusion and a global a summary of the work.

Part I

Background of an open-source appropriable medical device

The first part of this thesis sets the scene of an open-source appropriable medical device in three chapters, starting with the stakes of the Open-Source (OS) status followed by an assessment of what defines an appropriable medical device. The last chapter is dedicated to the identification of the needs for Open-Source Appropriable Medical Device (OSAMD). It discusses the reasons for development of this type of devices and gives information about the priority sectors for research.

Chapter 1

The Open-Source status

The first step toward the comprehension of this thesis is to understand what an OS device is. The OS status is defined under multiple aspects, as well for software than for hardware, from the legal, managing, design or even innovative point of view. Its advantages can respond to challenges of medical design.

1.1 The Open-Source definition

The term Open-Source is often used to describe a range of practices and approaches that involve the sharing and collaboration around the development and use of various forms of intellectual property, including software, hardware, and other types of content. The concept of OS is generally characterized by a focus on transparency, collaboration, and continuous improvement. It involves the sharing of information and ideas in order to create and enhance products and services.

It is difficult to identify a single leader in the field of OS that can serve as a reference, since the OS community is decentralized and includes a wide range of organizations and individuals working on a variety of projects. However, there are a number of organizations and initiatives that are widely recognized as key players in the open-source hardware community.

Here are several well-known and valuable organizations:

- The Open-Source Initiative (OSI), a non-profit organization dedicated to promoting the use and development of Open-Source Software (OSS) [8].
- The Free Software Foundation (FSF), a non-profit organization with a worldwide mission to promote computer user freedom. They defend the rights of all software users [9, 10].
- The Open-Source Hardware Association (OSHWA)[1], which is a non-profit organization dedicated to supporting the development and use of Open-Source Hardware (OSH).

[1] Previously called "Open Hardware Summit" [9].

- The Free Hardware Foundation (FH), which is a non-profit organization that promotes the use of Free and Open-Source Software (FOSS) and Free and Open-Source Hardware (FOSH).

In practice, there are many other organizations and individuals that are actively involved in the open-source hardware community.

The OSI has imposed a definition about OSS known as the Open-Source Definition (OSD). Later, the OSHWA guidelines define the OSH Definition as "*hardware whose design is made publicly available so that anyone can study, modify, distribute, make, and sell the design or hardware based on that design*". This definition is directly based on the OSD [11, 9]. The main difference breaking the isomorphism between the OSS and OSH development process is caused by the *physicality* of the hardwares : in addition to the requirements of a OSS project, an OSH project will require more skills, tools, a production phase[2], and logically, an adaptation of the Intellectual Property (IP) rights [12].

1.2 Open-Source licensing

It is essential to mention the impact of licenses[3] when talking about OS. A licence agreement is a contract under which the holder of intellectual property (licensor) grants permission for the use of its intellectual property to another person (licensee), within the limits set by the provisions of the contract. Without such an agreement, the use of the intellectual property would be considered an infringement [13].

Engelfriet, Lerner and Tirole explored the determinants of OS license choice, but only considering softwares and not hardwares. Since the approach is the same, the reader can make a generalization of the proposed arguments. At the beginning of FOSSs, they were usually publicly made available without any license governing their use. However, that would allow any private third party to use the source code as its own work and, for example, to monetize it, to the detriment of the OS principles. In the 1980s, the MIT programmer Richard Stallman developed a new approach to distributing FOSSs : the GNU General Public License (GPL). GPL requires that the source code must be freely available and that modifications to the code must be allowed. It also insures that any derived work remains subject to the same license (said as copyleft license) and prohibits the mixing of open and closed source software in any distributed work. In the case of OSH, the definition specifies that one must allow modification and commercial re-use of its design : licenses with a no-derivatives or non-commercial clause do not respect the definition [16].

Since then, more than 80 OS licenses have been created with respect to the OSD, and the impact of the license's selection on the course of an OS project is non-negligible. It affects :

[2] In case of failed experiments, this effort, needed for OSH may appear unnecessarily tedious [12].

[3] The difference between a license and a patent is crucial : A license protects the way a product is made (e.g. source code), while a patent protects the idea of the product itself (patents are therefore relatively out of scope in this work). If a private third party wants to re-create the source code of an OS project under any OS license and commercialize it as its own IP, it can.

- The appeal of the project to the OS community;
- The quality of the final product;
- Other OS projects that can complement (or compete with) the project;
- Commercial vendors, whoses opportunities depend on the license [12];
- The licensor's reputation.

OS licenses are divided into two main categories: Permissive and copyleft licenses. Permissive licenses do not require users to share any modifications they make to the software (so allowing the commercialization of any derivative of the product). On the other hand, copyleft licenses require users to share any modifications they make to the software and to release their own software under the same license.

The most widely used licenses within OS communities are listed in Table 1.1, and it is indicated whether they are specifically designed for use with software or hardware. Software licenses do not contain specific provisions related to hardware, such as provisions regarding the distribution and sale of hardware products. However, when selecting a license for a product, the nature of the product as either software or hardware is not a true relevant factor as long as the license respects the OSD or the OSH definition's criteria. For example, a GPL license could perfectly suit for a FOSH project.

Table 1.1: Table containing 13 of the most popular and used OS licenses by OS communities in the world. Identifying the publisher of a license helps to highlight the fact that the OS approach is a collaborative effort that emerges from various communities working towards a shared goal or purpose.

Open Source Licenses				
SPDX short identifier	Publisher	Category	Target	Source(s)
Apache-2.0	ASF	Permissive	software	[17]
BSD-3-Clause	UC Berkeley	Permissive	software	[17, 9, 14]
BSD-2-Clause	UC Berkeley	Permissive	software	[17, 9, 14]
GPL	FSF	Copyleft	software	[17, 9, 14, 16]
LGPL	FSF	Copyleft	software	[17, 9, 14]
MIT	MIT	Permissive	software	[17, 9, 14]
MPL-2.0	MPL	Permissive	software	[17]
CDDL-1.0	OSI	Permissive	software	[17]
EPL-2.0	Eclipse Foundation	Permissive	software	[17]
CC BY-SA	Creative Commons	Copyleft	hardware	[16]
CC BY	Creative Commons	Permissive	hardware	[16]
OHLs	CERN	Copyleft	hardware	[16]
HL	TAPR-OHLWG[4]	Permissive	hardware	[16]

1.3 Pros and cons of the Open-Source approach

Lerner and Tirole identified both advantages and disadvantages to using an OS approach for the conception of a software, compared to a classical approach. Most of them can also be applied to the case of OSHs (Table 1.2).

[4] A non-profit organization that promotes the development and use of OSH.

Table 1.2: Summary table of the pros and cons of an Open-Source approach while designing a software or a hardware.

Pros and cons of the OS model	
Advantages	Source(s)
Free to use and distribute	*OSI* and *OSHWA*
High quality-price ratio final products	[18, 19, 20, 12, 21, 22]
Inherent simplicity of the design	[23]
Innovation, competitivity and productivity source	[24, 25, 26, 20, 12, 23, 22]
Time winning	[18, 23]
Toward standardization and interoperability	[18, 27, 28, 29, 21]
Fiability and peer-reviewing	[20, 21, 23]
Learning and educational resources accessibility	[30]
Enjoyment, altruism and reputation-gaining	[30, 26, 31]
Drawbacks	Source(s)
Management difficulties	[32, 12]
Possible confusion about the objectives	[21]
Unmanaged forking, numerous versions	[15, 33, 34, 21]
Complexity and compatibiliy issues[5]	[27, 35, 12, 21]
Lack of user support, information stickiness[6]	[27, 21, 22]

An OS product is generally free to use and distribute (even if it can be sold, depending on the license chosen by the licensor[7]) [20]. Numbers of case-studies show that OS projects can most of the time result in low-cost, time-winning and customizable final products that concurrence the market [30, 18, 19]. The OS approach aims to improve the sharing into and between communities, with a will of standardization [35]. Moreover, the open-source approach to hardware design allows individuals to access the plans and documentation needed to create the product, which can facilitate learning and experimentation with new technologies [30]. It also serves as peer-reviewing and enhances fiability.

Among the benefits of the OS approach, one can also find an endless source of innovation. OS collectives work together to build and share information and ideas, which leads to increased creativity, productivity and critical review. Moreover, it gives the possibility to the contributors of a collective to gain in reputation and to fulfill a sense of altruism or social recognition [30].

While the community-driven development is a strength of the open-source model, it is also the cause of drawbacks regarding management, *forking*[8], responsibility and final

[5] Despite the efforts and the will to standardize the product, it may not be compatible with specific other parts, or a custom assembly may be required.

[6] The term "information stickiness" refers to the difficulty in accessing information about OSS or OSH. This difficulty may be caused by a variety of factors, such as the complexity of the system, the way the information is organized or stored, or the lack of documentation or resources available to help users access the information [20].

[7] It seems to be a slight confusion in the scientific litterature between the acronyms FOSH and OSH (or FOSS and OSS) : "OSH" is often used interchangeably with "FOSH", but it can also be used to refer to any hardware that is developed in an open and collaborative manner, regardless of the license used.

[8] Forking: A unique project can evolve in multiple parallel versions, which can increase the complexity and the confusion about the product and its versions [34], split the community and limit the support that

quality of the product, depending on the community that carries the project and the resources allowed [12]. The bigger the community, the most powerful it is to carry a project. For the licensor(s), the gathering [36] and management of the contributors towards a unique direction can be hard and chaotic, especially in cases where people are not retrieving any certain retribution for the work. From the potential confusion (or different wills) about the objectives of the project, contributors can diverge and start forking. Whether or not a OS project is forked, the support provided to users is typically offered by the community through open public forums or documentation, and may not be as comprehensive as the support provided by commercial products [27] [9]. Besides, since there is no single entity responsible for the development and maintenance of the software, if any issues or problems occur, it is harder to hold someone accountable for issues or bugs. It is also very important to stay aware of the limitations imposed by the OS license chosen for the project.

1.4 Open-Source Medical Devices

Raasch asked: "How can we apply OS methods to the rest of the world?". The answer is given by Shirky et al..

> [*The real question is how much of the rest of the world be made to work like a software project?* [...] *OS is not pixie dust, to be sprinkled at random, but if we concentrate on giving other sorts of work the characteristics of software production, OS methods are apt to be a much better fit.*]
>
> — Shirky, 2005

Their application to medical devices is in expansion and is the spirit of this thesis. To discuss this topic the definition of a medical device needs to be introduced. The European Parliament and the Council define the medical device as :

"Any instrument, apparatus, appliance, software, implant, reagent, material or other article intended by the manufacturer to be used, alone or in combination, for human beings for one or more of the following specific medical purposes:

- *diagnosis, prevention, monitoring, prediction, prognosis, treatment or alleviation of disease,*
- *diagnosis, monitoring, treatment, alleviation of, or compensation for, an injury or disability,*
- *investigation, replacement or modification of the anatomy or of a physiological or pathological process or state,*
- *providing information by means of in vitro examination of specimens derived from the human body, including organ, blood and tissue donations, and which does not achieve its principal intended action by pharmacological, immunological or metabolic means, in or on the human body, but which may be assisted in its function by such means."* [38]

the community is able to give to the users.

[9] In the case of a forked project, the user-support is split unequally between the branches, thus reduced.

1.4.1 Compromises between the OS model and the medical world

Open-Source Medical Devices (OSMDs) can be OSSs, OSHs, or a combination of several of them. They face thus limitations during their development that challenge and may make us reconsider the usual procedures[10] when conceiving a Medical Device (MD).

For a case-study about an Open-Source Hardware Mechanical Ventilator (OSH-MV), Mora et al. has developed a taxonomy to evaluate and rate the ability of an OSH product to meet specific scenario requirements (Figure 1.1). The *builtabilty* criterion denotes the necessary ressources and skills to build one unit (engineering aspect). The second one, *adoptability*, is relative to the amount of effort of the healthcare personnel to replace the usage of a conventional device with the OS one (healthcare personnel aspect). Finally, the third one, *scalability*, is related to the potential of the OSH-MV —here extended to any OSMD— initiatives for large scale fabrication and adoption.

Mora et al. also defined properties representing the OS approach and gathering the advantages and drawbacks discussed above (see section 1.3) in a qualitatively evaluable manner. After an evaluation of the OSMD among the three criteria (figure 1.1) regarding these properties, it can be located on a graph to either be compared to other equivalents devices, or to be categorized according to its quadrant (figure 1.2). Eligible OSMDs are found in the upper-right quadrant, where the *builtability* is high, and the *adoptability* is considered easy.

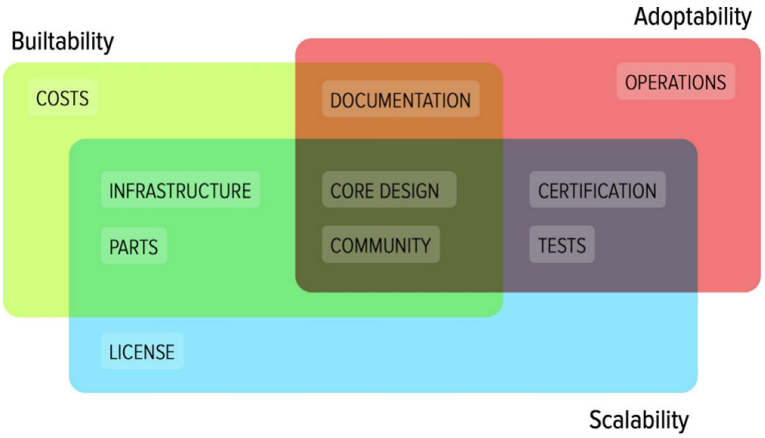

Figure 1.1: Relation between criteria lenses and properties from Mora et al..

Among the properties encompassed by these two criteria, some stand out before even having an idea of what device to develop and should act as development constraints during the OS approach : cost, parts (or simplicity of design), documentation, certification and community.

Any properties visible on figure 1.1 are well-described in the paper and extendable to any OSMD project:

[10] Among other things, to fulfill the requirements in terms of medical design, such as those of the U.S. Food and Drug Administration, the International Organization for Standardization or the European Medical Agency.

- **Core Design**: the core components common to all devices of this type.
- **Operations**: the minimum set of features required by the MD to fulfill duties.
- **Documentation**: types and amount of information provided to describe the system (evaluation of the information stickiness).
- **Infrastructure**: the material resources and skills required for manufacturing.
- **Parts**: number of parts that compose the system (evaluation of the complexity of the system).
- **Cost**: cost/unit estimation.
- **Test**: protocols, procedure and results for validation and benchmark.
- **Certification**: device design is submitted or approved by a competent organization such as International Organization for Standardization (ISO) or U.S. Food and Drug Administration (FDA).
- **License**: the kind of license that rules the OS device development and share.
- **Community**: the extent of contributors, adopters as well as tools to engage with the community to contribute to the project.

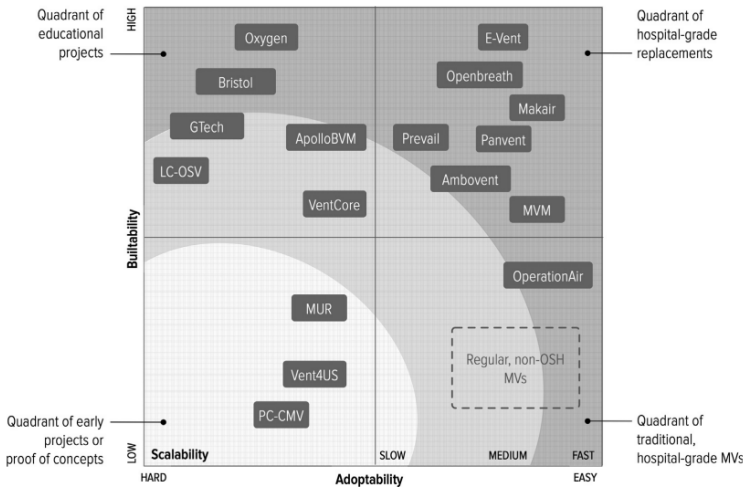

Figure 1.2: The four quadrants with respect to investigation criteria from Mora et al..

The major advantages of the OS we want to see with MDs are respectively the inherent simplicity [23] of the OS designs and the resulting low-cost final products. The workload and costs of research, which are generally amortized in the selling price of the product, are distributed between voluntaries and/or other external fundings, subsidies, etc. Almost only the manufacturing cost remains. Acosta highlighted the fact that in the case of highly available products, the cost of building an OS solution is higher than using a closed-system because. It may also be the case for MD since a license for medical use is required: these certifications can be very expensive (both in time and money). Despite that last point, investment differences of several million dollars have already been observed thanks to

the use of OSMD which is simpler and cheaper than a conventional manufacturer [19, 22]. Moreover, there are already different mathematical formulae to quantify the economical value of an OS project [19], and they can be adapted to OSMD.

Secondly, stickiness of information and the lack of user-support and training is a disease of the OS method and is a very important drawback of OS tech regarding the medical world. According to the World Health Organization (WHO), between 70% and 90% of all MD donated to the developing world never function as intended [22]. End-users need two kind of information, respectively relative to *builtability* and *adoptability* (figure 1.3) to first conceive the OSMD and second to use it. According to Mora et al., usage manuals should not always be necessary if the device follows standard guidelines for MD of the same type, but it may arise a confusion due to the uncertainty about the usage : *what about people not aware of usual standards?* In addition, Bonvoisin and Mies clarifies the requirements of OSH's documentation and measures the openness[11] of an OS project, as well for contributors as for end-users[12]. The paper highlights that the product documentation should be addressed (in term of complexity and prerequisites) to people who have access to sufficient means of production to make the OSH and has at least to contain: the license, the bill of materials (references, cost, procurement information, photos), and fabrication instructions (source files, materials, machine parameters, step-by-step assembly instructions).

The 3 types of information needed in an OSMD project

	Participability	*Builtability*	*Adaptability*
Bonvoisin and Mies, 2018	Process Openness	Product Openness	Product Openness
Mora et al., 2020	/	Builtability	Adaptability
Beneficiaries	Contributors	End-users	End-users

Essential to the healthcare world

Figure 1.3: The 3 types of information and their denomination noted in Mora et al. and Bonvoisin and Mies. *Participability* refers to the documentation for contributors such as original files, contribution guide, file formats or license.

Finally, Medical Design has its own procedures that have to be integrated into the OS model for OSMDs, and medical certification[13] is a big challenge but manageable for an OS project [22]. The main obstacle is the procedure needed to certify the usage of a MD, an iterative process that usually demands very specific skills, takes years and costs a lot of money: That obstacle should not be skipped. Depending on the geographical area and on the situation where an MD is used, it could be used without medical certification but it should always be under the authority of a competent organism. Moreover, in case of emergency, civil disobedience has already been seen, if no other similar MD is available. The risks for the patient of the MD usage has to be evaluated and compared to the benefits.

[11] *Open-o-Meter*, Bonvoisin and Mies.

[12] There is a nuance to bring regarding the needs and usage of information: A end-user needs to know how to build the OSMD and how to use it, where information destined to contribution to the project is also crucial for the project but not essential for use (Figure 1.3). Bonvoisin make the distinction between the two kinds of information using the terms "Product Openness" and "Process Openness".

[13] Medical device certification is made by entities like ISO, EMA, FDA or SAHPRA, depending the geographical zone og usage of the device.

Regarding the challenges discussed above, it is clear that the community of contributors for OSMD should be composed of engineers and members of the healthcare world. Medicine is a very complex art, and the requirements of MD in terms of risk management, ethics[14] and standards are high. Contributors have to integrate the *MD design thinking* in their work methodology.

1.4.2 Impacts of the COVID-19 pandemic on the OSMD approach

The COVID-19 rise resulted in a stress of the hospital sector and consequently in many researches and inventories of available MDs (OSMDs included), motivated by the volume of patients that critical infrastructures cannot handle, increasing the mortality rate [40, 41]. More than observations, these studies also assess the readiness of the needed technologies. Most of them show their will to empowering people to take action, favoring collaboration in- and outside the communities [4].

The lack of ressources susmentioned could not be fought using pre-fabricated stockpiles. First because it is a difficult bet to anticipate the future challenges in medical urgency and medical crisis. Secondly because of the high costs associated with maintaining the stockpiles. To correctly access to all the benefits of the OSMDs, the nature of manufacturing from the usual large-scale, slow and centralized will change to be small-scale, fast and decentralized. The consumer will be geographically close to the device production site, and the answer to the medical needs will be locally autonomous [40].

That new distributed manufacturing paradigm can only be reliable if the OSMDs designs and specifications are shared before the crisis, ensuring them to be available in any way (the Internet could go down during the crisis, preventing global communication, which is a key element to the community aspect of OS thinking). Moreover, sharing before the apparition of any disaster enables the medical staff around the world to train itself, making the OSMD easier to deploy [40].

During the COVID-19 crisis, in order to increase their production rate, Medical and Vaccine companies and governments made partnerships with industries like car manufacturers instead of working with OSH communities (for example: GE Healthcare and Ford, Ventec and GM, Medtronic and Tesla). It is a worthy solution, but it was not sufficient. Moreover, the gain of such a method is temporary: These companies are not working toward OS, consequently not releasing their files. There is no contribution to the OSMD field for the future years [4, 42].

Despite the fiablity of the OS approach to answer to a medical crisis, it has shown that OS distributed manufacturing ensures the widest possible dispersion, as well in term of devices as of fabrication knowledge. FOSH is maximizing the number of possible legal fabricators by definition [40]. These fabricators were mostly independents, using 3D printers based on Fused Deposition Modeling (FDM) technology. Altought these printers are not fast [41], the manufacturing speed emerges from the fabrication parallelism. Despite all, the

[14] For example, data privacy will be a big challenge because is can be difficulte to integrate to the OS approach [39].

reader has to note that developping nations are particularly vulnerable to medical crisis [40], either using the traditional manufacturing paradigm or the decentralized one. The situation is only minimized thanks to the low costs of OSMDs.

1.4.3 Famous OS initiatives and databases suitable for medical usage

During our researches, multiple reference to OSMD communities or initiatives where found and are presented at table 1.3. Unfortunately, most of them where referenced using web links that are broken today. We do not have any hypothesis to explain the situation.

Table 1.3: Summary table of famous OS initiatives and databases suitable for medical usage.

Famous OS initiatives and databases suitable for medical usage	
Name	Description
Journal of Open Hardware	*Scientific journal*
Open Know How/Where	*Sharing the OS approach*
The ARDUINO Project	*Movement, documentations and repositories*
Wikipedia	/
Thingiverse	*DIY Hardware repository*
Youmagine	*DIY Hardware repository*
Hackster.io	*FOSH repository*
Open Source Pharma	*OS pharmaceuticals*

It seems that more complex OSMDs are not shared using popular OS-sharing media yet. They are isolated, difficult to find in the vast expense of the Internet. These projects seem drowned by thousands of smaller other projects, whose web indexing also use the same keys. To get to know them, an intensive research is needed or through word of mouth. This way, members of the healthcare world are not sure to have a bird's-eye view of all the OSMDs they are looking for. It is essential for the OSMDs development that one build an indexing protocol and a platform to create an OS reliable directory usable and editable by the healthcare world.

In addition to OSMD databases and big initiatives, in the physical world, there are also community-operated laboratories where makers can meet, share resources, socialize and collaborate about projects. These spaces are commonly called: *fablabs*, *hackerspaces*, *hackspaces*, *hacklabs* or *makerspaces* and are present all over the world.

To summarize

This chapter has for goal to understand the open-source status and bring perspective on its use for medical devices. The open-source status is often used to describe a range of practices and approaches that involve the sharing and collaboration around the development and use of various forms of intellectual property, including software, hardware, and other types of content. It is characterized by a focus on transparency, collaboration, and continuous improvement. Advantages are related to that dynamic like the gain in time, the low price, enhanced fiability through multiple reviews, good accessibility, innovation, and simplicity. On the other side, drawbacks also appear: management difficulties,

confusion on the objectives, compatibility issues between resources, lack of user support and thickness of information. The ability of a medical device to meet specific scenario requirements can be evaluated through three criteria that are builtability, scalability, and adoptability. Difficulties of open-source applications on medical devices include the thickness of information and the certification.

Chapter 2

The meaning of an appropriable medical device

In 2007, the WHO worked in hands with the Dutch Ministry of Health, Welfare and Sport on an project called *"Priority Medical Devices"*[43]. They defined the *4-A's* (*Availability, Accessibility, Appropriateness and Affordability*) that a priority medical device should respect.

In the same spirit, with regard to chapter 1, an appropriable MD should respect several aspects that stem from its context of use. From the moment a specific MD is needed to the point where it has served its purpose, the members of the healthcare world have to face delays, the costs of the device, then its understanding and finally its usage protocol. In this thesis, an appropriable MD is a MD designed in order to facilitate the overcoming of these obstacles. Overviews and answers to these challenges are discussed in following sections. The reader will notice that the appropriable medical device is defined in a spirit very close to the OSH thinking described in section 1.4.1, where the compromises between the medical world and OS are discussed.

2.1 Acquisition speed

The delays of acquisition of a medical device generally depend on the manufacturer's constraint. Before selling the device, they encounter different challenges when starting the production. From a legal point of view, they take responsibility for the device to be conform to the applicable medical devices regulations and requirements. If the device design has not be designed and documented to be certifiable from the beginning of its conception, the certification process will last longer. A period during which the device will not be available for sale.

Another source of time loss is the technologies used. Depending on the available workforce or the device size and complexity, the device manufacturing delays will be impacted.

Last but not least, the availability of resources needed to manufacture the device plays a crucial role in the production process. It can be assessed from two perspectives: the existence of adequate stockpiles and also their geographical proximity, since delays in resource delivery are a determining factor of the manufacturing speed.

The consideration of these timings and a concern to minimize them are necessary aspect of an appropriable medical device.

2.2 Development, acquisition, usage and maintenance costs

Given long researches-and-development cycles, the financial aspect in the development is of great importance in the MD sector [44]. Moreover, the development of the technologies used in the healthcare world in the recent years and the need to pace with these technologies influences the cost of investment [45]. Added to the development and acquisition costs, the cost of the formation and of the maintenance is not to be left apart. The maintenance of a MD can be taken care of by the health infrastructure that owns it or by subcontractors or the manufacturer with payment[1]. Depending on the risk categorisation of the MD, its technology level and its frequency of usage, the maintenance and monitoring[2] routine must be put in place, requiring human intervention and materials.

Not only financial and labor costs should be considered, but also the resources required for integrating the device into the considered medical environment, when estimating the overall cost. Since the costs and means of medical entities depend on the region (figures 2.1 and 2.2) [47, 48, 49] it is essential to carefully evaluate the specific needs, priorities, resources, and capabilities when developing health services, as highlighted by Bektemur et al..

The goal with an appropriable device is to minimize all the listed costs. It should be accessible to a certain extent for the price point and required resources.

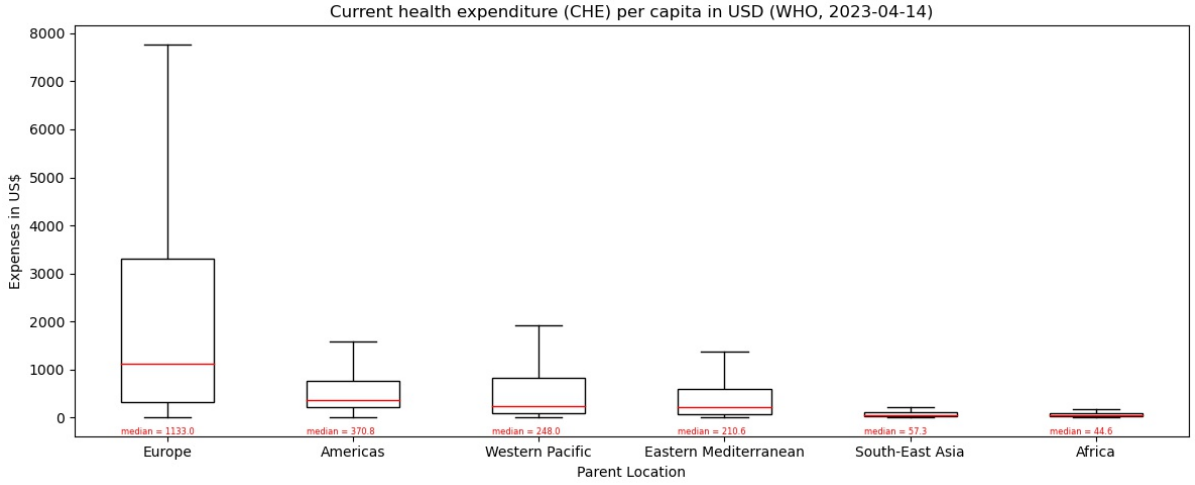

Figure 2.1: Boxplots of the current mean health expenditure per person (CHE) per capita in US-dollard, clustered according their parent location. Medians are colored in red for better visualisation. Data provided by the World Health Organisation (WHO) on the 03/04/2023.

[1] Included or not in the MD buying price.
[2] For surveillance and vigilance [46].

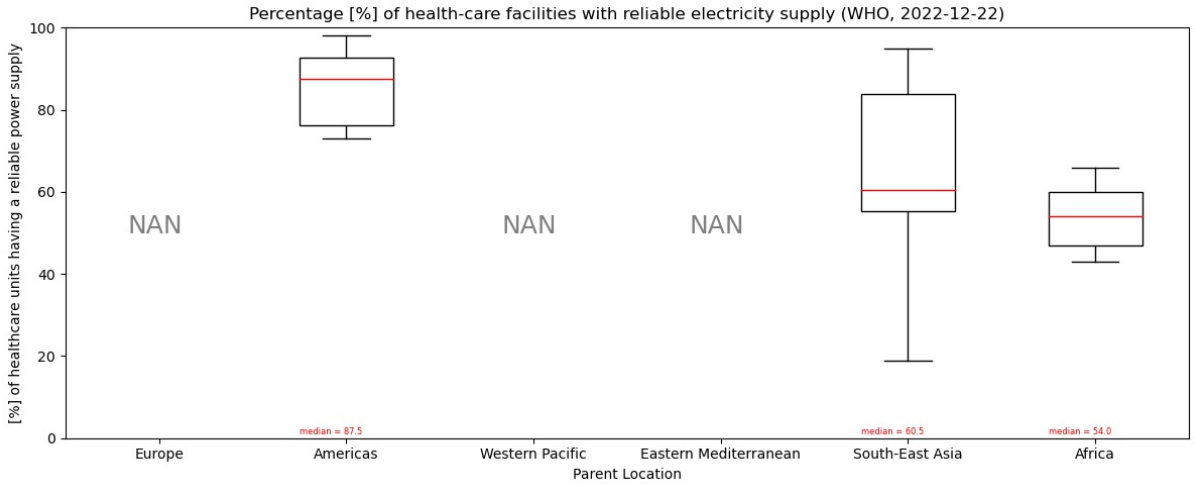

Figure 2.2: Boxplots of the percentage of the health-care facilities with reliable electricity supply, clustered according their parent location. *NAN* is indicated where no information was given and medians are colored in red for better visualisation. Data provided by the World Health Organisation (WHO) on the 22/12/2022.

2.3 Documentation

The documentation accompanying a MD, whether it is an OSMD or a simple MD, plays a critical role in ensuring a comprehensive understanding of the device. This documentation must contain pertinent information concerning the device's applicable contexts, as well as detailed descriptions of the therapies and functions it performs. According to the perspective put forth by Bonvoisin and Mies, the documentation should be tailored to the prerequisite knowledge and aptitude levels of individuals capable of performing associated medical procedures and actions.

To ensure its accessibility and usefulness, the documentation must be available in convenient formats, regularly updated if needed, and written in clear and concise language understandable by the target audience. Moreover, it must provide unambiguous instructions for device operation, maintenance, and troubleshooting to minimize the risk of errors or adverse events.

The appropriable medical device should be correctly documented in order to make usage as easy as possible. The content should be clear and accessible.

2.4 Usage protocol and user interface

This section is directly related to section 2.3 and pertains to the documentation associated with the standard utilization of the MD, more practical than theoretical, an aspect briefly touched upon earlier but not discussed. This is in line with the idea of "*Adoptability*" defined in the OSMD framework (chapter 1, section 1.4.1).

Regardless of the media used, formation and documentation on the usage of the MD must be available for members of the healthcare world destined to use it. Even if the

formation and the documentation is deemed flawless, the ease and speed of learning of the MD are also directly impacted by the complexity of its usage protocol and User Interface (UI). A consciously designed UI, along with adherence to established standards, is an effective tools to enhance the adoptability and the integration of the device in the medical infrastructure.

Therefore, an appropriable medical device is designed to correspond to its users, here particularly the actors of the clinical world.

Chapter 3

Need for open-source appropriable medical devices

As stated in the introduction, the COVID-19 pandemic inspired this thesis, the unusual high flow of patients needing urgent and intensive care created a lack of medical devices to treat them all. This triggered initiatives to provide the necessary medical technologies as fast and reliably as possible: It was a *medical emergency*[1] situation.

The initial idea of this thesis was to focus on OSAMD for specifically medical emergencies. However, it quickly appeared that OSMD could also be of great help for other circumstances. Actually, OS devices are useful for all situations where medical devices are needed at low-costs, in large number, in emergency or in precarious environments.

Theses situations are non well-defined. This chapter clarifies them and identifies their needs in order to build a selection method for devices that deserve OS prototyping. Here are presented different problematics where open-source medical devices could bring help.

3.1 Major causes of death

As first step, the situations that impact a lot of people were clearly identified. One way of creating added value with OSMD is to pin point main causes of death and try to answer to them.

The website Our World in Data shares data about the number of deaths by cause visible on figure 3.1. Three categories of causes of death can be identified:

- **Physical diseases** such as cardiovascular, respiratory and digestive diseases, cancer, diabetes, and so on.
- **Mental conditions** or psychiatry related ground. For example dementia, alcohol and drug use.
- **Injuries** linked to road injuries, falls, homicide attempts, terrorism and and natural disasters.

[1] Medical emergency definition: An illness, injury, symptom or condition so serious that a reasonable person would seek care right away to avoid severe harm [50].

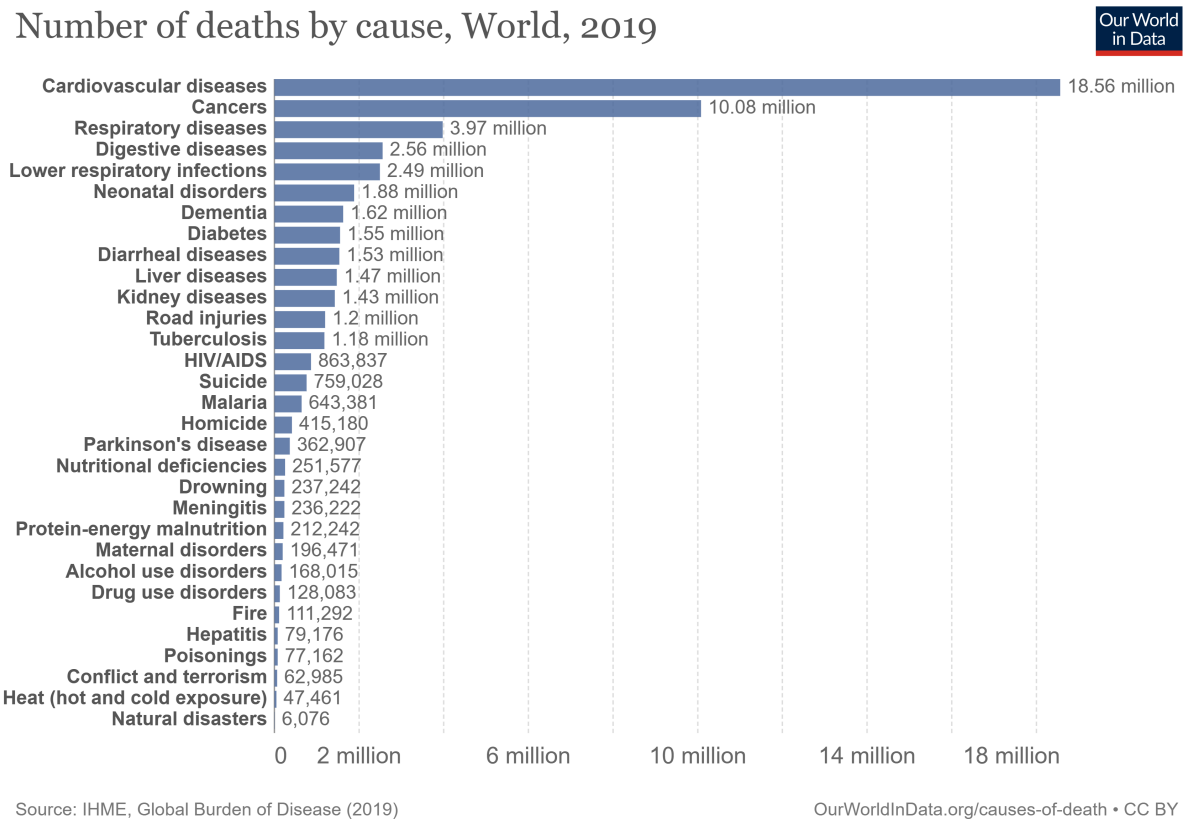

Figure 3.1: Number of deaths by cause in the world in 2019 [51].

3.1.1 Physical diseases

For all physical diseases, diagnostics and treatments could benefit from open-source medical devices. The next paragraphs describe the appropriate tools for these areas. They concern all physical diseases but particular attention can be brought to cardiovascular diseases. They lead the causes of death by far with 18.56 millions of deaths when the second cause provoked 10.08 millions of deaths.

Diagnostic

Tools for diagnostic include monitoring devices and medical imaging devices. There are single parameter monitoring systems and multi-parameter monitoring systems [52]. The most used monitoring devices are the stethoscope (used to listen to heart but also lungs and intestine noises), blood pressure monitors [53], the pulse oxymeter, the thermometer and the electrocardiogram machine, among others [? 54]. For the medical imaging the main techniques are X-rays, magnetic resonance imaging, computed tomography, fluoroscopy, ultrasound, echocardiography and nuclear medicine. Most of these tecnhiques can serve for multiple regions of the body[55]. The diagnostic devices are candidates to the device selection protocol developed in chapter 4 because of their high utility.

Treatment

For treatments the main options are medication, surgery and medical procedures. Drugs are not considered a medical device. Therefore, they are not part of the subject of this

thesis but the medical devices used for surgery are considered for the OSAMD selection process.

3.1.2 Mental conditions

Mental conditions are usually handled with psychotherapy, medication, support groups, hospital or residential treatment program for continuous support [56, 57]. Those solutions relate to medical staff, organizations and pharmacology. Therefore, they are not part of this study.

3.1.3 Injuries

The remaining items on the chart of leading death causes are injuries that appear during road injuries, falls, homicides, terrorism and natural disasters. The proportions of injuries from these causes are displayed on figure 3.2. Most of them are traumatic injuries[58, 59].

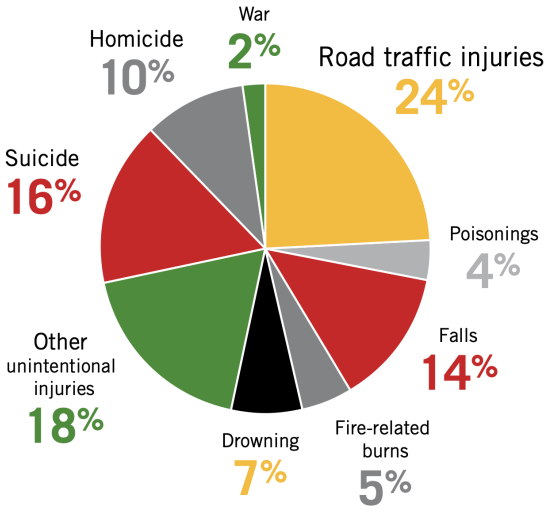

Figure 3.2: Pie chart of the causes of injury deaths in 2012 around the world [60].

Traumatic injuries are defined by University of Florida Health as *"physical injuries of sudden onset and severity which require immediate medical attention"* [61]. They include blunt traumatic injuries such as fractures, lacerations, amputation, and crush related injuries. Another common type of injury is soft tissue injuries. These are injuries that impact skin as burns or skin irritations but also tendons, muscles or any soft tissue. The most frequently harmed areas are chest and abdomen, extremities and spine [62, 63, 59].

Traumatic injuries needs immediate attention or surgical intervention and many victims are taken to the hospital emergency units. In order to address this factor with an open-source medical device, focus can be brought on surgical and emergency departments and their use of medical devices[64, 65, 66].

3.2 Overflow of medical resources

When medical services experience higher flow of incoming patients than usual, they have to face many challenges and can easily be overwhelmed by the number of persons to treat, the severeness of casualties and the shortfall of adapted equipment or personnel. Open-source appropriable medical devices can be a solution because they offer reduced costs and relative local production. Open-source appropriable technologies are thought to be easily made and are less expensive because the design is delivered freely.

A Mass casualty incident (MCI) is defined as *"an incident in which emergency medical services resources, such as personnel and equipment, are overwhelmed by the number and severity of casualties"* [67]. The main type of events that cause MCIs are *Mass disasters*[2]. They are of different nature : natural incidents, accidents or man made. Natural incidents include tsunamis, fires, earthquakes or even pandemics. Example of accidents are collisions, crashes and derailments. Finally, examples of man-made mass disasters can be acts of terrorism of bombings [68]. All those events can cause the medical healthcare world to be overwhelmed and lacking resources. This are typically cases where OS devices are very useful.

The question is how to select the best devices to face these situations. As an anwser, two axis have been identified. The first one is to focus on the devices that are used to treat the kind injuries that happen in mass disasters. A lot of patients will arrive at the hospital at the same time, mostly with traumatic injuries. This meets subsection 3.1.3 and the solution is the same : focus on devices of the emergency and surgery units of hospitals. The second part of answer is to focus on the duration of stay at hospital. Situation where patients have to be treated for longer periods are difficult to handle because that increases the shortfall. The longer a person has to stay the more it consumes and needs medical resources and thus creates a bigger shortfall. All medical devices needed for intensive care and for bedridden patients would be suited for open-source development. Equipment that is used for long periods of time or continuously also falls in this category. The essential intensive care unit equipment under general care are [69, 70, 71]:

- ICU Bed
- Patient monitor
- Vital signs monitor
- Sequential compression device
- Syringe driver or syringe pump
- Respiratory ventilator
- Infusion Pump
- Anesthesia Machine
- Medical Stretcher

[2] Mass disaster definition: An unexpected, sometimes catastrophic event, causing serious injury and several deaths[68].

- Ultrasound Machine
- EKG Machine
- Enteral Feeding Pump

All listed equipment are eligible for the selection protocol of OSAMD defined in chapter 4.

3.3 Future trends in healthcare

The healthcare industry will face many changes over the next decades. The evolution of technology, of demographics and of culture impact the medical world. There will be major changes related to development of artificial intelligence (in medical imaging, diagnostic, individualisation of treatment, etc.)

The next trend is related to the changing demographics. The ageing of population is a stake that will take more importance in the future[72]. On figure 3.3 the variation of median age of the world population over time is shown. There is a rise observed since the seventies until today and predictions dictate a continuous growth over the next twenty years. Ageing goes with growing risks of health problems [73]. As you get older, all systems decline : the muscles, joints, bones, the digestive system, sensorial systems among others. Especially the cardiovascular system experiences changes. The blood vessels become stiffer and provokes pumping for blood more difficult. Blood pressure tends to rise and so does the risk for pathologies [74].

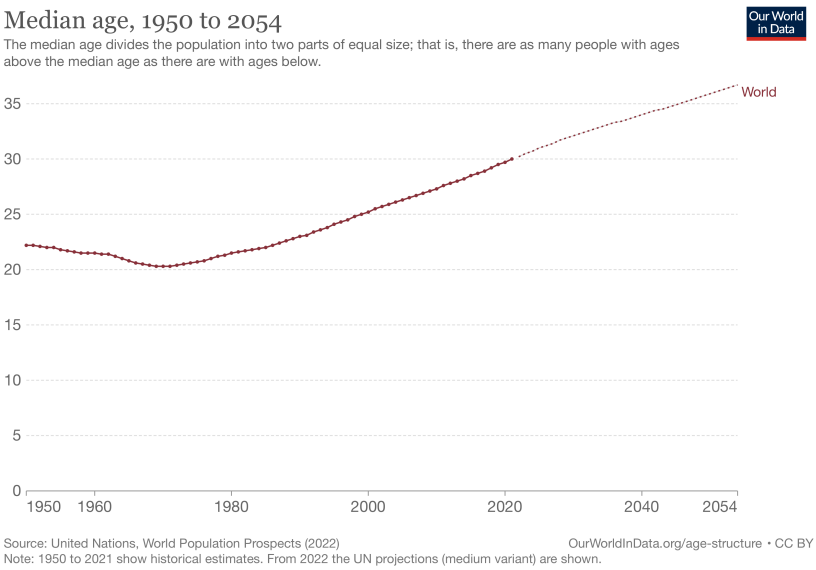

Figure 3.3: Median age evolution and prediction between 1950 and 2054[72]. The full line corresponds to the data and the dotted line is the prediction.

Figure 3.4 shows age specific incidence of confirmed major cardiovascular disease by type of first event. The trend shows a clear rise over lifetime with a steeper increase starting in the sixty to sixty-nine age group. This type of diseases mostly occur in population over sixty [75, 76]. Consequently, this cause of death should see an increase in the next decades as a result of the aging population [77]. Therefore, medical devices adapted to cardiovascular

diseases specifically are important to be developed in an open-source version.

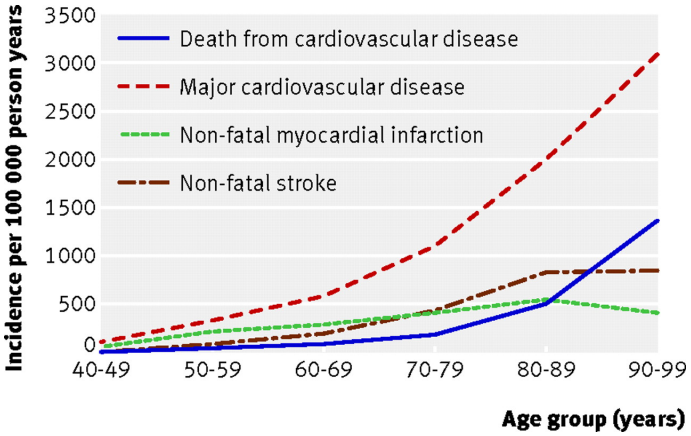

Figure 3.4: Age specific crude incidence of confirmed major cardiovascular disease by type of first event (non-fatal myocardial infarction, non-fatal stroke, and death from cardiovascular disease) [75].

The second trend that could lead to a different prioritization of medical devices is the shift towards less hospitalization and more at-home medicine. The point-of-care [3] is progressively moving towards home. Remote care and monitoring are increasing and will continue over the next decades [78]. Remote and wearable medical devices will also be more and more favoured [79]. Thus open-source development is of interest.

To summarize

This chapter aims to identify specific needs for open-source appropriable medical device development. The first problematic that could benefit from these kind of devices it the major causes of death. The impact of more affordable and appropriable devices would benefit the medical system by the number of persons it would help. Devices that were identified useful for that category are devices related to cardiovascular conditions, tools for diagnostic, the essential devices for surgery and of the emergency department. The overflow of medical resources would also benefit from affordable devices that can rapidly and locally be produced. Sectors that are usually overflowed are the emergency and the surgery departments as well as the intensive care unit. The important devices of those departments are thus important to develop. Finally, open-source can also help to prepare to adapt to the future trends and make the necessary tools more affordable. In the medical world, that relates to the aging population, therefore cardiovascular diseased, and remote care. Those fields would also benefit from open-source appropriable propositions.

[3] The location where care is delivered.

Part II

Sequential Compression Devices

In part I of this thesis, the background of *open-source appropriable medical device* is investigated. The different terms of the concept of these devices were defined and the needs for such devices were justified. This part is dedicated to the selection of a medical device that corresponds to the frame of this thesis and to its presentation. Firstly, the methodology of selection is presented with specific information about the medical device database that was used and the selection protocol applied to it. All criteria are detailed and justified to allow future researchers to adapt the protocol. Following this selection process the sequential compression device was chosen. The next chapters present this device starting with an explanation of its basic operating principles and the need for such device in the context of an open-source appropriable hospital. Finally, the existing sequential compression devices with their regulations and classification are presented.

Chapter 4

Medical device selection protocol

The creation of a medical device selection protocol had to start with a database that is a large census of medical devices. The idea is to then apply on this list several filters and criteria. Since this thesis subject was initiated by Mr. Louis Breels during the academic year 2021-2021, his work served as starting point. As included, the use of the MeDevIS (priority Medical Devices Information System) database.

4.1 Medical device database

MeDevIS is defined as an open-access World Health Organization (WHO) electronic database of medical devices [80]. This database is a free resource accessible to all public. It is supplied by the WHO and lists MDs and their specifications: the type of MD, the service where it is used, the type of patients it is addressed to and its European and FDA risk classification, among others.

This website finds its origin in a state members' resolution[1] that was taken during the 2007 WHO assembly [81]. The resolution called for the creation of a web-based database of health technologies that incorporated up-to-date evidence and functions as a central resource. The goal was to improve access to medical devices worldwide. Moreover, it would allow governments and public health bodies to have a general overview of MDs and assess all related topics (procurement, reimbursement, planning, etc.). It could also help to face emergencies by being well prepared and thus respond in a more efficient way.[82]

As a reaction, WHO started the Priority Medical Devices (PMDs) project. Methodology of selection of PMDs was published in 2010 in a document named "*Medical devices: managing the mismatch: an outcome of the priority medical devices project*" [43]. They based their process on availability, accessibility, appropriateness, and affordability, as mentioned in chapter 2. Firstly, diseases with significant risk factor estimations were identified and given priority. Subsequently, evidence-based clinical guidelines were used to determine the crucial interventions for prevention, diagnosis and treatment of these diseases. Finally, a team of specialists from various disciplines collaborated to develop lists of MDs that could help managing high-burden diseases in various situations.

[1] Resolution WHA60.29: Global strategy and plan of action on public health, innovation and intellectual property.

The following lists of WHO PMDs were published [80]:

- Interagency list of priority medical devices for essential interventions for reproductive, maternal, newborn and child health [83];
- WHO list of PMDs for cancer management [84];
- WHO list of PMDs for management of cardiac diseases, stroke and diabetes [85].

MeDevIS was initially intended to cover these three publications. However, the SARS-COV-2 pandemic provoked the addition of the *"Priority Medical Devices list for the COVID-19 response and associated technical specifications"* in 2021[86]. More information has been included: The *"WHO Package of eye care"* interventions released in 2022 [87] and the MDs of the *"Trauma and Emergency Surgery Kit (TESK) 2019"*[88]. This last addition has for objective to list the tools to treat 50 patients that need surgical intervention at the same time.

MeDevIS is therefore a good starting point for the selection of the device that will be prototyped in an open-source appropriable mindset. MeDevIs was created with for goal the worldwide access to detailed medical device lists and with a priority mindset. This is rather close to the open-source ambitions. It lists a selection of devices that are the most important in today's climate. The next step is to apply to the set of data filters that are appropriate to our work frame.

4.2 Selection method

Our goal is to select a medical device and create or improve an open-source appropriable version as a subject of our biomedical engineering master thesis. Therefore, the device has to compile with a number of requirements. Some requirements are stated by the students according to their specific abilities, personal preferences and the frame of the thesis.

1. It has to be a medical device;
2. The device should respond to the needs for OSAMDs. Therefore, it has to fit the stakes that where presented in chapter 3. This includes major causes of death, overflow problem and future health trends;
3. The device should require some scientific and technical knowledge;
4. The device should be manufacturable or completely modelled by the students in the time of the academic year.

Requirement 1 is respected inherently by the database. For the other ones, the MeDevIS website makes possible to select several filters to obtain the list of devices corresponding to your criteria. At the time of the selection, the database included 1723 devices. Today, it has been modified and counts 2099 devices.

The first filter selected is the *Sector of use*. General surgery, emergency care, intensive care and medical imaging and "across all" categories where chosen. They all fit requirement 2. The emergency and intensive care categories allow to select devices that are important

because of their necessity in urgent situations where patients are facing immediate danger and need medical support. They also correspond to the overflow problem because they are usually the first units affected: emergency unit faces the most influx of patients. On the other side, intensive care units are made to help only a few patients that need continuous and high maintenance care, making it easy for such units to overflow. Finally, for the future trends with the ageing population, intensive care are likely to need further development. Regarding general surgery, medical imaging and *"across all"* categories are also appropriate for the needs of chapter 3. They target general problems and various types of patients. The associated medical devices are appropriable to many situations and crucial to prevent to various death causes. They will fit to the future trends because of the broad medical range they cover.

The next filter is on the *General vs. specific use (health condition)* category. The *Various* criteria, in opposition with *Disease specific* is chosen. Avoiding very specific use cases increases the interest and fit for an open-source version of the device and the relevance for requirement 2. For the same reasons, "single use" devices were excluded and "capital" and "reusable" devices were selected. Today those three option are not included in one category anymore. In the present time, there are three separated categories: capital, reusable and consumable, each with two options `Yes` or `No`. Yes should be selected in the first two categories and no should be chosen for the consumable aspect.

Next, suppression of devices requiring only a basic level of knowledge was added to fit requirement 3.

At the time of the selection, MeDevIs offered a selection category with the regulatory risk classification. The class III and IV devices, and related equipment, were excluded. Their high level of complexity exceeds the fit for requirement 4. Currently, this category does not appear as a filter on the website.

Once all these filters are selected, the next step is to export the remaining list as an Excel file. On that document, devices considered too basic[2] for an engineering master thesis were manually removed, in order to satisfy requirement 3. Further selection was made with more specific criteria. The size of the device was taken into account and devices exceeding around 1[m^3] were rejected. The complexity of the technology and possibility of prototyping were also considered. Devices that could not be fabricated in the time of the academic year because of their difficulty were kept out of the selection to satisfy requirement 4. Finally, seven devices were selected based on personal interests and competences of the writers. Both wanted to prioritize the hardware work, one having a background in robotics and the other in electronics.

Each of the seven devices was investigated in more details with several questions in mind:

- Does an OS version already exist?
- Is it possible to find enough documentation about the device?

[2] For example, scissors, cables, tables and trays were suppressed.

- What is its price on the market? Would it be possible to create a more affordable version?
- How well does the use fit the open-source appropriable frame?

Finally the sequential compression device was chosen. This device corresponds to the requirements set and all reasons will be discussed more in details in the next chapter but a brief recapitulation can already be made. The device can be developed by two engineering student and is interesting for a master thesis because of the broad skills fabrication involves: Research, modeling, electronic handling and use of laboratory fabrication methods. The size of the device corresponds to the limit set and documentation on the functioning is largely available. Moreover an Open-Source version was released recently and could be improved towards the appropriable frame. The price will also be discussed later but it can be significantly lowered. In addition, this device fits the needs for open-source appropriable conception.

Now that we went through the selection process that led to choose the SCD, the next chapter will present this medical device. It will explain the functioning principle, the settings for administration and why it finds its place in the appropriable hospital theme.

Chapter 5

Understanding Sequential Compression Devices

The previous section explained how the Sequential Compression Device was selected, it is now time to understand what this technology is about and how it works. Figure 5.1 shows an exemple of that type of device on a patient's legs.

Figure 5.1: Commercial image of the Koleno Flowtron Excel DVT Pumps, which is an example of SCD [89].

5.1 Anatomy and principles

A SCD is a MD wrapped around either one or both of a patient's legs. It helps blood flow return towards the heart by applying repeated compressions on the limb. It thus enhances the blood circulation in the veins. This process is called Sequential Compression Therapy (SCT). It reduces the risk of blood clots and associated problems [90].

5.1.1 The basis of the venous return

Venous return from the lower-limbs to the heart is an intricate process essential for the maintenance of an adequate circulatory function. After the blood passes through the capillaries, moving from arterioles to veins, the pressure wave generated by the contraction

of the left ventricle of the heart is dissipated [91]. To counteract the effects of gravity and get back to the heart, potential energy must be introduced into the system to define what is called *venous return*.

In the lower limbs, where a SCD is designed to act, this process involves an interplay between the musculovenous pump, the venous valves, and the respiratory and cardiac pumps [91]. If the action of the latter two are evident, the musculovenous pump and the valves deserve particular attention.

The musculovenous pump is composed of the popliteal vein, anterior and posterior tibial veins, and peroneal vein, along with the muscular tributaries that connect to these veins. As visible on figure 5.2, the arrangement of the leg muscles surrounding these vessels restricts passive dilation of the veins during periods of rest, while during periods of normal muscular activity, the pressure on the veins increases and decreases rhythmically. This action effectively constrains the blood to flow in the proximal direction, which is the only route permitted by the valves of the venous system [92]. However, when this process is harmed by pathologies or immobility, for instance when a patient is bedridden, blood circulation is highly impacted. This is where SCD intervenes.

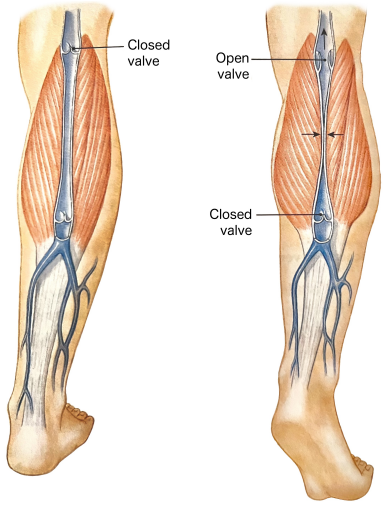

Figure 5.2: Schematic of the musculovenous pump from Silverthorn and Brun.

5.1.2 Pathologies

The main pathology that a SCD is used to prevent is *Deep Vein Thrombosis (DVT)*. This situation occurs when a blood clot is formed in one of the deep veins of the body. These clots mostly form in the lower body. It can lead to pulmonary embolism which corresponds to the blood clot travelling to the lungs and causing serious blockage. Factors that increase the risk of developing DVT include: slow blood flow[1], injury to a vein, increased oestrogen, chronic illnesses, age, etc. DVT can show no symptoms at all or cause swelling, pain and change in skin colour [93].

SCDs are also used to treat *Lymphedema*[94], where a disruption of the lymphatic system causes fluid accumulation and produces swelling and discomfort. Severe cases will affect

[1] Due to confinement to bed, limited movements, etc.

movement and can cause infections and sepsis. This pathology can be caused by surgery, when lymph nodes are suppressed, or by trauma, infection, lack of activity, etc. No cure exists at the time, but the symptoms are treated with compression and physical therapy. The SCD is intended to target the lymphatic system rather than the musculovenous pump.

Another pathology that SCD is used to treat is *Critical Limb Ischemia (CLI)*. This disease is a "severe blockage in the arteries of the lower extremities, which markedly reduces blood-flow" [95, 96]. CLI happens because of thickening and stiffening of the vessel's lining. This is the result of the build-up of blood components like fats and cholesterol on the walls of the arteries [97]. This pathology provokes severe pain in the feet and/or toes even when they are at rest. If not treated, it results in amputation of the limb. Apart from the pain, symptoms include open sores, skin infections or ulcers that will not heal, cold extremities, skin that appear smooth, shiny, hairless or very dry, weak or no pulse in your legs or feet, numbness in your legs, feet or hands [98, 96]. Risk factors include age, smoking, obesity, sedentary lifestyle, high cholesterol, etc[96]. The main treatments are revascularization through surgical procedure or endovascular treatments. Treatment via surgical procedure usually consists of replacing the problematic area with a graft [96]. Endovascular treatments are less invasive and consist of balloons or stents placed in the vessel to open the artery [71]. For patients where revascularization is not possible, SCT has been shown to be an efficient and non invasive treatment [99, 100]. In addition, medication is another tool to fight against CLI. It is used to lower blood pressure and cholesterol, prevent blood clots and reduce pain [96, 98].

5.1.3 Administration

SCT consists in sequential compression-deflation of multiple bands, using a peristaltic principle to help the blood to get back to the upper-body. Each sequence consist of consecutive inflation of each bands, starting at the ankle and moving to the knee. Such a sequence lasts between 20 and 60 seconds (each compression lasts around 10 seconds), with a rest period of about 15 seconds. During compression sequences, bands are inflated with an inner-pressure range of 30 to 120 mmHg, depending on the physiology of the patient [101]. When a medical doctor prescribes SCT, his order should specify the exact protocol. The positioning of the device, the impulsion time[2], the duration of the therapy, and the compression protocol should all be mentioned [102]. Before placing the SCD on the leg, a complete assessment of the patient's pathology is required, as well as a skin and neurovascular assessment. This is to avoid risk that will be mentioned in section 5.1.4. The skin and neurovascular assessment should be repeated every eight hours by removing the device. The patient should be educated to the use of the device, notably on notifying the medical staff when removing it and reporting pain sensations. For placement, the device needs to fit the leg correctly. Two finger should be able to fit between the leg and the device but it should hold in place. Manufacturers usually refer to how correctly position the sleeve in the device documentation [102].

5.1.4 Risks

Adverse conditions associated with compression therapy mostly include skin irritation, discomfort and pain [103]. Another risk is patient falls. The Patient Safety Authority

[2] An *impulsion* is the term for one compression sequence of the sleeve.

indicates from fall reports that "*the proportion of serious events reported in patients who fell wearing SCDs was 15%*" [104]. The majority of falls occur when toileting because patients trip over or get tangled up in the SCD tubing[104]. Severe adverse events are very rare (below 0,01% of incidence) and include soft tissue damage and nerve palsy [105].

5.1.5 Other treatments

Other types of compression therapy include bandages and wraps or compression stockings. Those options aim to achieve the same results but are completely passive. They do not allow control of the variation of the administered pressure which is useful to face interpersonal variation[3] and personal variation[4] of needs. They are also usually less effective than pneumatic compression [?].
Another treatment to ameliorate blood circulation is the administration of blood-thinning medicine. Those drugs may work better than compression devices, but they also entail other risks[103]. They are not advised for people at high risk of excessive bleeding, pregnant woman or during certain surgeries. They can also produce side effects[5] [106].

5.2 SCD for an appropriable hospital

The information presented in section 5.1 confirms the need for an OS appropriable SCD. First of all, it treats diseases that are the results of immobility. So if a high number of persons are bedridden because of any disease or incident, appropriable SCD that could be acquired rapidly would be very useful. In addition, the pathologies mentioned above include age as a risk factor and the increasingly aging population will likely become a prevalent issue in the future, further enhancing the need for solutions. The number of patient needing SCT should rise over time. Furthermore, because the SCD is one of the essential intensive care unit equipments, it is likely to rapidly reach maximum capacity. Finally, this device is used for long periods of time and patients need to wear it nearly continuously. One device can treat only one patient at the time, and so for usually a few weeks. This makes the eventuality of an open-source and appropriable version even more interesting.

All these elements allow us to reach the conclusion that an open-source appropriable SCD would be useful to develop. In order to do so, the next chapter will present the existing devices. It will touch on regulations and classification of the products on the market. This will allow us to have a complete vision on the information about this MD for next steps of prototyping.

[3] Different patients have different needs.

[4] One specific patient can have different needs along its medical journey.

[5] Side-effects examples are: passing blood through urine, excessive nose bleeding, severe bruising, headaches, digestive discomfort, etc.

Chapter 6

Existing Sequential Compression Devices

Sequential Compression Devices (SCDs) are a considerable field when talking about MDs. As medical devices, their are subject to law's constraints impacting their design. The technologies used have to ensure the safety of all the stakeholders and the proper functioning of the treatment. Moreover, there are already numerous SCD existing on the market. They were assessed and referenced to evaluate the advantages of the OSAMD-SCD.

6.1 Legal regulations

According to MeDevIS, SCDs are only subject to standard regulations on applied to medical devices depending the geographical area where the device will be sold/used. In the European Union (EU) medical devices regulation, a SCD is classified as a medical devices of risk class IIa[1].

In EU, the application of risk management to MDs is specified by the *ISO14971* standard and done using a case-specific risk management plan. It implies a sustained and iterative research aiming at the identification of potential risks of use of the device. Once the risks have been identified, their consequences must be evaluated, notably via their probability of occurrence, their severity and the ratio of benefit to risk. Depending on the score obtained, risk reduction may or may not be required. This reduction will be done through a change in the design of the device, in its method of use[2] or by additional safety information. Once the new design is proposed, the risk analysis is repeated. As briefly mentionned in section 1.4.1, the risk management process is inherent to the design process of a device that aims to be medical.

6.2 Devices classification

Schara et al. already listed 9 SCDs to evaluate the price advantage of their OS SCD but their identification presented shortcomings such as a lack of sources or the use of renting

[1] The classification of medical devices in the EU is determined by their intended use and potential risks, ranging from I (lowest risk) to III (highest risk), all prioritizing public health and safety.

[2] For example, using protective measures.

prices which is not relevant in the context of an appropriable hospital, since an hospital is most of the time the owner of the device. An updated assessment of FDA and/or EU-approved MD banks reveals a good representation of the types of SCDs on the market [107, 108]. The research has made it possible to situate the various technologies of SCDs in respect to each other according to four components:

- Compression technology;
- Compression control;
- Portability;
- Price.

All these aspects where articulated into table 6.1 and an associated graph that allows the reader to compare the devices (figure 6.1).

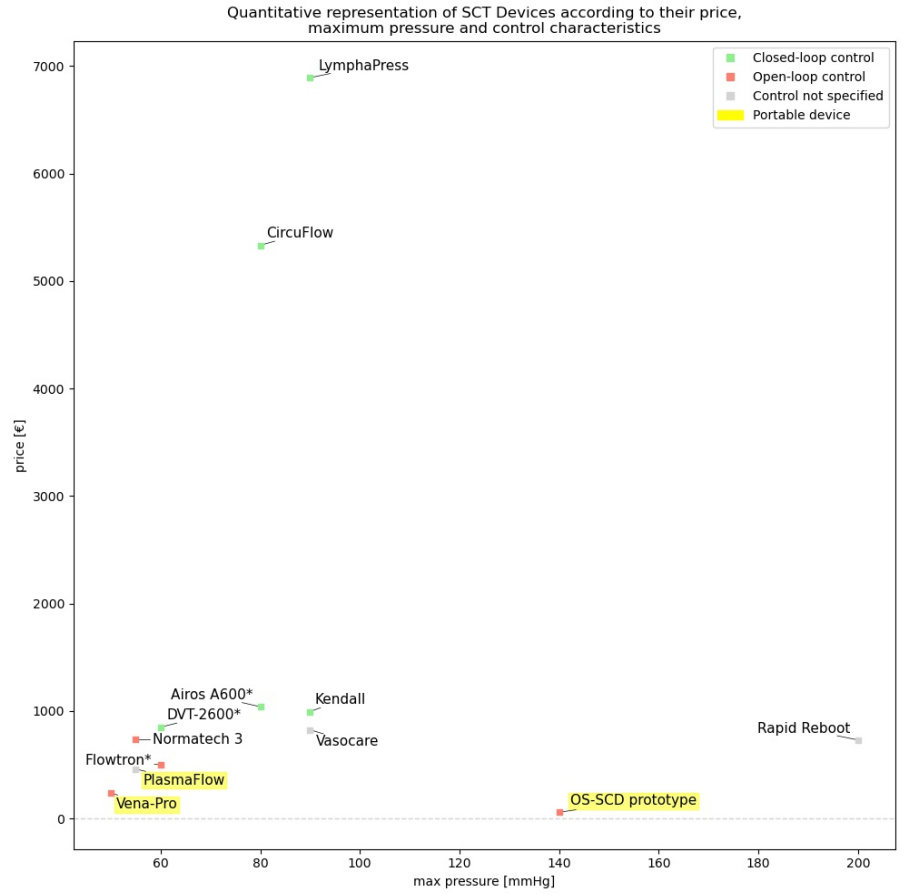

Figure 6.1: Quantitative positioning of the different SCDs evaluated in table 6.1. A more precise identification of the studied devices is available in the table. Not available information is not represented, except for the pressure control method of the devices. *OS-SCD prototype* refers to the prototype discussed in part III of the thesis. (* = price for pressure controller only).

6.2.1 Compression technologies

Various devices are available for SCT. Intermittent Pneumatic Compression Devices (IPC Devices) are the most commonly used due to their efficiency. Most of them are

suitable for SCT as well as for IPC therapy. The difference between these two therapy modes is visible on figure 6.2. However, this difference is often confused in scientific literature [109] since they are used to treat similar pathologies. These devices commonly utilize an air-pump to inflate a constrained structure that apply pressure on the limbs. However, newer technologies that use electro-stimulation of the muscles involved in the musculovenous pump are claiming to offer comparable results to IPC Devices [110].

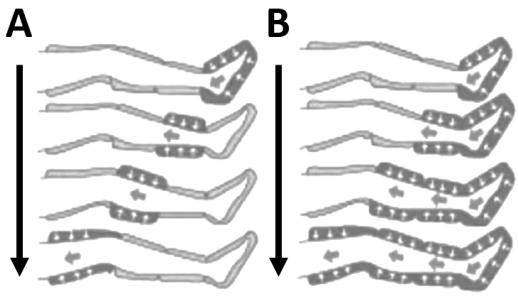

Figure 6.2: Different SCT impulsion modes available from Rapid Reboot Recovery Products. Figure **A**: Sequential compression, figure **B**: Peristaltic compression. Sequential compression mode is used during a SCT while the peristaltic compression mode is used during IPC therapy.

In the context of IPC Devices, their inflatable structures are of various designs, depending on the desired location of the SCT and the desired behavior of the pressure profile. Among the IPC Device of table 6.1, the most common design is a pair of sleeves made of polyurethane and nylon [111] wrapping the limb, with between three to five air chambers connected to the controller of the device.

Controllers are specifically designed to accommodate the connection of two sleeves or are sold in pairs, directly connected to their associated sleeve, like the *Legfit* (table 6.1). In case the therapy is wanted to be unilateral, an *air-blocker* is sold with the device in order to block the airflow of one of the two controller output (figure 6.3).

Figure 6.3: CircuFlow IPC Device controller[112] (*right*), associated air-blocker (*left*) and user-manual (*behind*). Complementary specifications about this device are given in table 6.1.

Among all the devices encountered, *Venowave* stands out. It announces the use of undulatory mechanical compression on the calf using a contoured plastic plate (figure 6.4).

The movement of blood for this technology should be more continuous, thus inducing less turbulence. However, this device is the only FDA and EU certified device of this type and is not commercialized for the moment. The manufacturer does not provide any specific information regarding the performance of the device that would enable a comparison with the other devices.

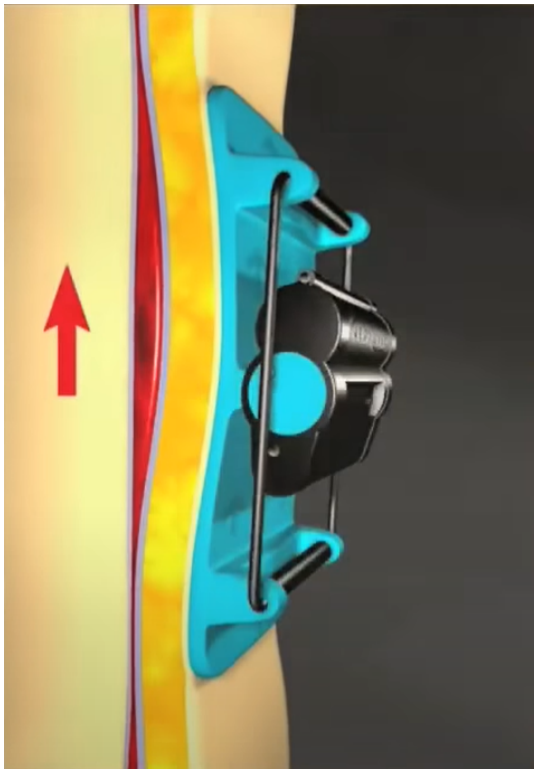

Figure 6.4: Design of the *Venowave VW5 peristaltic pump* [113]. FDA GUDID: 00683601000053. Technology protected by US Patents.

6.2.2 Compression controls

Compression control of SCDs is most often an *open-loop control*, where the timing and the pressure of the compression sequence are initially set using the UI of the device. It allows a basic design regarding the UI but more importantly for the electronics behind. However, a feedback allows the device to adapt the airflow to ensure a continuously appropriate treatment.

Various types of feedback can be utilized to observe the efficacy of the device, such as measuring the relative pressure between the inflatable band and the patient's limb, monitoring the patient's blood pressure and blood flow, or assessing the patient's blood oxygen saturation level using an oximeter. For simplicity reasons, the pressure feedback is predominant and the only one found among all the devices of table 6.1.

The pressure indicated by all manufacturers of SCDs is the inner-chamber pressures, and not the exact pressure applied by the sleeve's band on the patient's leg. Delis et al. have studied the optimum IPC stimulus for lower-limb[3] venous emptying and determined

[3] considering the foot, the calf and both of them together.

the best compromise between the different parameters of a SCT to induce a significant and lasting reduction in venous pressure. In this study, the analysed parameters are:

- Frequency of the impulses[4];
- Applied pressure;
- Delay time between the steps of an impulse.

An equivalent study specific to SCT does not appear to have been conducted to this date. However, some of the results can hypothetically be extended to the SCT, such as the applied pressure and indications about the impulse characteristics. Considering a compression of both the calf and the foot, higher applied pressures (up to 140[mmHg]) and higher frequencies (up to 4[impulse/minute]) of impulses lead to better blood pressure reduction.

6.2.3 Portability

In the context of SCDs, *portability* refers to the ability of the user to maintain freedom of movement while using the device. The portability is constrained by the electrical autonomy of the device and its pneumatic design. That aspect appeared to be relevant since it reduces the risk of falls discussed in section 5.1.4, and implies a lower need in term of medical manpower since manipulations (placement or removal) are less frequent. Thanks to a possible everyday-use of portable devices, therapies can also be performed for longer period, not impacting the personal life of the patient, hence freeing up precious hospital space.

For most of the IPC Devices, each chamber of the sleeve is connected separately to the controller, thus favoring the presence of tubes in the system. Of all the considered devices, portable designs implies two controllers, one for each sleeve, fixed directly on the sleeve. Batteries are also a constraint for mobility. They have to be small and to supply the device for long period therapy. *Venowave*, *Legfit*, *PlasmaFlow* and *Vena Pro* are portable designs.

6.2.4 Selling price

Development and manufacturing prices were never published by manufacturers of the considered devices, which is why only the selling price is considered. Selling prices of SCDs are generally not publicly available since their sale is not directly to the public but to professionals. When information about the price of a SCD has been found, it is from a reseller or from user-feedback. To perform a more precise price analysis, a deeper research involving manufacturers and professionals of the healthcare world is needed.

From table 6.1, the mean and the median price of a SCD can be evaluated at 1471€ and 735€, respectively, with a minimal value of 238€ and a maximal value of 6892€. The reader has to keep in mind that this list is not exhaustive and potentially not representative of all the SCDs currently available on the market. Moreover, the prices of the two legs sleeves associated to the controller are sometimes missing, meaning that the previously

[4] An impulse is one train of contraction as it is represented on figure 6.2.B. The frequency of the impulse is generally given in [impulse/minute].

computed minimal, maximal and mean values are likely to be higher.

Figure 6.1 strengthens the hypothesis that the presence of a feedback loop in the controller of the device makes the price substantially higher. If having a closed-loop control in the device is not mandatory[5] or necessary for the proper conduct of a SCT, one can reduce the device manufacturing budget. Research raised the hypothesis that the absence of closed-loop control could be compensated by an initial calibration of the device pressure and a reduced SCT session duration.

To summarize

Sequential compression devices are classified as a IIa risks class devices and are subject to the medical devices regulations of the sale/use, the EU regulation for Europe. Numerous devices are present on the market and a large variety of them was classified according to the compression technology, the compression control, portability and price. Most of the devices can provide as well sequential compression therapy as intermittent compression therapy. Both open-loop and closed-loop devices are available but the feedback-loop seems to increase the cost. Some devices are wearable, other are not, once again wearable devices are not especially more expensive. Price vary among the devices. Most of them cost less than 1500€ but a few exceed the 5000€ mark. However information on prices was difficult to obtain and this research could be reviewed by hospital members that have access to the exact selling prices. Therefore, an affordable SCD should cost significantly less that most devices on the market. It can or not be wearable and have or not closed-loop control. However if these features are not present in the first iterations it would be an advantage to add them to fight the most competitive devices on the market. Possibility of providing both types of compression therapy would also be a good feature to add progressively through updates of the open-source solution.

[5] Regarding the risk analysis.

Table 6.1: Table containing 16 devices found during research about SCDs, their regulation approvement, an overview of their specifications and their prices. Since SCD and IPC Device are only slightly different, IPC Device have been differentiated but are part of the research. The reader has to note that the table is not exhaustive and that the indicated prices may vary and were found without using the conventional ways for medical instances. *ID* refers to the GUDID (FDA) or the EUDAMED-ID (EU) medical device identification number of the device. *Leg* p_{pouch} indicates the inner leg-cuffs pressure. Information about *control* is not always included. If not announced clearly, closed-loop control has been assumed based on the presence of pressure error indicators and pressure feedback. *Portability* means the device doesn't restrict movement. Price denotes the price demanded for the entire device, leg sleeves included. All prices have been converted to € (1 USD = 0.92€ on may the 5th, 10:48) for easier comparison.
(NAN = not available information, * = pressure controller only, † = Not in commercial distribution.).

Sequential Compression Therapy Devices								
Shortname	ID	Regulation	Leg p_{band}[mmHg]	Control	Portability	Autonomy	Price [€]	Source(s)
Normatec 3 Legs	NAN	FDA	$0-55$	Open-loop	No	Battery (3hrs)	734.68	[115]
Kendall	10884521129634	FDA	$6-90$	Closed-loop	No	On sector only	995.00	[116, 117, 118]
Venowave†	00683601000053	FDA, EU	NOT APPLICABLE	Open-loop	Yes	Battery (NAN)	465.07	[113]
CircuFlow	00879766005358	FDA, EU	$20-80$	Closed-loop	No	On sector only	5333.10	[119, 120]
DS MK300L	08809315678957	FDA	$10-200$	NAN	No	On sector only	NAN	[121]
DS DVT-2600	18809315678398	FDA	$20-60$	Closed-loop	No	Battery (8hrs)	*849.68	[122, 123]
Airos A600	00855682007010	FDA	$30-80$	Closed-loop	No	On sector only	*1039.49	[124, 125, 126]
POWER-Q2300	08809277423466	FDA, EU	$20-200$	NAN	No	Battery (NAN)	NAN	[127]
Rapid Reboot	B691SPCL021	FDA	$0-200$	NAN	No	Battery (NAN)	731.00	[128]
LymphaPress	07290105878946	FDA, EU	$20-90$	Closed-loop	No	On sector only	6891.65	[129, 130]
PlasmaFlow	00850998008003	FDA	$0-55$	NAN	Yes	Battery (10hrs)	460.00	[131]
Vasocare	00812311021540	FDA	$20-90$	NAN	No	On sector only	824.60	[132][133]
Vena-Pro	00190446273288	FDA	$0-50$	Open-loop	Yes	Battery (20hrs)	238.00	[134]
LGT-2201DVT	06971410780254	FDA, EU	$40-190$	NAN	No	Battery (NAN)	NAN	[135]
IPC Device only								
Legfit	59052149440014	EU	NAN	Open-loop	Yes	Battery (NAN)	NAN	[136, 137]
Flowtron	05055982700016	FDA	$30-60$	Open-loop	No	Battery (NAN)	*499.00	[89, 138, 139]

Part III

Development of the prototype

In November 2022, Schara et al. published a research paper titled "A low-cost wearable device for portable sequential compression therapy". This paper presents the development of an open-source SCD. We studied their methods and results to produce an updated and more appropriable version. The first chapter of this part (chapter 7) is a presentation of the paper that served as basis for our prototype with a review of its openness as it is an open-source resource. The chapter 8 details the modeling and dimensioning of the prototype. Lastly, the entire fabrication process is detailed in chapter 9, with the updates that were made to the Schara et al.'s suggestion in order to enhance the open-source appropriable properties of this future medical device.

Chapter 7

Overview of the taken-up work

Schara et al. from the Department of Mechanical Engineering from Rice University published an article about a low-cost wearable device for SCT in November 2022. This open-source devise had as goal to be affordable in order to provide better treatment conditions for socioeconomically disadvantaged people[7]. It is the only OS SCD that we found during research and we based our development on their proposition. Their SCD project is published under a Creative Commons CC-BY licence. This chapter presents their work.

7.1 The paper

This section focuses on the paper that was published to present the device. It reports the motivation for the work, the methods and the results that are presented in the article.

The paper starts by presenting the high impact of cardiovascular diseases and the relation between socioeconomic status and the risk for these diseases. People with a low income have higher prevalences of risks factors for developing cardiovascular diseases [7] . Authors then proceed to present the treatments for the Cardiovascular Diseases (CDs) with the highest prevalences. Those are long-term medications, revascularization surgeries and lifestyle changes. They say SCT is usually prescribed along these treatment options to enhance efficacy and that it has been demonstrated to lower the risks after undergoing surgery [7]. Also, they explain that SCT can be used during rehabilitative sessions because it has been shown that the combination is more effective than each individually [7]. Authors also mention that SCT devices are associated with high cost, between 100$ and 500$ over a 1 month treatment cycle and over 1000$ for purchase [7]. This justifies the importance of creating and affordable and wearable SCD. The following point is the interest of soft-robotics for the prototype since it makes the interface between human and the device safer with good compliance [7]. They state that textile is advantageous because of his strength and compliance. They add that it has been shown to fit well soft-robotics [7]. Furthermore, they also cite research that has already been made about soft-robotics for mechanotherapy via leg wraps as basis of their work [7]. Nevertheless, these works are not open-source and not specifically for SCT unlike this new prototype. This is how they justify the method of soft-robotics and the use of textile for this device.

Their devices consists of inflatable bands of *pouches*. Pouches are flat rectangular sections that transform into chambers when inflated. The input pressure creates a retraction

in the length and thus a longitudinal tensile force. This type of device is called a *pouch motor*. When a band is attached around the leg, the retraction translates in a circumference reduction which induces radial pressure by the Laplace pressure relationship [7]. Most SCD are under the form of a sleeve composed of a number of pouches that inflate to provide compression the the leg contrarily to the straps of multiple pouches presented here. Three bands are attached to a common perpendicular section so that their relative position is maintained. Each strap is composed of five squared shaped pouches of 3cm of side [7].

Schara et al. claim that their device costs 62$ and that all parts are available commercially.

7.1.1 Fabrication

The chosen fabrication method of the bands consists of the stacking of three layers. The two outer layers where cut out of a nylon textile coated on one side with Thermoplastic Polyurethan (TPU). This material makes the textile heat-sealable. The TPU sides are placed on the inside of the stacking in order to bound together with heat press. The intermediate layer is has to be non-stick, here parchment paper was used. It creates non-adhesive chambers for inflation. The authors mentioned that the layers can be cut by laser or any fabric cutting technique, as simple as scissor. For sealing, the protocol used was heat-press for 30[s] at 345[kPa] and 200[°C] [7]. However, it is specified that any other source of sufficient heat and pressure, such as an iron, can by used. This fabrication protocol as the advantage of being very simple and inexpensive. It can be applied anywhere without very specific machines [7]. The inlets of the bands were connected to tubes with Luerlocks. Researchers applied heat to the TPU around the locks so that is shrunk, then they applied epoxy for complete adhesion and isolation [7]. They attached adhesive-backed hook-and-loop fasteners to each band. This allows to adapt fitting to the leg and the the height of the band [7].

An electronic system controls pressure and timing of the inflation of the device [7]. To do so they used an Arduino Nano to impose the pressure by modulating the opening of the valves with control on their duty-cycles. The other main electronic components are a pneumatic micropump, three miniature pneumatic valves and two batteries. Transistors connected to outputs of the Arduino allow the regulation of the pump and the valves. During their SCT, the pump is in steady-state and the valves are opened one after the other to let air in the bands and obtain the SCT. The researchers also implemented 3 knobs, each connected to a valve via the Arduino board to adjust the pressure of each strap individually. This is justified because the straps will be attached at different heights on the leg, each having a different diameter [7]. Since the pressure on the leg is related not only to the pressure in the strap but also to the radius of the leg (by the Laplace pressure), input pressure could need to be different in each strap.

7.1.2 Analytical modeling

To predict the behavior of the fabricated bands, made of 5 serial pouch motors, the pouch model of Niiyama et al. was used. It relates the input pressure to the Laplace pressure applied on the leg with. With the pouch motor model, the input pressure, P_{pouch}, is linked to the force of one strap due to its retraction, F_{strap}. L_O and L_1 are the length and width

of one pouch and θ the tangential angle of the inflated pouch with the ridge of the pouch perpendicular to the longitudinal axis of the strap (see figure 7.1). The relation is the equation 7.1.

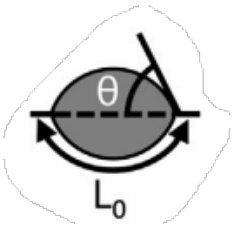

Figure 7.1: Schematic from Schara et al.. defining the variables L_0 and θ as parameters for the pouch model of Niiyama et al..

$$F_{strap} = L_0 L_1 \frac{cos(\theta)}{\theta} P_{pouch} \tag{7.1}$$

In the article the leg is considered a near-rigid body and θ does not vary around it. The consequence is that the relation in equation 7.1 is linear.

Then the relation between F_{strap} and the pressure on the leg, P_{leg} is formulated using the relationship of Laplace pressure, see equation 7.2. This pressure state is derived from the Young-Laplace relation and is a function of the surface tension γ and the radius, r. In this case r is the radius of the leg. γ is defined in the article as a "force per perpendicular unit length". It corresponds here to F_{strap}/L_1.

$$P_{leg} = \frac{\gamma}{r} = \frac{F_{strap}}{L_1 r} \tag{7.2}$$

For SCT it is important to relate the pressure applied on the leg P_{leg} to the input pressure, P_{pouch}. By combining all equations above this relation appears, see equation 7.3.

$$P_{leg} = \frac{L_0 \frac{cos(\theta)}{\theta}}{r} P_{pouch} \tag{7.3}$$

The controlling of P_{pouch} to achieve specific P_{leg} was done through varying the duty-cycle of the pumps. To identify the pressure on the leg and the relation of the pressure with the duty-cycle the researchers used a force sensor to measure the force on the leg, F_{leg}. The relation between this force and the P_{leg} is equation 7.4.

$$P_{leg} = \frac{F_{leg}}{A_{eff}} \tag{7.4}$$

A_{eff} is the effective surface area of the force sensor. Then with this measured force, F_{leg} served to identify the calibration factors C_1 and C_2 of their pumps and find the relation between the force on the leg and the duty-cycles of the pumps, see equation 7.5.

$$F_{leg} = C_1 DC + C_2 \tag{7.5}$$

7.1.3 Testing, results and discussion

They used a universal testing machine to quantify the relation between F_{strap} and P_{pouch}. The results confirmed the linear relation as seen on figure 7.2.A [7]. The band was fixed to the testing machine and the force it exerted for different pressures was measured. θ remained approximately constant throughout this experience and was deducted to equal 46° to fit the niiyama model [7]. The second test performed was the measure of F_L with three force sensors placed between each strap and the device and a mannequin leg anatomically proportionate. The fake leg was covered with a silicone elastomer layer. The layer simulated skin tissue and the plastic leg simulated the musculoskeletal part of the leg. They considered that the effect of position of the pouch motor on F_L was mitigated by the silicone material that distributed the force and that this effect is similar to the human tissue [7]. The empirical data shows a linear relation between F_L and P_{pouch} as seen on figure 7.2.B.

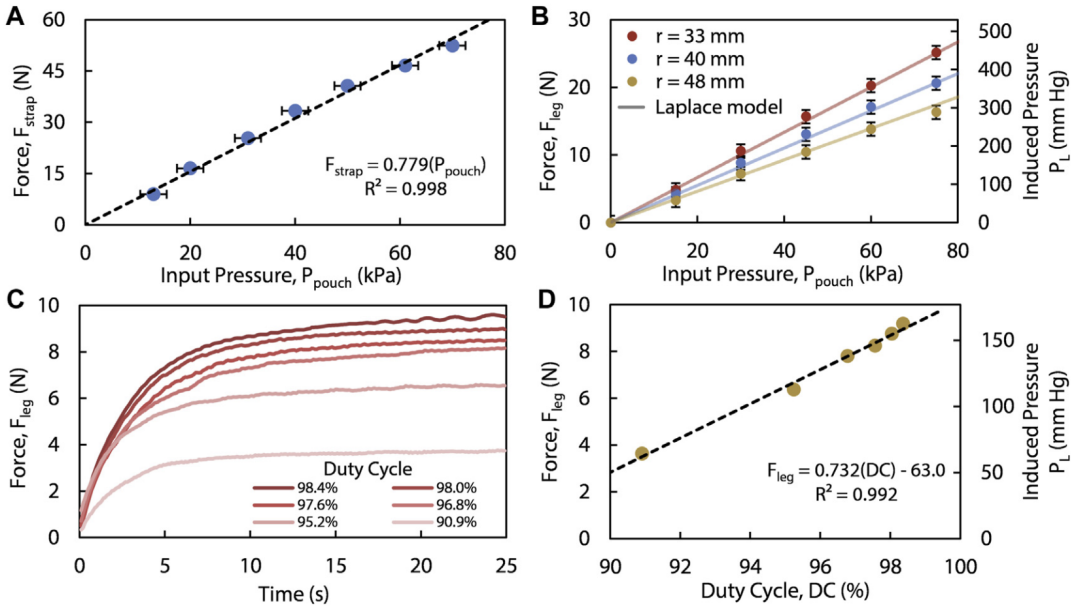

Figure 7.2: Image from Schara et al.: (A)F_{strap} for different pressure inputs. The doted line is a linear regression and the blue points are the experimental measures. (B)F_{leg} at different input pressures and for different leg radius's. The lines corresponds to the Laplace model and the points are experimental results. (C) Measured F_{leg} over time at different duty-cycles. (D)F_{leg} over the duty-cycle. The dotted line is a linear regression and the yellow points are experimental results[7].

The researchers also measured the force applied on the leg depending on the Duty Cycle (DC) chosen with the same set up as the previous experiment. The results showed that specific steady-state F_{leg} and thus P_{leg} could be achieved by varying the DC, this is shown in figure 7.2.C. Figure 7.2D shows a linear regression that was performed to find the link between F_{leg} and the duty-cycle. This served to easily calibrate the DC to obtain a specific P_{leg} for treatment [7].

Since all straps are attached at different leg diameter but need to deliver the same pressure on the patient, the relation between F_{leg} and P_{pouch} is not exactly the same depending on the diameter. Therefore, the DC of each strap were made to be calibrated independently. One potentiometer was associated to each valve in order to fix the DC independently for

each strap, and tailor the pressure to the diameter of the leg. Test were performed on a human leg and showed that controlled compression sequence fits the medical guidelines of 40–120 mm Hg of induced pressure for SCT, as shown on figure 7.3 [7]. Moreover, the paper says that even when the device is not controlled, the maximal pressure reached on the leg is of 450[mmHg] [7]. It also cites another paper that had shown that essays of mechanoterapeutic devices that apply greater pressures on the leg did not report adverse effects[7]. This suggests that even without the control board the device would cause no harm.

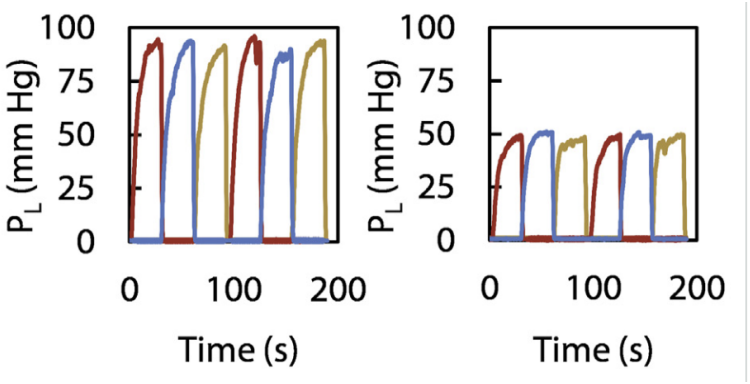

Figure 7.3: Image from Schara et al.: P_{leg} was measured over time and each color corresponds to a strap. All the straps produced the same radial pressure, with different input pressures according to the leg radius they were fixed on. On the left the results on the mannequin, on the right right the results on a human leg [7].

The authors conclude that they provided an affordable solution that fills the requirements for SCT in terms of duration and applied pressure [7]. They also insist on the fact that this solution is wearable and that that could lead to better use of the device. Additionally they say that the simplicity of the approach makes the device accessible and makes sense for the open-source dynamic [7]. Finally they conclude on future enhancements that could be brought to it. They mention the possibility of integrating the device in a piece of clothing to further improve the portability and low-profile. They also suggest the implementation of textile-based energy harvesting so that the whole device would only be mode of textile. It would be entirely soft with even better compliance [7]. They also suggest to further develop the device to deliver SCT with a closed-loop control [7].

7.2 Additional material

At the end of the article there is a section named "supplementary material". In provides a link to the rest of the material that is not included in the paper. This material is addressed to people with purpose to reproduce the device or the results of the paper [7]. It consists of one pdf document called "Data sheet 1" and a folder named "Data sheet 2" that contains eight documents.

7.2.1 Data sheet 1

The first data sheet gets into the details of the experimental procedures. Then it provides details on the fabrication process and provides supplementary figures and tables.

The authors specify the reference of the universal testing machine and of the pressure gauge used to quantify F_{strap} in relation with P_{pouch}. They explain that they fixed the strap in the machine's grips and measured the lateral tensile force exerted by the strap via a 2kN load cell integrated in the machine [7]. Air was supplied in the strap and adjusted with a regulator. Then the pneumatic pressure was measured with the pressure gauge.
For the quantification of the radial pressure via the radial force small, flat and flexible sensor were used and their specifications are mentioned in the document. The other used devices and their references are also listed : a digital pressure gauge, a data acquisition device a layer of silicone elastomer and a laboratory air supply [7]. The text proceed to explain that three force-sensing resistors were placed on a mannequin leg and that this structure was thereafter wrapped with the silicone layer. A specific input pressure was imposed with the pressure gauge and with the specification of the sensor, the inward pressure could be quantified. The device was then used to apply sequential compression and the applied pressure on the leg was calculated. The same test was performed on a human leg [7].
The last relation that was quantified is the one between the duty-cycles of the pump and the exerted force. The set-up was similar to the one described above with the acquisition of the force exerted radially. However this time DC were applied to the pump.

Consequently, the process of fabrication is detailed. It is specified that provided .svg files with the patter of the sheets (of TPU textile and non-stick layer) can be used as input for a laser cutter or vinyl cutting device. It is also said that is these devices are not available, the sheet can be obtained by using a simple scissor. The design could be printed with a A3 printer. In spite of that, no schematics provide the exact dimensions of the layers. To find them, someone needs to extract them from the svg files by converting the pixels in *cm*. The next step in the fabrication is the heat pressing of the layers together. It is mentioned that the layers where pressed together for 30 seconds at 345 kPa and 200C. The authors suggest to use a standard clothes iron if a heat press is not available. To facilitate the alignment, slotted tabs were included in the design. They can be seen on figure 7.6. Cardstock can be threaded through to keep the alignment during heat pressing [7] . Problem is, this only ensures that the external layers are aligned, it does not help to keep the non-sick layer well positioned. A fabrication process to fight this problem is discussed in chapter 12. After the device has cooled down, "three 16-ga, 1-in blunt-tip dispensing needles with threaded (twist-to-connect) Luerlock tapers (CML Supply, 901-16-100) are inserted and glued into the three openings created by the non-stick channels" [7]. Then the fasteners need to be attached to the straps.

The data sheet also describes the files for 3D impression of the box that will enclose the electronical components. They recommend polyactic acid or "other reasonably durable materials". They then suggest to use a strip of fabric with hoop-and-loop fasteners to serve as a strap to fix the box on the patient's leg.

Finally the document discusses the fabrication of the emulated leg. The writers give the reference of the mannequin leg they used and so of the 1 cm layer of silicone elastomer. They followed the indications of the manufacturer and then embedded the force sensing resistors (after their calibration) between the mannequin's leg and the elastomer [7].

It also includes a number of figures and tables.

- An image of "the setup for measuring the lateral force exerted by the pouch motor at a given pneumatic pressure input on a universal testing machine" [7].
- An image of the electronic circuit wiring schematic and of the electropneumatic controller. This imagine can be seen on figure 9.1.
- A picture of the experimental set up of the testing of the pressure on the test bench with the force sensors.
- A figure with graphs of the input pressure over time for the results obtained in figure 7.3.
- A table with the costs of SCT with hospitalization, different equipment rentals or different device prices and for mutiple time frames. This chart shows that the device of the article is less expensive and increasingly advantages over time.
- A table of the major components of the device. The table is reported on figure 7.4. Components that can easily be replaced were not included in the table [7].

Part Names	**Model Number (#)**
Arduino Nano IOT 33	ABX00032
Skoocom Miniature Pneumatic Pump	SC3101PM
Lee Co. Pneumatic Valves	LHDA0531115H
Galaxy 2S (7.4V) 120 mAh Lipoly Battery Pack	UPC: 04429784075
Seattle Fabrics: Heat Sealable Coated Nylon Taffeta	FHST
Reynolds Kitchens Parchment Paper	G74991

Figure 7.4: Table from Schara et al. : The major part names and their model number[7].

7.2.2 Data sheet 2

This folder contains 8 files :

- Two .STL files for the 3D impression of a box that was designed to hold the electronical circuit of the device. One file for the top and one for the bottom part of the box, visible on figure 7.5.
- Two .svg files, one with the dimensions and pattern of the textile layers and the other for the parchment paper layer. This file can be used as input for a laser cutter.
- Two .ino files. On one the Arduino code to upload on the device to perform the SCT. On the other side the Arduino code that was used for the experiments for the leg force experiment.
- a .m file with the MATLAB code used to translate the data of the force sensor into the Laplace pressure.
- A README.txt document that contains a description of the other files.

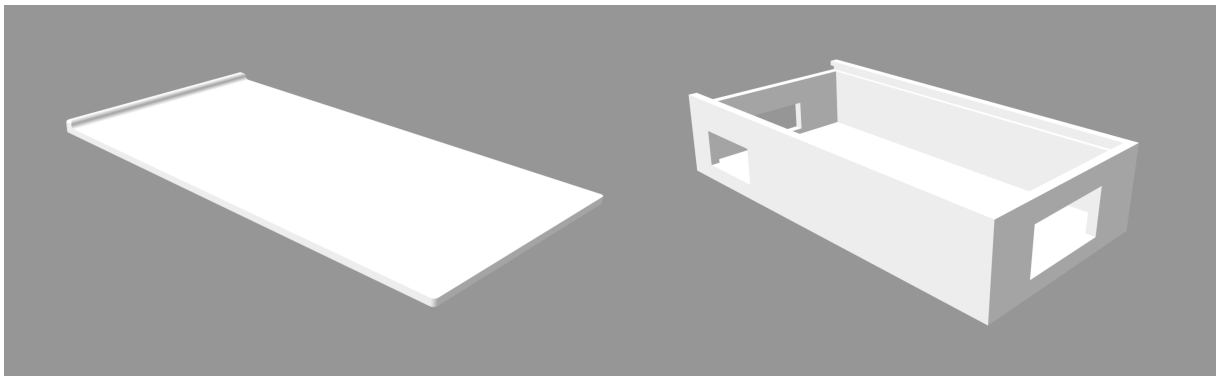

Figure 7.5: Left: Illustration of Schara et al. of the top part of the box for which the 3D impression file is provided in Data Sheet 2 [7]. **Right:** Illustration of Schara et al. of the bottom part of the box for which the 3D impression file is provided in Data Sheet 2 [7].

The .svg files with the patterns for cutting are visible on the following figures. Figure 7.6 shows the pattern for the two heat sealable textile layers. The three bands are visible and they are attached to a perpendicular section that holds their relative position. The same figure also shows the shape of the non-stick layer, with the three arrays of five pouches and the air access.

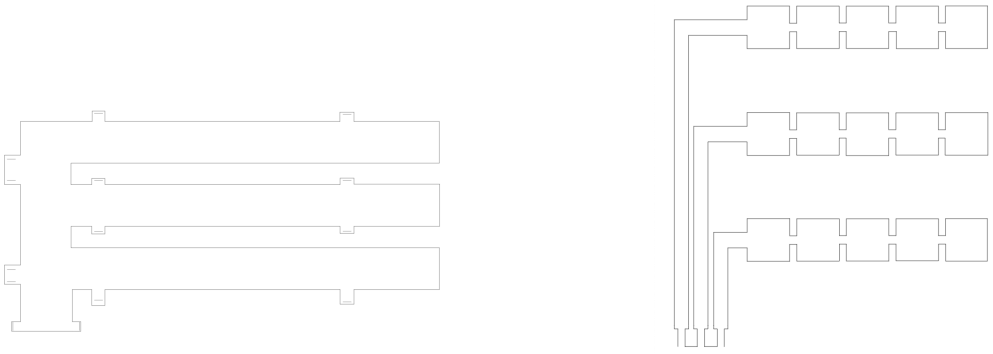

Figure 7.6: Left: Illustration of pattern the heat-sealable layers[7].**Right:** Illustration of pattern the intermediate layer[7].

The SCT_Run.ino file contains the SCT protocol to upload to the Arduino and run automatically when its start button is pressed.

Arduino code: initiation Their Arduino code developed for SCT is very basic. After defining the pins used for the potentiometers (*inputs*) and valves (*outputs*), the conversion rate from the input tension values is hardcoded. A counter is initiated to `counter=0` and will be used to handle the timing of the impulses regarding the internal board clock.

Arduino code: loop The code will loop over 3 code blocks almost identical, one for each band, and finish by a hardcoded waiting time that delays the next impulse. The block 1 states that until a given time flag (depending on the current `counter` value) is not reached by the clock, the output of the valve 1 will oscillate between `LOW` and `HIGH` according to a hardcoded *off time* specific to the considered band and the converted value

of the relative potentiometer input. Once the time flag is reached, the valve is set to `LOW` and the Arduino executes the next block.

7.2.3 Openness review

The article that was just presented served as base to our research. It is the first open-source SCD and presents promising results. However a few drawbacks about the openess of the work need to be addressed.

Dimensioning The calculation behind the choice of components is not presented. Especially the pump and valves had to be dimensioned to fit the air flow and pressure requirements but the development is nowhere to be found. This is a breach to the open-source dynamic since it complicates the taking-up of their work. A justification of the chosen components would facilitate the review and improvement of their work.

Referencing They managed to give a good referencing (using model number) of the principal components of the devices (fig. 7.4). However, nothing about their specification were given, resulting supplementary researches and uncertainties about components acquisition.

SCDs pricing In the same spirit, the existing SCDs prices used to situate their work were not sufficiently identified and not sourced.

Pressure performance inaccuracy They announce that their device reaches a maximum of 450[mmHg] when unregulated. This corresponds to nearly 60[kPa] and their pump performances do not allow such a high pressure. It is limited to 40[kPa]. The maximum pressure on a leg must have been tested with an external pressure source.

Hardcoded SCT Their `SCT_run.ino` code was hardcoded specifically for their prototype, hence fully dependant of the used components, meaning that the code has to be completely rethinked for every little modifications of the circuit. The times values defined for their SCT protocol are also hardcoded and not related to any formula, making it impossible to adapt consciously the SCT.

Chapter 8

Dimensioning

Mathematical modeling is used during the conception of the device, for its analysis and characterization. It involves the dimensioning of the pneumatic circuit and the related performances of the device. The pneumatic band designed for our thesis is named *StandardL* and is visible on figure 8.1, a precise plan is given in appendix A. It is an update from the one of Schara et al., this will be discussed in chapter 9.

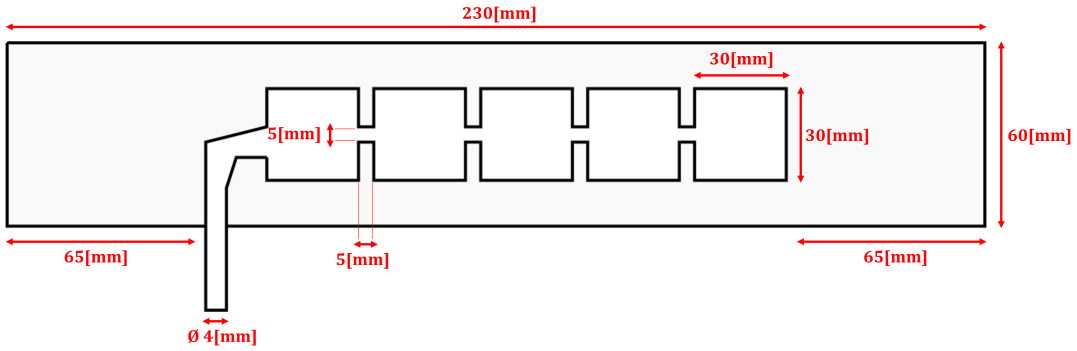

Figure 8.1: Schematic of the design of the *standardL* pneumatic band developed for the thesis. The band is composed of 5 identical pouches. More detailed measurements are available in appendix A.

8.1 Pouch geometry models

To understand and characterize the technology developed and used for the SCT prototype, Schara et al. based their study on a volumetric model used in soft robotic developed by Niiyama et al., hereinafter referred to as *pouch model*. It is assumed that a pouch is equivalent to the intersection of two cylinders (figure 8.2.A). With this hypothesis fixed, only three parameters are needed to define the inflation state of a pouch. Niiyama et al. introduce L_0, L_1 and θ_N, being respectively the initial length, width and tangential angle of the pouch model curved surface with the middle line (figure 8.4).

For a squared pouch as the one of the *StandardL* band, the variable L_1 can be replaced by L_0 and it simplifies the model's geometrical equations.

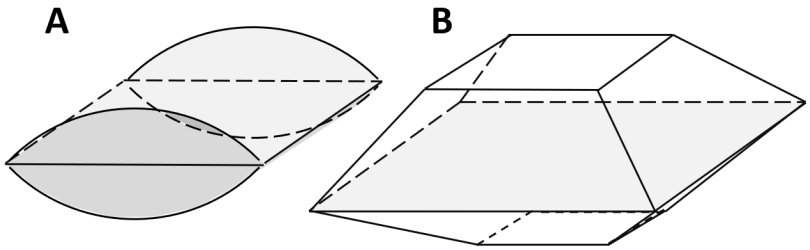

Figure 8.2: A: Geometric representation of a pouch according to the model of Niiyama et al.. It is the intersection volume of two identical cylinders. **B:** Geometric representation of a pouch according to the truncated pyramidal model.

Due to the real geometry of a pouch (figure 8.3), a *truncated pyramid model* has been imagined and approached. It aims to be more realistic and closer to the real geometry of an inflated squared pouch since the pouch model presents a non-conservation[1] of the total surface of the pouch during inflation.

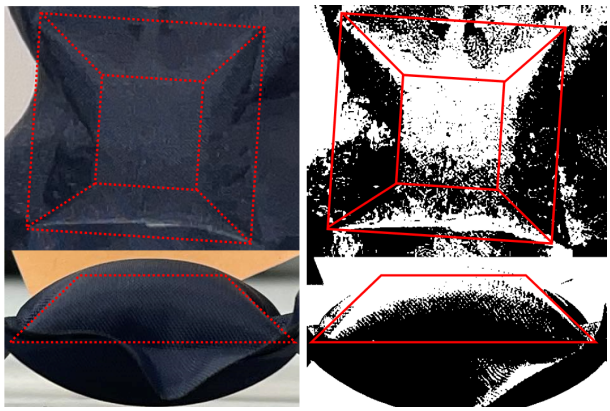

Figure 8.3: Picture of one squared pouch of a developed band of the thesis. The reader can observe that the geometry of the pouch is closer to the truncated pyramidal model than to the pouch model from Niiyama et al.

8.1.1 Truncated pyramid model

Figure 8.4 describes the variables L, L_0 and θ_N as defined by Niiyama et al. for a squared pouch. In the context of use of the model, the relation of interest is the one that links L to L_0 using θ, which is an indicator of the level of inflation of the pouch. These 3 variables are fully transposable to the truncated pyramid model (figure 8.4). The main hypothesis of both of the models is the conservation of L_0.

Constraint 1: Upper basis constraint If one considers a triangle of basis length $(L - L')$, of height h and angle θ between a lateral face of the truncated pyramid and its

[1] The upper and upper basis surface of the cylinder-intersection is added up to the initial surface of the pouch.

basis (figure 8.4.B), the following relation can be expressed :

$$h = tan(\theta) \times \left(\frac{L - L'}{2}\right)$$

$$L' = L - \frac{2 \times h}{tan(\theta)} \tag{8.1}$$

The profile of $L'(\theta)$ can be observed on figure 8.5 for better visualization of the constraint.

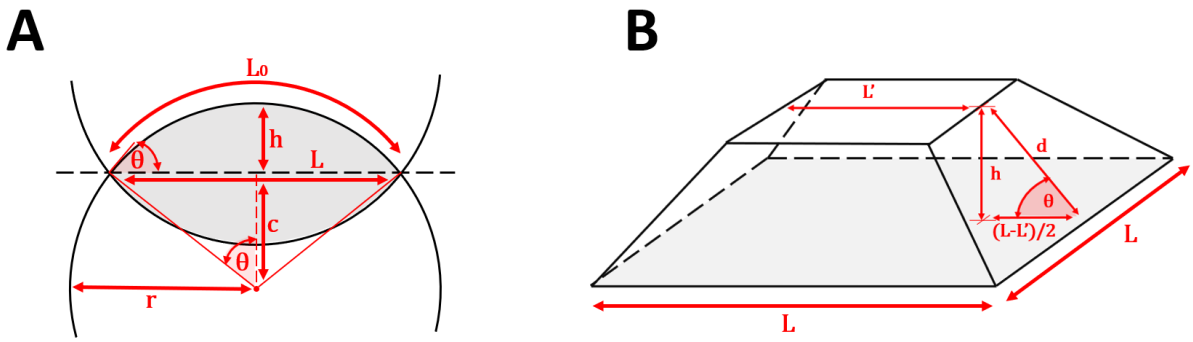

Figure 8.4: **A**: 2D geometry profile of the pouch model developed by Niiyama et al. $\theta \in [0, 90°]$ defines the tangent to the circle; L and L_0 are respectively the actual and initial lengths of the pouch. Other variables are referenced for further calculations. **B**: Geometry of the truncated pyramid model. $\theta \in [0, 90°]$ defines the tangent to the circle; L and $L_0 = 2 \times d + L'$ are respectively the actual and initial lengths of the pouch. Other variables are referenced for further calculations. The equivalent to the L_0 of the pouch model is $2 \times d + L'$.

Constraint 2: Height constraint Because of the unknown mechanical properties of the fabric used for the band, it is difficult to estimate the pouch height behavior. Since a constraint between the height of the pouch and its length exist implicitly[2] in the pouch model, it can be extracted and injected in the truncated pyramid model.

Figure 8.4.A shows the pouch model with a height[3] h equivalent to the h of our model. In Niiyama's model, this constraint is implicitly expressed by the fact that the profile of the air cushion half fits in a perfect circle, consequently to the conservation hypothesis of L_0 during inflation. Using the law of sine, the half-height of inflation (h) is thus:

$$c(r) = r \times \frac{sin(\pi/2 - \theta)}{sin(\pi/2)} = r \times cos(\theta)$$

$$h = r - c(r) = r \times (1 - cos(\theta))$$

By taking the conservation hypothesis of L_0, we finally find a relation for the constraint between h and θ:

$$h = r(\theta) \times (1 - cos(\theta))$$

[2] by the fact that the profile of the air cushion half fits in a perfect circle.

[3] h is the height of a half pouch geometry. Since that geometry is symmetrical (figure 8.2), all the developments are involving the upper part only.

$$h = \frac{L_0}{2 \times \theta} \times (1 - cos(\theta)) \tag{8.2}$$

For an arbitrary initial length of $L_0 = 30$[mm], the graphs on figure 8.5 allows the reader to visualise the inflation behavior of a truncated-pyramidal pouch.

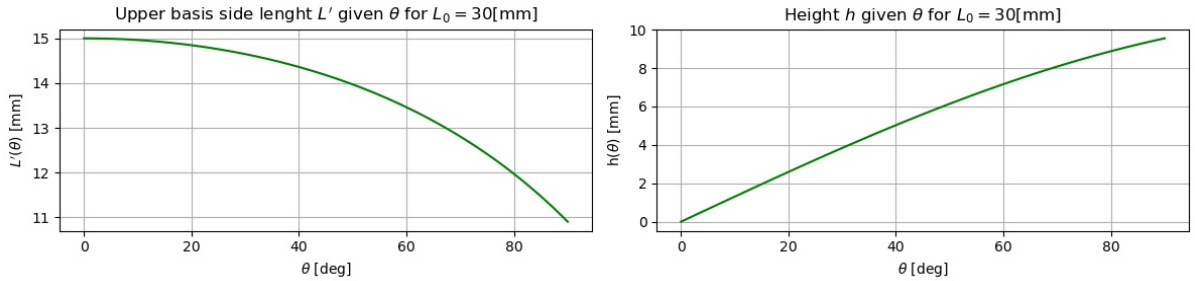

Figure 8.5: Left: Behavior of the upper basis (squared) dimensions over the tangential angle of the pouch θ as defined on figure 8.4. L' depends on $L(\theta)$ and is computed using the final strain equation of the reasoning (eq. 8.6). **Right:** Behaviour of the height h of a pouch for an initial squared pouch of 30×30[mm] over θ, the tangential angle of the pouch. These variables are defined on figure 8.4.

Constraint 3: Surface area conservation Since the equations are only applied to the upper part of the pouch geometry, the constraint on the surface area[4] S can be obtained as follow:

$$S = 4 \times A_{trapeze} + L'^2 = L_0^2$$

with $A_{trapeze} = d \times (L - h \times cot(\theta))$ and $d = \frac{h}{sin(\theta)}$ from figure 8.4.B, a new relation between L_0, L, h and θ is obtained.

$$L_0^2 = 4h \times \frac{(L - h \times cot(\theta))}{sin(\theta)} + L'^2 \tag{8.3}$$

Final relation between L, L_0 and θ By combining equations 8.1, 8.2 and 8.3, we obtain:

$$L_0^2 = \frac{2L_0L}{sin(\theta)} \times \frac{1 - cos(\theta)}{\theta} - L_0^2 \times \left(\frac{1 - cos(\theta)}{\theta}\right)^2 \times cot(\theta) + \left(L - L_0 \times \frac{1 - cos(\theta)}{\theta} \times cot(\theta)\right)^2$$

using $\phi = \frac{1-cos(\theta)}{\theta}$,

$$L_0^2 = \frac{2L_0L}{sin(\theta)} \times \phi - L_0^2 \times \phi^2 \times cot(\theta) + (L - L_0 \times \phi \times cot(\theta))^2$$

$$L_0^2 = \frac{2L_0L}{sin(\theta)} \times \phi - L_0^2 \times \phi^2 \times cot(\theta) + \left(L^2 - 2 \times L \times L_0 \times \phi \times cot(\theta) + (L_0 \times \phi \times cot(\theta))^2\right)$$

$$1 = \frac{L}{L_0} \times \frac{2}{sin(\theta)} \times \phi - \phi^2 \times \frac{cos(\theta)}{sin(\theta)} + \left((\frac{L}{L_0})^2 - 2 \times \frac{L}{L_0} \times \phi \times \frac{cos(\theta)}{sin(\theta)} + \left(\phi \times \frac{cos(\theta)}{sin(\theta)}\right)^2\right)$$

[4] Considering the four sides and the upper basis surfaces.

With the relative length variation $\gamma = \frac{L}{L_0}$,

$$1 = \gamma \times \frac{2}{sin(\theta)} \times \phi - \phi^2 \times \frac{cos(\theta)}{sin(\theta)} + \gamma^2 - 2 \times \gamma \times \phi \times \frac{cos(\theta)}{sin(\theta)} + \left(\phi \times \frac{cos(\theta)}{sin(\theta)}\right)^2$$

$$sin(\theta) = 2\gamma\phi - \phi^2 cos(\theta) + \gamma^2 \times sin(\theta) - 2\gamma\phi \times cos(\theta) + \phi^2 \times \frac{cos(\theta)^2}{sin(\theta)}$$

We then have a quadratic equation for the relative length variation γ,

$$sin(\theta) \times \gamma^2 + 2\phi(1 - cos(\theta)) \times \gamma + \left(\phi^2 \frac{cos(\theta)^2}{sin(\theta)} - sin(\theta)\right) = 0 \tag{8.4}$$

After a numerical resolution of the equation 8.4, the reader can observe on figure 8.6 that although the values of γ obtained are almost roots of the quadratic equation, the system has to violate the surface conservation constraint to be resolved.

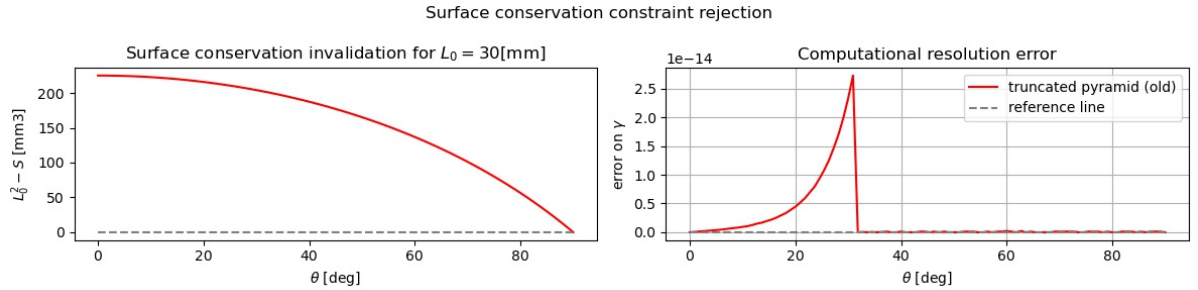

Figure 8.6: Left: Computation of the value $L_0^2 - S$ along the tangential angle θ, where S is the surface obtained using the right side of equation 8.3. The profile of the surface is computed using the numerical evaluation of the relative length variation γ obtained from equation 8.4, since S depends on L' which depends on $L = \gamma \times L_0$ (eq. 8.1). The reference line refers to the desired profile of the red curve. **Right:** The γ values returned by the numerical resolution show an error (values of the left term of eq. 8.4 for the numerically obtained γ). The reference line refers to the desired profile of the red curve.

Alleviated constraint (3bis): Since the surface conservation is not compatible with the profile of $h(\theta)$, one can do a step backward and alleviate the surface conservation constraint by imposing instead:

$$L_0 = 2 \times d + L' = 2 \times \frac{h}{sin(\theta)} + L' \tag{8.5}$$

This constraint is identical to the one of Niiyama et al. but on a geometrical model that considers a more realistic geometry of the pouch. Using equation 8.1 and trigonometric relations on figure 8.4.A, the equation constraint 8.5 becomes:

$$L_0 = \frac{2h}{sin(\theta)} + L - \frac{2h \times cos(\theta)}{sin(\theta)} = L + \frac{2h}{sin(\theta)} \times (1 - cos(\theta))$$

with the relative length variation $\gamma = \frac{L}{L_0}$,

$$\gamma = 1 - \frac{2h}{L_0} \times \frac{1 - cos(\theta)}{sin(\theta)}$$

injecting h from equation 8.2 and defining the strain $\epsilon_{pyr} = \frac{L_0 - L}{L_0}$,

$$\epsilon_{pyr} = \frac{(1 - cos(\theta))^2}{\theta \times sin(\theta)} \tag{8.6}$$

This final strain formula does not need numerical computation to be obtained and can directly be compared to the pouch model (figure 8.7). If the truncated pyramidal model fits better to the real behavior of a inflating pouch, we could expect a greater retraction from the pouch.

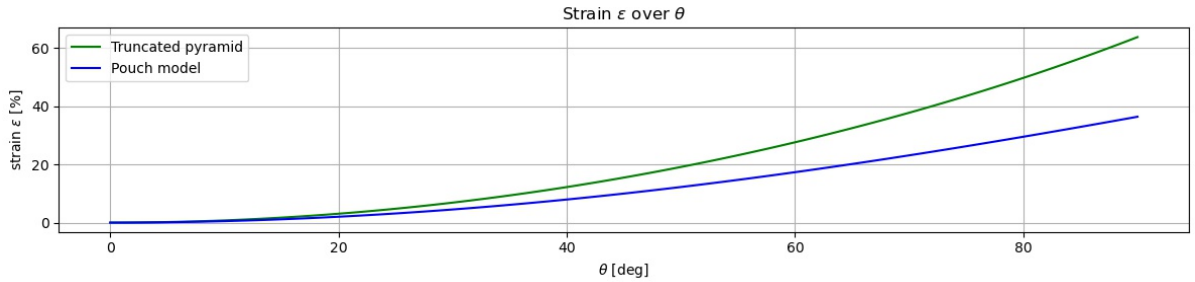

Figure 8.7: The strain ϵ is given in [%] of the initial length of the pouch L_0 along θ for the truncated pyramid model (eq. 8.6) and the pouch model. The tangential angle θ is an indicator of the inflation level of the pouch since it evolves accordingly to the quantity of air injected in the pouch.

Since the pouch model also defines pressure-to-force equations according to θ that will be used further, the inverse relations between the strain and the tangential angle are required:

$$\theta_{pyr}(\epsilon) := \epsilon_{pyr}^{-1}(\theta) \text{ and } \theta_N(\epsilon) := \epsilon_N^{-1}(\theta) \tag{8.7}$$

These relations can be numerically computed using the Newton-Raphson algorithm (figure 8.8).

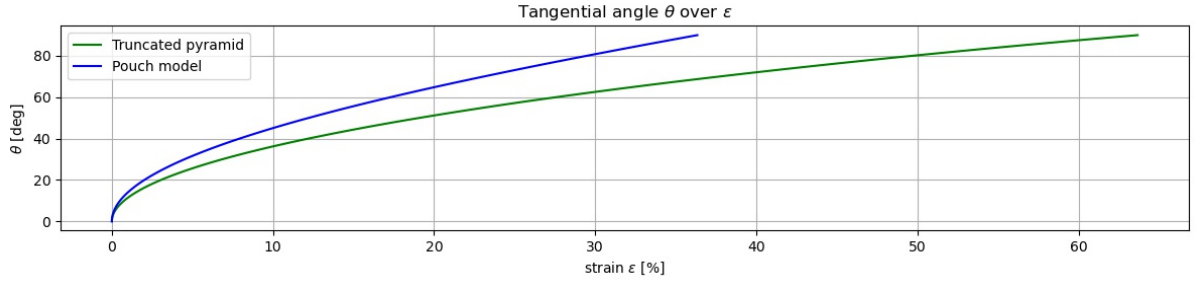

Figure 8.8: Inverse functions $\theta_{pyr}(\epsilon)$ and $\theta_N(\epsilon)$ numerically obtain from the strain models equations $\epsilon_{pyr}(\theta)$ and $\epsilon_N(\theta)$. *Pouch model* refers to the model developed by Niiyama et al..

8.1.2 Volume during inflation: Truncated pyramidal vs. Niiyama

The formula of the volume of a pouch made of two truncated pyramids for the parameters visible on figure 8.4.B is given below:

$$V^{pyr}(\theta) = \frac{2}{3} \times h(\theta) \times (L(\theta)^2 + L'(\theta)^2 + L(\theta) \times L'(\theta)) \tag{8.8}$$

In the work of Niiyama et al., the volume for a squared pouch is expressed as follow:

$$V^N(\theta) = \frac{L_0^3}{2} \times \frac{\theta - cos(\theta) \times sin(\theta)}{\theta^2} \tag{8.9}$$

Using the truncated pyramidal model equations 8.1, 8.2 and 8.6, the expression of the volume over θ (eq. 8.8) can be obtained (figure 8.9). The decrease in V^{pyr} beyond $\theta = 50°$ does not align with the actual physical constraints. The domain of validity of θ can potentially be constrained to $[0, 50°]$ or else the constraints on $h(\theta)$ or $L'(\theta)$ could be modified to address this decrease.

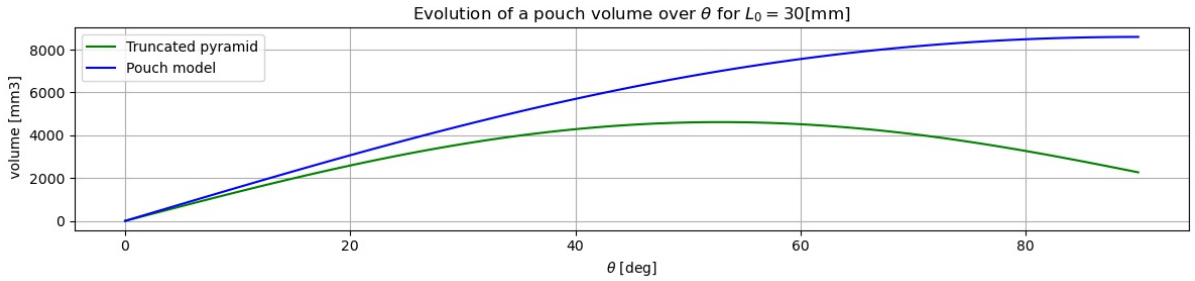

Figure 8.9: Pouch model and Truncated pyramidal estimations of a squared pouch volume along the augmentation of its tangential angle θ as defined on figure 8.4.

8.2 Pump dimensioning

In order to dimension the pump needed to perform a SCT with 3 identical pneumatic bands whose geometry is given by the figure 8.1, the volume of these bands and the rest of the pneumatic circuit must be estimated. Thanks to the two geometrical models, two estimates can be calculated.

8.2.1 Estimations of the pneumatic band volume

The volume is a function of the inflation state of the band, directly linked to the value of θ. The geometry of the band (figure 8.1) is such that the connections (elbows and intersections) are approximable using the pouch model, and the volume of the pouches can be estimated using Niiyama or the truncated pyramidal model. For further needs, the equations are developed using the Niiyama model with an angle $\theta = 45°$, while the complete relations between the estimated total volume of the band and θ are showed on figure 8.10. The value $\theta = 45°$ will be justified in section 8.2.3. By doing the hypothesis that all the sections of the tube respect the same tangential angle at the same time, all the values needed to approximate the volume V_{band} are thus known:

$$V_{band}(\theta) = V_{elbow}(\theta) + 4 \times V_{is}(\theta) + 5 \times V_{pouch}(\theta)$$

with $V_{is}(\theta)$ the volume of a intersection segment.

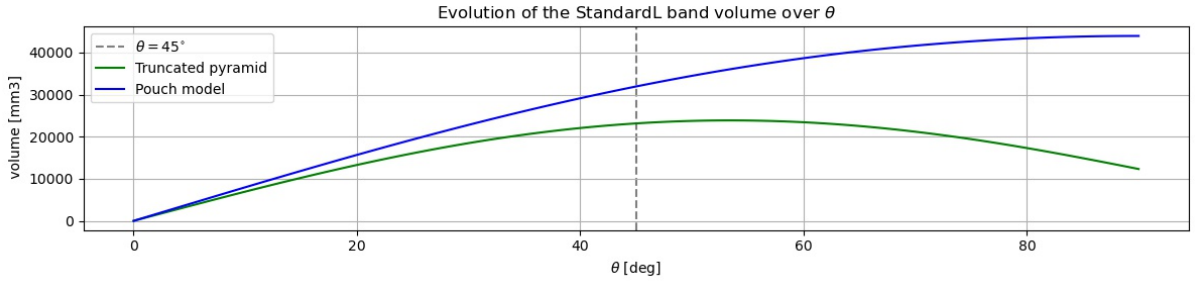

Figure 8.10: Estimation of the *StandardL* band total volume using the Niiyama's pouch geometric model for tubular sections and using both the pouch model and the truncated pyramid model to estimate the volume of the pouch along the tangential angle θ, considered the same for any section of the band.

Since the elbow and the intersection segments are almost tubular, they can correctly be estimated by the pouch model of Niiyama. Given the precises dimensions of the band given in appendix A, the elbow volume is computed. Since some parts of its profile are conical, we can adapt the Niiyama formula by integrating it:

$$\begin{aligned} V_{elbow} &\simeq V_N(L0 = 6.28, L1 = 15, \theta = 45°) \\ &\quad + \int_{6.28}^{9.28} V^N(L0 = l, L1 = \tfrac{10.50}{3.00} dl, \theta = 45°) dl \\ &\quad + \int_{6.28}^{10.00} V^N(L0 = l, L1 = \tfrac{20.00}{3.72} dl, \theta = 45°) dl \\ V_{elbow} &\simeq 597.612[\text{mm}^3] \end{aligned} \tag{8.10}$$

$$\begin{aligned} V_{is} &\simeq V^N(L0 = 6.00, L1 = 5.00, \theta = 45°) \\ V_{is} &\simeq 28.917[\text{mm}^3] \end{aligned} \tag{8.11}$$

Estimating the volume V_{pouch} from V^N or V^{pyr},

$$V^N_{pouch} \simeq V^N(L0 = 30.00, L1 = 30.00, \theta = 45°) = 6246.046[\text{mm}^3] \tag{8.12}$$

$$V^{pyr}_{pouch} \simeq V^{pyr}(L0 = 30.00, \theta = 45°) = 4490.345[\text{mm}^3] \tag{8.13}$$

Using the results from equation 8.10 to 8.13, two estimations of the volume of a band can be made:

$$V^N_{band} \simeq 31943.509[\text{mm}^3] \tag{8.14}$$

$$V^{pyr}_{band} \simeq 23165.005[\text{mm}^3] \tag{8.15}$$

Since the truncated pyramidal model volume (eq: 8.8) was not verified at the time of the pump dimensioning, the pouch model has been selected to estimate the volume of the *StandardL* band to reduce the risk of sub-dimensioning[5].

[5]The truncated pyramidal model volume approximation being much smaller than the Niiyama's model obtained volume.

8.2.2 Estimations of the pneumatic circuit volume

The total pneumatic circuit of the device is composed of three pneumatic bands discussed earlier and of 7 tubes connexions, neglecting the pump and the valves used (figure 8.11). The standard tube inner diameter used for our device is 2[mm]. In order to allow mobility between the components of the prototype, the lengths A, B_{1-3} were arbitrary set to 100[mm]. The lengths C_{1-3} where posed to 1000[mm]. These lengths will be adjusted later, but this gives us a good margin of maneuverability.

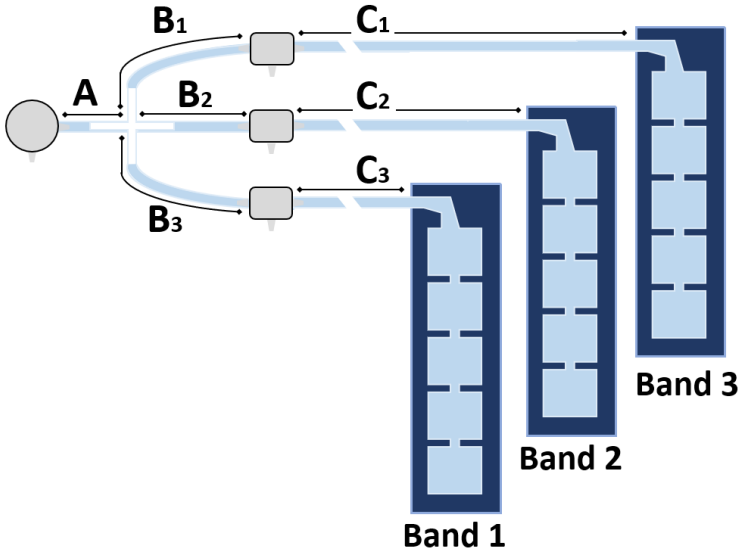

Figure 8.11: Schematic of the pneumatic design of the OS SCD updated prototype. Pump (all on the left) and the three valves are coloured in grey to allow the understanding of the pneumatic behavior of the device. A four-ways junction (white) connects the pump to all of the valves. The light-blue color indicates the presence of air. A, B_{1-3} and C_{1-3} refers to the length of their respective tube. The scale is not representative.

The total volume[6] of the pneumatic system can then easily be approximated:

$$V^N_{system} \simeq \left(A + \sum_i (B_i + C_i)\right) \times \pi \times 1^2 + 3 \times V^N_{band} \tag{8.16}$$

Using equation 8.16, the following volume is obtained:

$$V^N_{system}(\theta = 45°) \simeq 106511.943[\text{mm}^3]$$

According to that result, we observe that the tubes volume counts for 10.03% of the total volume and should not be neglected for dimensioning at first sight. Due to the functioning principle[7] of the device, the pump only compresses one band at a time, meaning that only the following volume is concerned for the contraction of the band j during impulsion $j \in [1, 2, 3]$:

$$V^N_{contraction,j} \simeq \left(A + \sum_i (B_i) + C_j\right) \times \pi \times 1^2 + V^N_{band} \tag{8.17}$$

$$V^N_{contraction,j}(\theta = 45°) \simeq 36341.739[\text{mm}^3] \qquad \forall j \in [1, 2, 3]$$

The value obtained from 8.17 will be used to dimension the pump requirements.

[6] Using the Niiyama et al. approximation.

[7] One and always one valve let the airflow pass through to a band at a time.

8.2.3 Performance requirements

The pump used for the prototype has to meet constraints defined by the context of use of the device. The SCT requires a given range of pressures applied on the leg and a given range of impulsion speed. The optimal parameters were discussed in section 6.2.2.

Desired inner pressure

The selected maximum applied pressure p_{leg} is 140[mmHg]. According to the observation of Schara et al., p_{leg} will depend on the inner pressure of the band p_{band} and of the radius r' of the leg around which it is wrapped.

$$p_{leg} = \xi \times p_{band} \text{ avec } \xi = \frac{L_0 \times \frac{cos(\theta)}{\theta}}{r'} \tag{8.18}$$

After an evaluation of the calf radius r', the approximation the desired pressure p_{band} can be determined.

Estimation of the calf radius Using the table 69 of the statistical measures of Todd and Lindala, one can define an interval of values regarding the perimeters of the human calf:

$$P_{calf}^{min} = 260.4 - 5.745 - 48.18 - 4.062 = 202.413[\text{mm}]$$
$$P_{calf}^{max} = 288.5 + 2.581 + 38.26 + 1.825 = 331.166[\text{mm}]$$

Resulting in the following interval for the calf radius:

$$r' \in [32.215 \rightarrow 52.707][\text{mm}] \tag{8.19}$$

Selected pressure requirement From the values selected for p_{leg} and r' (eq. 8.19), the relation 8.18 allows to obtain an interval for p_{band}, assuming $\theta = 46°$:

$$p_{band} \in [74.465, 284.275][\text{mmHg}]$$

Logically, the maximum value of that interval is selected for the dimensioning.

$$p_{band} = 284.275[\text{mmHg}] = 379.027[\text{mbar}]$$

Impulsion speed

The desired frequency of impulsion of the device is 4 impulses per minute. Consequently, for a 3-bands impulsion, the estimated volume $V_{contraction}^{N}$ (eq. 8.17) has to be compressed of 379.027[mbar] in 5[s]. In practice, the band length will be constrained by the calf and thus the compressed volume will not reach its maximal inflation. An arbitrary maximal value of $\theta = 45°$ is fixed for the computation of the volume during a band contraction: $V_{contraction}^{N}(\theta = 45°)$. If it is relevant to consider the worst case while dimensioning, which would mean to choose $\theta = 90°$, it is not relevant to use values that are not compatible with the prototype's physics and operating principle. Being a central value of the validity domain of the pouch model, $\theta = 45°$ seems to be a fair estimation. Moreover, we expect the pouch model to overestimate the real volume due to its geometric difference with a real pouch. The inflation process is thereafter divided in two phases: an isobaric volume

expansion and then isochoric compression. For a pneumatic band filled with dry air, the law of perfect gases applies:

$$p \times V = n \times R \times T$$

Considering the air state inside the pouch during the isobaric volume expansion phase:

$$p = p_{atm}, \quad V(\theta) \simeq V^{N}_{contraction}(\theta), \quad n_{as} = \frac{p_{atm} \times V(\theta)}{R \times T} \quad |\theta \in [0 \rightarrow 45^{\circ}]$$

Given the following constants,

$$\begin{cases} R = 8.314[\text{J/mol/K}] \\ T^{s} = 298.15[\text{K}] \end{cases}$$

For the very first volume expansion phase of the band, during which θ goes from 0° to 45°, the inner pressure of the band is constantly equal to the external pressure assumed standard at $p_{atm} = 101.325$[kPa]. In view of the above equations, this phase requires a molar input of:

$$\Delta n^{00}_{as} = \frac{p_{atm} \times V(\theta = 45^{\circ})}{R \times T^{s}} = 1.486 \times 10^{-3}[\text{mol}]$$

For any following volume expansion phase, considering the *buffering volume* (eq. 8.20) previously compressed, the Δn_{as} is slightly different:

$$V_{buf} = \left(A + \sum_{i} (B_i) \right) \times \pi \times 1^{2} = 4398.230[\text{mm}^3] \tag{8.20}$$

$$\Delta n^{0}_{as} = \Delta n^{00}_{as} - \frac{p_{band} \times V_{buf}}{R \times T^{s}} = 1.421 \times 10^{-3}[\text{mol}] \tag{8.21}$$

The volume V_{buf} could later be optimized to minimize the duration of the volume expansion phase, but one has to consider that the isochoric compression phase may last longer. For the rest of the dimensioning, Δn^{00}_{as} is neglected because a simple isochoric compression of of the volume V_{buf} before starting the SCT can increase the pressure of p_{band}.

In the second phase, where the internal pressure of the band goes from $p = p_{atm}$ to $p = p_{atm} + p_{band}$ with a constant volume (isochoric compression), and therefore $V(\theta = 46^{\circ}) \simeq 36870.081 \times 10^{-9}[\text{m}^3]$. Using the law of perfect gases and assuming that the compression is isothermic, the estimated molar input needed is:

$$\Delta n_{as} = \Delta p \times \frac{V(\theta = 45^{\circ})}{R \times T^{s}} = 0.534 \times 10^{-3}[\text{mol}] \tag{8.22}$$

Thanks to equations 8.21 and 8.22, the complete compression of a working volume as defined by equation 8.17 requires the input of a total molar number of dry air of :

$$n_{as} = \Delta n^{0}_{as} + \Delta n_{as} = 1.955 \times 10^{-3}[\text{mol}]$$

The nominal air volume sucked in $\Delta t = 5$[s] by the pump for a complete contraction of a band is then expressed:

$$V^{0\prime} + V' \simeq (\Delta n^{0}_{as} + \Delta n_{as}) \times \frac{R \times T^{s}}{p_{atm}} = 34760.698 + 13063.841[\text{mm}^3] \tag{8.23}$$

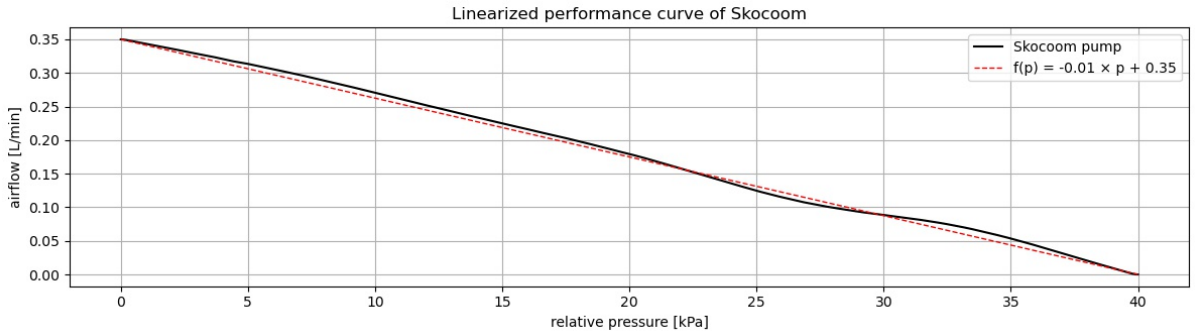

Figure 8.12: Performance curve (black) of the airflow [L/min] along with the pressure difference [kPa] of Skoocom's SC0801SPX pump, the pump used to build the first version of the OS SCD prototype. The linear approximation used for dimensioning is showed with its formula in red. The maximal error of approximation is 0.011[L/min].

For the isobaric volume expansion phase, the airflow will be constant, but not during the isochoric compression. Figure 8.12 shows that any pressure difference with the environment results in a decrease in the nominal airflow sucked by the pump.

For an isochoric and isothermic perfect gas compression from p_{atm} to $p_{atm} + p_{band}$, the nominal airflow is:

$$Q'_{pump} = m \times \Delta p + Q^{0\prime}_{pump} \tag{8.24}$$

where m[m^3/s/kPa] is the angular coefficient of the linear approximation of the performance curve of the pump.

Therefore, the equation expressing the contraction time of a band is :

$$\Delta t = \frac{V^{0\prime}}{Q^{0\prime}_{pump}} + \frac{V'}{\int_0^{p_{band}} Q'_{pump}(p)dp} \tag{8.25}$$

By injecting equations 8.23 and 8.24, the previous relation can be developed:

$$\Delta t = \frac{R \times T^s}{p_{atm}} \times \left(\frac{\Delta n^0_{as}}{Q^{0\prime}_{pump}} + \frac{\Delta n_{as}}{\int_0^{p_{band}} m \times p + Q^{0\prime}_{pump} dp} \right)$$

Using equations 8.17, 8.21, 8.22, 8.24 and the values of $m = -1.458 \times 10^{-10}$[m^3/s/kPa] and $Q^{0\prime}_{pump} = 5.833 \times 10^{-6}$[m^3/s] characterizing the *Skocoom* pump of the prototype of Schara et al. (figure 8.12), the final time spent by the pump for the contraction of a band during the SCT is:

$$\Delta t = 5.959[\text{s}] \tag{8.26}$$

With regard to the result 8.26, the *Skocoom* pump is not sufficient to perform the desired SCT of 4 impulses per minute regarding the design of the *StandardL* band and its volume approximation using the Niiyama et al. However, as discussed in section 8.1 the pouch model probably overestimates the total volume of the system due to the real geometry of the pouches of the *StandardL* band.

8.3 Selection of the components

The selection of components needs to fit the OS appropriable frame. Therefore, they were chosen to be affordable, easily available[8] and rather small. This last point makes the prototype more manipulable and could later serve to transform it in a portable equipment. All prices and references of the components are listed in appendix A The specifications for each of them is also detailed. The average price for one device was calculated to be 71.2€. This number does not include TVA and delivery.

The *ZR320* pump that was acquired according to our means respond to the performances requirements of $p_{band} = 379.027$[mbar] and 4 impulses per minute. The linear approximation of its performance curve is compared to the *Skocoom* curve on figure 8.13.

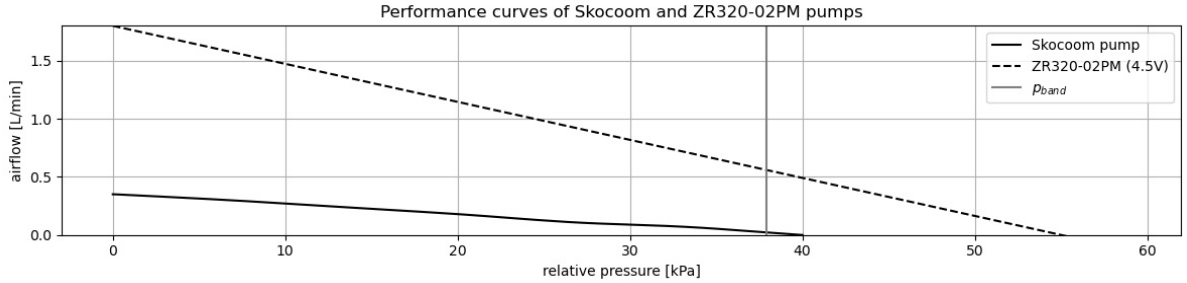

Figure 8.13: Linear approximation of the *ZR320-02PM-4.5V* performance curve compared to the *Skocoom SC8001SPX* pump performance curve.

Using equation 8.25 with the parameters of the linear approximation of the *ZR320* pump, $m = -5.455 \times 10^{-10}$[m^3/s/kPa] and $Q^{0\prime}_{pump} = 3.000 \times 10^{-5}$[m^3/s], the resulting contraction time of a band is estimated at:

$$\Delta t = 1.159[\text{s}]$$

This value is below the threshold of 5[s] per contraction, allowing to contract the band even if the θ of the isobaric phase is higher than the initial guess of 45°. Figure 8.14 describes the estimated pressure behavior of the *StandardL* band under the *ZR320* pump for different allowed volumes expansion during the isobaric phase. According to the graph, the pump should be efficient enough to apply a high enough pressure in less than 5[s] even if the band has clearance with the patient leg. The two phases decomposition can be discussed since the deformation of the band, creating a unknown dependency between the pressure and the volume according to the physical properties of the fabric, is not considered. The pump also offer new perspectives, allowing to increase the number of bands for a smoother sequential compression profile.

Next, the valves should be selected carefully. The valves need to be able to handle the maximal pressure imposed by the pump. We selected the a solenoid pneumatic valve of model Fa0520E. this three-way valve allows the air to come in from one path and go out from another one. However we realized that this valve was tested to only 300[$mmHg$], which is approximately equal to 40[kPa], whereas our pump can provide until 55[kPa]. Another valve should be selected for further fabrication or study of the prototype.

[8] All material should be orderable online by any individual, in Belgium.

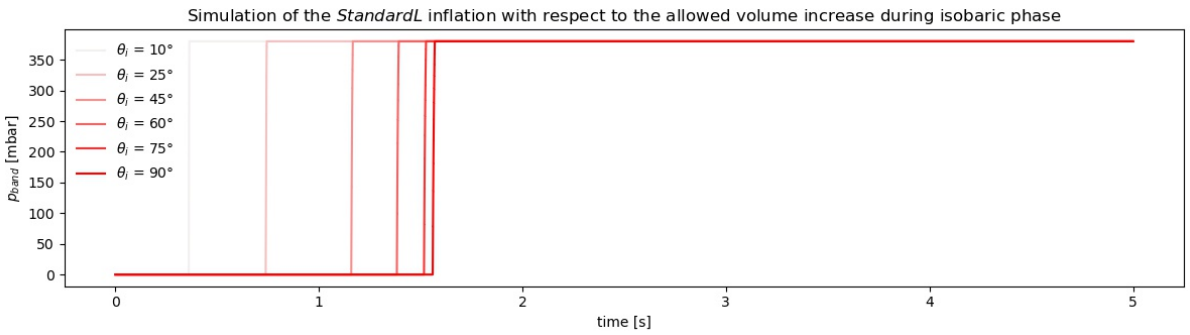

Figure 8.14: Pressure profile simulation of the *StandardL* band under the *ZR320* pump using the pouch model volume estimation for given values of θ_i. The inflation is simplified in two phases: isobaric for $\theta = 0°$ to θ_i and then isochoric.

Chapter 9

Fabrication of the device

After having selected the components needed to build the OS-SCD, the manufacturing phase begins. Updates are brought to the Schara et al. version in both the software and the hardware. The continuity of the project has to stay under the same Creative Commons CC-BY licence.

All material and resources useful to the prototype production has been made available freely, on Forge UCLouvain in the OpenMedTech group:

`https://forge.uclouvain.be/openmedtech/sequential-compression-device.git`

9.1 Components list

All the components needed to construct the prototype are listed in table 9.1. The specifications of the needed components and the references of the exact components that were chosen for this work are detailed in annex 9.1.

9.2 Electronic circuit conception

The electronic circuit schematic given in the paper we based our work on is shown in figure 9.1. This schematic contains a few errors that we modified to obtain a functioning prototype.

The updated electronic circuit used in our prototype is visible in figure 9.2. An Arduino Nano IOT33 handles the activation of the pump and the valves of the system via NPN transistors. A 4.5[V] voltage source, potentially a battery as in the original paper, supplies the valves and the pump. For each of those motorized components, a protective diode allows to protect the rest of the circuit from inductive kickbacks[1] when the motor shutdown.

The schematics on figure 9.2 presents a few differences with the original one (fig. 9.1). First of all, a few errors were corrected. On the original one, the ground and input voltage are connected at the bottom of the schematics. This must have been an error of transcription of the schematic because the circuit would not have worked if it was

[1] Inductive kickback refers to the voltage generated when an inductive load is switched off or the current through it is rapidly changed.

Table 9.1: List of the components needed for the prototype fabrication and their function. A precise referencing an description of the components is available in appendix A.

Components list	
Component	Function
Pump	Supplies the pneumatic circuit with air.
Valves	Control the flow of air in the bands.
TPU tubes	Connect the pump to the valves.
4-way valve	Splits the air flow toward the three valves.
Arduino nano IOT33	Acts as controller of the pump and the valves.
LCD screen	Displays the SCT status and parameters.
Transistors	Act as switch controlled by the Arduino on the pump and the valves.
Resistors	Allow to regulate the current to the Arduino.
Diodes	Protect the circuit components from inductive kickbacks.
Potentiometers	Allow regulation of the SCT parameters.
TPU-coated nylon	Material of the bands.
Parchement paper	Allows to create inflatable chambers in the bands.
Needles with female Luerlock	Supply the air from the tubes to the bands.
TPU tubes with male Luerlock	Connect the valves to needles.
Epoxy	Serves to seal the air entry by the needles with the band.
Hook&loop fasteners	Serve to attach the band to the leg.
Fastening loops	Serve to attach the hook&loop fasteners to the textile.

connected in this way. Another error is the direction of the diodes. The next modification is the number of knobs. We added one knob to regulate the impulse duration directly on the interface of the device rather than having to modify the Arduino code each time. Finally the last modification that was brought to the electronical circuit is the addition of a screen to allows a precise control of the user-parameters of the device.

9.3 Arduino code update

In order to manage the features added to the electronic circuit of the OS SCT, the .ino code made available has been completely revised. It is more relevant regarding the control parameters and adaptable to some potential modifications of the device, such as parameter handling addition or a difference in the number of pneumatic bands of the device. The software code is available at Appendix C.

9.3.1 Pin attribution

Each pin is wisely selected to ensure a clear understanding of the system. The pump transistor in connected to pin `D10`, at the extremity of the board but avoiding SPI communication channels (`D12` and `D11`). Pins `D10` to `D2` are destined to the transistors of the valves.

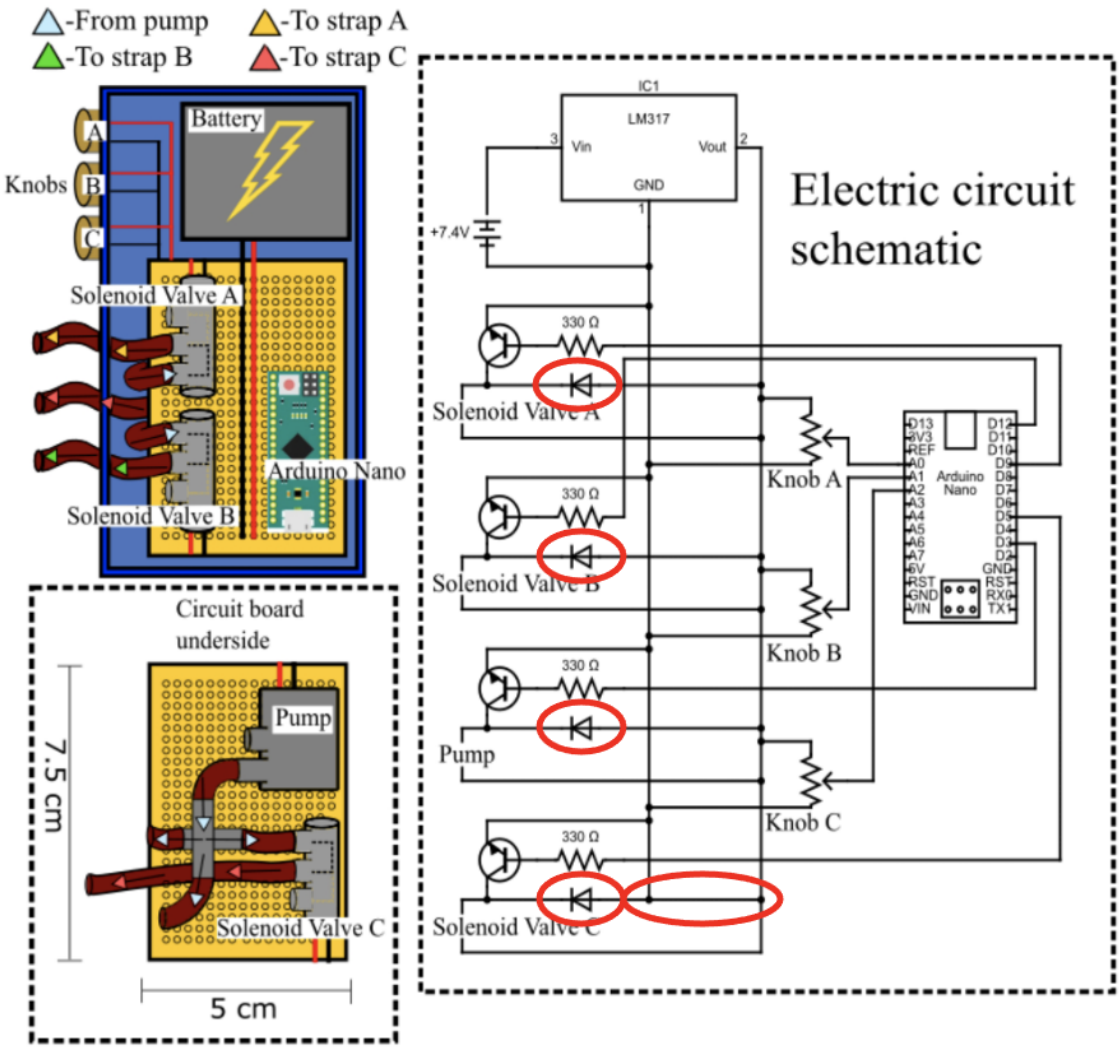

Figure 9.1: Schematic from Schara et al. of the electronic circuit used for the Sequential Compression Device prototype. The errors are indicated in red.

Pin `A0` receives the potentiometer input that drives the *impulse duration* parameter. Pins `A1` to `A7` (except `A4` and `A5`) are reserved for the analog inputs of the potentiometers that control the *duty cycle* relative to each valve of the device, allowing a maximum capacity of 5 pneumatic bands for this version of the OS SCD. A LCD screen is connected to the board using an I2C converter. Due to its specific communication protocol, pins `A4` and `A5` are reserved for these connections.

For the `D9-D4` as for the `A1-A7` pins, the chosen pins have to be indicated in the `valvesPins` and `potDCPins` arrays, respectively, in the user-zone of the code. The implementation requires to indicate them from distal to proximal regarding their respective pneumatic band.

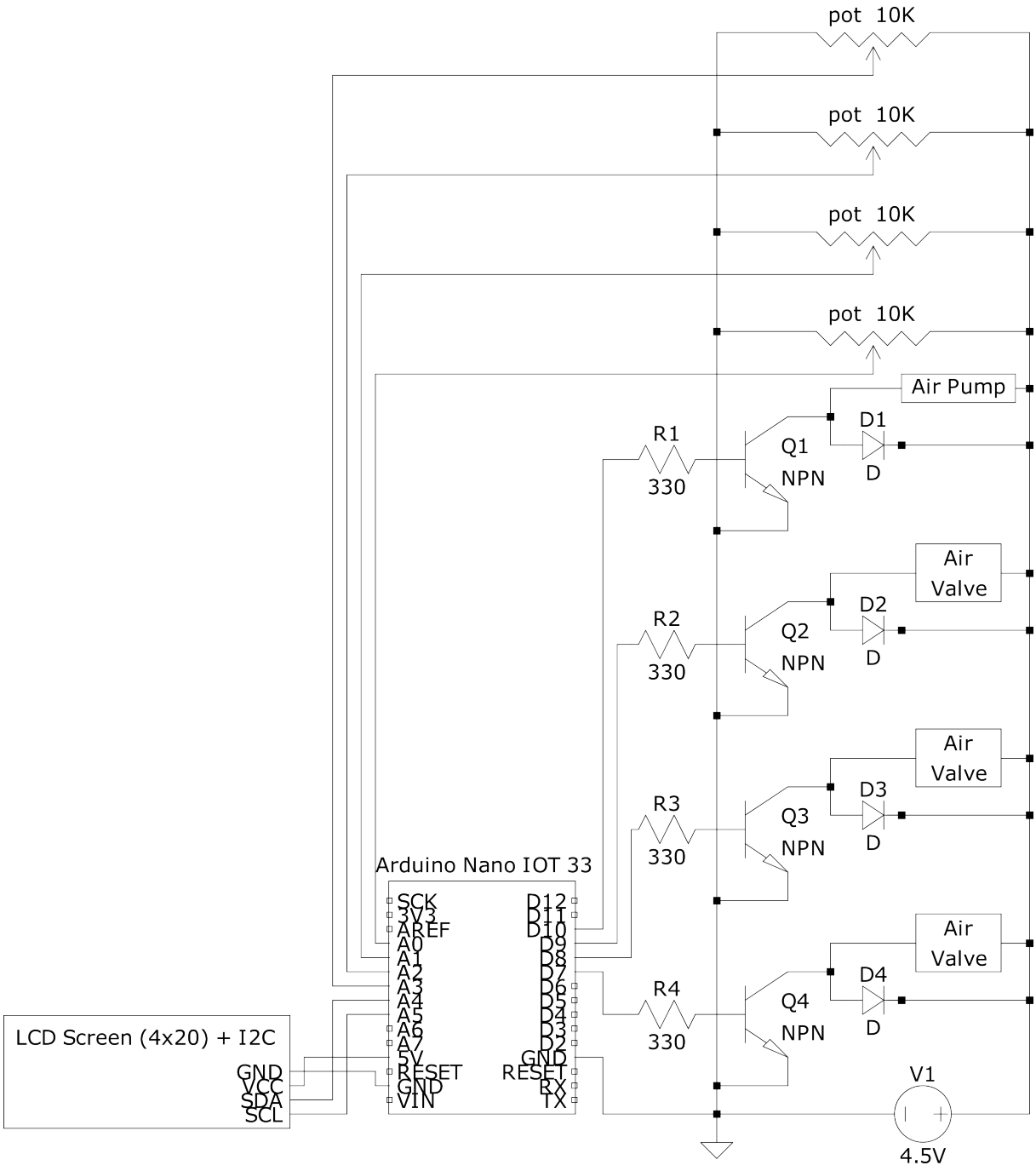

Figure 9.2: updated electronic schematic of the circuit of the OS-SCT device.

9.3.2 Therapy parameters

The technological research about SCDs (section 6.2) highlights the difference of applied pressures between the devices themselves but also the timing of the impulsion and the difference in pressure according to the position of the pneumatic band. In our opinion, the SCT parameters that deserve the most a direct user control are the *impulse duration* and the *duty cycle* relative to each valve of the device, controlling each the mean pressure of one pneumatic band. They allow to therapy to be easily adapted to the needs of each patient. The total duration from the start of the SCT is also displayed.

Concerning the hardcoded parameters, the timing of each compression can be tuned by setting a percentage of the total impulsion duration for each band (`impulse_repartition`). A waiting time at the end of each impulsion can also be set up using the `end_waiting_time` variable. Finally, the `period` variable allows to define the period on which the *duty cycles* are applied, impacting the mean pressures of the bands.

9.3.3 Main code

Manufacturing Apart from the arrays of used pins and the potential therapy parameters mentioned above, the manufacturer never needs to modify the code itself, which adapts according to the size of these arrays and parameters.

Usage Once the Arduino is turned on, its orange led blinks 3 times to indicate the launch of the code, then the user has 5 minutes[2] to set up the $1+n_{bands}$ manual parameters using the potentiometers and the LCD screen (left on figure 9.3). A timer indicates the remaining time at the bottom of the screen to avoid any misuse.

After the 5 minutes, the SCT protocol starts running. As visible on the right of figure 9.3, the parameters selected during the settings phase stays displayed on the screen, they are no more changeable. The title of the screen change to *SCT RUNNING* and a new timer at the bottom of the screen indicates the amount of time of performed SCT expressed in minutes (from 0 to 999).

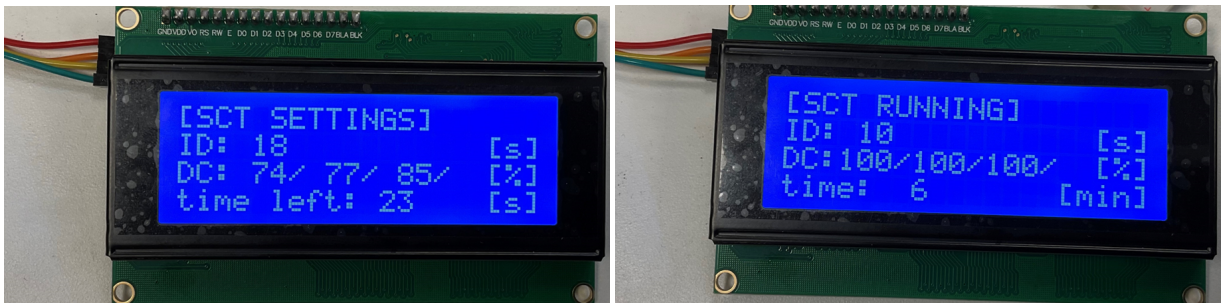

Figure 9.3: Left: Picture of the OS-SCD screen in setting mode. *ID* refers to the *impulse duration* parameter, and *DC* refers to the differents *duty-cycles* set for their respective band. *Time left* display the remaining time of the setting phase. **Right:** Picture of the OS SCD screen in running mode. *ID* refers to the *impulse duration* parameter, and *DC* refers to the differents *duty-cycles* set for their respective band. *Time* display the time elapsed since the start of the SCT after the setting phase.

Implementation The SCT protocol of the OS SCD is by definition a loop of *impulses*. For each impulse, the pneumatic bands are iterated from distal to proximal via their respective transistor. When a pneumatic band is considered during iteration, a *sequence* is initiated. That sequence defines the *open-closed* profile of the valve of the considered band according to the desired duty-cycle parameters and compression duration. The use of time-flags and conversion factors is the only remains of the initial code of Schara et al..

[2]This duration has to be adapted to the ease of use of the potentiometers.

9.4 Pneumatic bands conception

9.4.1 Original idea

The original idea of the work of Schara et al. to build the three compression bands consisted in three steps detailed below:

1. Cut two complementary layers of a specific pattern that will be heat-sealed together.
2. Cut an intermediate layer that will be placed between the two heat-sealable layers and prevent them to melt at some places.
3. The sealing process.

A schematic of Schara et al,. can be observed on figure 9.4 for better understanding.

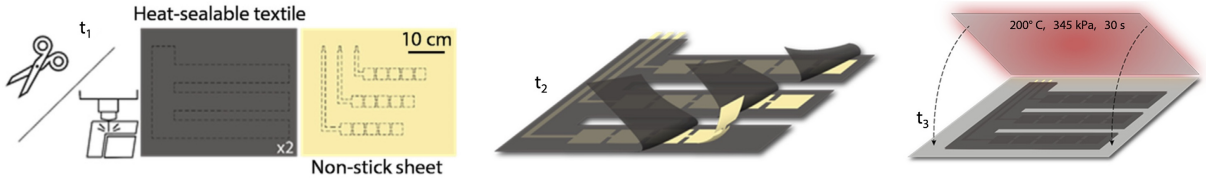

Figure 9.4: The three first steps of the pneumatic bands conception from Schara et al.. The denomination t_1, t_2 and t_3 designs the order of the operations.

The idea to put a non-stick middle layer to only merge the part of the heat-sealable textile where it is needed is efficient. However, one can encounter non-negligible challenges during the conception of this prototype.

Complexity of the design The precise design (figure 9.5) of Schara et al. is relatively complex. The three bands intermediate layers are different and the pneumatic bands are tied together in essence, which highly complicate the fusion process: Firstly, the materials used are very light and are then subject to perturbations due to the ventilation and the air-cooling systems of laser-cutters and heat-presses. With a big and intricate design, the perturbations create wrong cuts. Secondly, this lightness and shape also complicates the precise superposition needed for the layers before entering the heat-press. Human-hand manipulations also create perturbations and result in a non-proper geometry of the pouches. Finally, their design completely attached the hook and loop fasteners on the band. This creates longer bands and demands an area of $520 \times 263[\text{mm}^2]$ for the heat-pressing. Like the one of the *Makilab*[3], all heat-presses do not offer such an area, and sealing the pneumatic bands in multiple heating session is not a good option if one wants an efficient and reliable fabrication process.

Variability of the materials properties The materials used are cooking paper for the intermediate non-sticky layer and one-sided TPU-coated nylon fabric for the heat-sealable layers. For the parchment paper, one has to test the non-stickiness of the paper pressed against melted TPU. For textile, heating temperature should be tested in order to avoid the TPU to pass through the nylon mesh. The melting temperature of TPU is between

[3]The *Makilab* is the fablab of UCLouvain that hosted our pneumatic circuit fabrication work.

Figure 9.5: The design of the heat-sealable and intermediate layer used for the pneumatic bands conception by Schara et al.. Notches external to the bands main bodies are added in order to facilitate their alignement during the fusion process. Overflowing heat-sealable layer is intended for further fixation system on the leg.

170[°C] and 235[°C] [142]. Depending on the textile acquired, the best melting temperature and duration have to be evaluated experimentally to ensure the best impermeability and resistance to the inner-air conditions, leading to numerous trial-errors.

9.4.2 Updates towards a more reliable and simple design

By keeping the same process idea as Schara et al. for the pneumatic bands fabrication, the design can be modified to answer some of the cited challenges.

Schara et al. connected the bands together in order to maintain their relative position on the leg. However, regarding the complexity of the design observable on figure 9.6, there is no obligation for the three bands to be attached together from the beginning of the fabrication process. It is the same with regard to the additional length at the extremities of the bands that is intended to the further fixation of the band on the leg.

Another observation is that the pneumatic part following each elbow could simply be replaced with a medical tube[4] that does not need to be hand-manufactured. The elbows are conserved but were to updated with smoother angles[5].

Considering these observations, the design has been improved towards a more reliable and simple design (figure 9.6). This design is *economic*, with almost zero loss of fabric during the process, and easily *reproducible* thanks to its simpler geometry. The *surface of*

[4] Medical tubes are also needed for other parts of the pneumatic circuit, so it does not increase the number of needed components of the OS prototype.

[5] This version has smoothed the elbow angle and act like a funnel to reduce air turbulence. Perspectives of an improvement of this design to minimize dissipations can be seen here.

textile needed, considering any loss, is *reduced* by 58[%] for our *StandardL* band. Moreover, the *work plan* used for the bands conception[6] is also *reduced* by to about 86[%] for three bands. Additional spaces at the band extremities have been designed to allow the fixation of a scratch band in further steps. That design also allows to *control the spacing* between the compression bands while placed on a patient, which was not the case with the previous design.

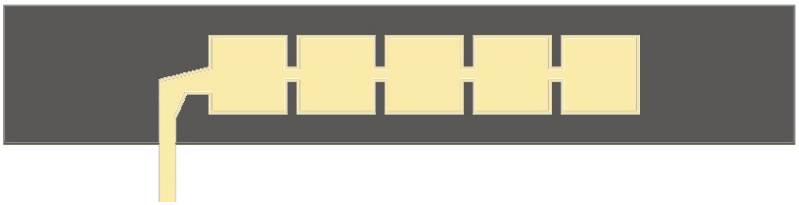

Figure 9.6: Render of the updated version of the design for an equivalent set of pneumatic bands.

9.4.3 Modification of the fabrication process

The update of the design answers the complexity challenge of the design of Schara et al. As seen on figure 9.7, a soldering iron pre-heating of the extremities and the use of a heat-resistant support plate to manipulate the layering improve the quality of the result.

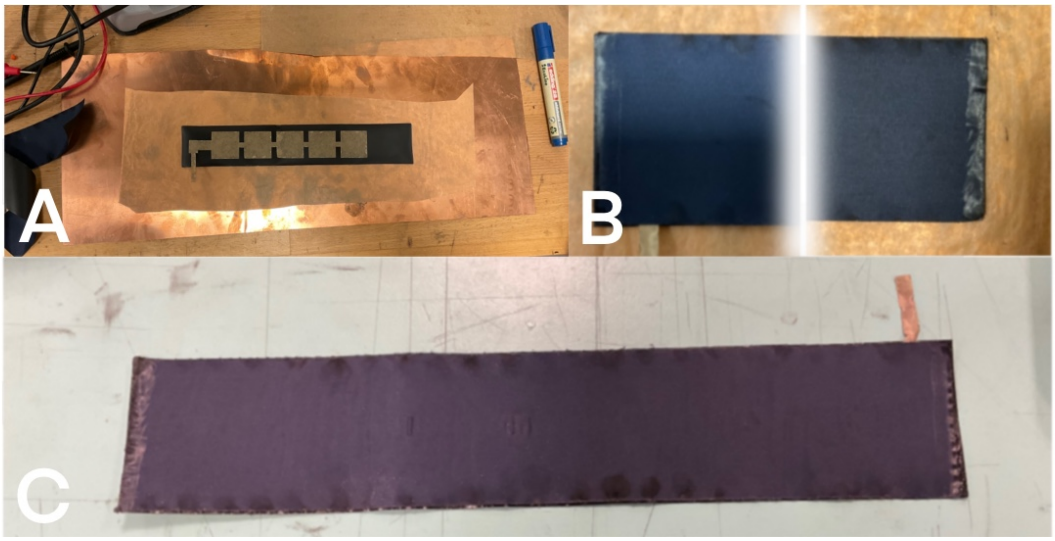

Figure 9.7: Before (A and B) and after the fusion process (C). One can observe that the heat-sealable layers alignment is correct, but there is no garanty on the intermediate layer position.

9.4.4 Automation of the design process

In order to test the performances and the reliability of the prototype regarding its settings, its geometry and its fabrication process, a high amount of designs is needed. To avoid time loss, a python script has been coded and takes as input the parameters visible on figure 9.8. In the OS spirit, this modularity is a powerful tool to anyone that would bring the project further.

[6] This is an advantage for the size of the heat-press required.

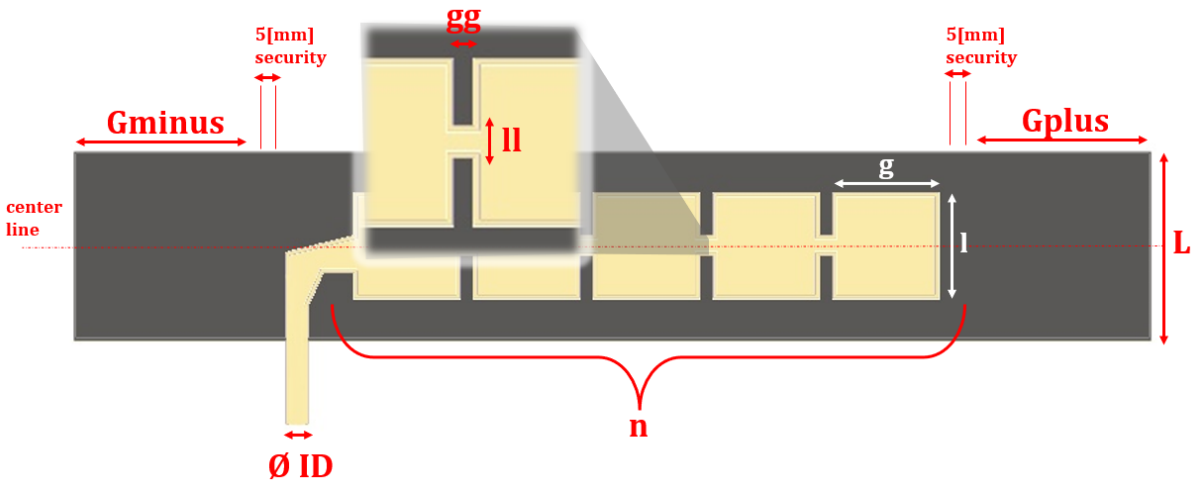

Figure 9.8: Schematic of the parameters used to design a pneumatic band. ID is the input inner-diameter of the band; n is the number of pouches; l and g are the 2D-dimensions of a single pouch; L is the width of the pneumatic band; G^+ and G^- are the additional lengths at the extremities; ll and gg are the 2D-dimensions of the interconnections between each pouch.

As output, the script returns a folder containing the following files (appendix B):

- a .svg file containing the desired design of the intermediate layer, ready to be set in the laser-cutter;
- a .svg file containing the desired design of the two heat-sealable layers, ready to be set in the laser-cutter;
- a .svg file containing a render of the desired design, to prevent any errors;
- a .txt file containing all the specifications relative to that design and additional information for the maker.

To keep all these bands well organised, an identification system has been implemented directly into the script, linking each file to the others using an automatic identification number (Appendix B). The fabricated band is tagged with that number so that its specifications are never lost (figure 9.9).

[n - ID - l - g - L - ll - gg - Gplus - Gminus]_tag

Figure 9.9: Design of the identification number attributed to a band according to its specifications as defined on figure 9.8. The tag, for example *StandardL*, is the surname attributed to the band for easy identification during discussions.

9.5 Risk management during conception

During conception, processes and implementation of a number of features were added to reduce potential risks, both during manufacture and usage of the device.

Fabrication process for minimization of poor manufacturing The iterative process to choose the optimal parameters of sealing allows to minimize the damage of the textile. It was chosen in order to have efficient sealing but no melting of the nylon and thus possible breakage. The testing methods for the sealing is further explained in the next chapter (10). In addition, the larger bands than the ones of Schara et al. permit to reduce the consequences of wrong stacking of the layers. If layers are a little shifted the risk that the chamber part is not included in both layers of textile is reduced and the impact of a small shift is mitigated. The pre-heating with the soldering iron as well as the support plate also facilitate the stacking and reduce shifts of the layers until the heat press. Finally, the simplified design reduces risks of poor manufacturing in general.

Starting indicator To ensure that the SCT protocol is starting, a flashing led was added to indicate the start of the device, reducing the risk on starting misuse.

Device comprehension To minimize the risk of misuse, the device is operated via a unique screen, where the two phases of the device (*settings* and *running*) are well distinct and defined by a clear denomination at the top of the LCD screen.

Settings indicator To avoid the risk of incorrect therapy, a precise control of the parameters is allowed, with a settings screen to visualize the actual values of these parameters during the manipulation of the knobs. The units of the parameters are given. Moreover, to avoid any misuse of the settings system due to haste, a sufficiently long timer indicating the remaining time before the start of the therapy is implemented.

Status indicator To minimize the risk of incorrect therapy, a LCD screen indicates the current parameters for the SCT in progress. This screen also validate the well-functioning of the SCT script, since a timer is updated after every impulse. That timer allows to assess the total duration of the SCT since the start of the device.

Locking parameters The risk of modifying the user-parameters (impacting pressures and impulse duration) during the usage of the device is set to zero thanks to a locking of the potentiometers after the setting phase via the Arduino script.

Part IV

Study

The previous chapters have presented the principle and the construction of the prototype. This part will describe the study of the performances of pneumatic bands. The assessment of the model, its performances and the future prospects are presented here. The first chapter details the material and methods for the study of the device. It will present all the parameters that were assessed and how. This includes the variables for the validation of the model and some qualitative evaluation. The following chapter relates to the results and discussion of this study. The last chapter will presents the future prospects for research. All things that have not been studied for this thesis but that would help with the characterization or improvement of the prototype are listed in that chapter.

Chapter 10

Material and methods

The methods for the study of the prototype are explained in this chapter, results will be addressed in the next chapter. Testing was conducted around two main directions. At first a qualitative evaluation of tightness. Then the study of the prototype's performances. This second part served to compare the resulting measurements with the geometrical and force-pressures models.

10.1 Qualitative evaluation of the tightness

Qualitative evaluation can give insights on specific aspects even though it is less precise than quantitative evaluation. Here it was used to investigate the air tightness of the bands, and the effect of different parameters on it. It was the first thing that was tested, before the validation of the model and characterization of the prototype.

To evaluate the air tightness, a leak detector spray was used. It makes a thin deposit of soap and bubbles appear where any leakages exist. We wanted to investigate the effect of different parameters on the tightness.

10.1.1 Effect of sealing protocol

The effect of the sealing temperature and duration was tested. To evaluate the sealing protocol, we created a model of individual pouches. The pouches had the format of squares of 30[mm] side for the chamber and 5[mm] of borders. Those pouches were heat-pressed at different temperatures and for different durations. The heat-press of the fabrication laboratory we had access to did not specify information about its pressure. We used four different protocols :

- 170[°C] for 45[s]
- 200[°C] for 45[s]
- 200[°C] for 60[s]
- 230[°C] for 15[s]

Then the leak detector was sprayed on the pouches that seemed viable after heat-pressing. The pouches were covered in leak detector and observed with attention to detect all possible bubbles.

10.1.2 Effect of borders and intersection dimensions

To identify the impact of size of the borders and intersections we created bands with different characteristics to compare the leaks on them. The dimensions of the bands could easily be adapted with the python script for design automation described in chapter 9. We created five different types of bands for this test :

- A band similar to the *StandardL* but with borders all around the chambers of 5mm and not 15mm. This band will be called *StandardS* during the rest of the manuscript.
- A bands with the standards dimensions.
- A band similar to the standard one but the intersections between pouches were 8mm large.
- A band similar to the standard one but the intersections between pouches were 2mm long.
- A band similar to the standard one but the intersections between pouches were 15mm long.

Then we sprayed the leaks detector on all of them and observed with attention if any leaks were visible.

10.1.3 Effect of fatigue

The evaluate the effect of fatigue on the air tightness of the bands, two bands underwent a fatigue protocol[1]. The two bands had for difference the length of the intersection canal between pouches. One band had an intersection of 5[mm] which is the standard dimension, the other one had was 3[mm] long. Two bands with the same characteristics were kept never-inflated before the sealing test to compare the effect of fatigue on the air leakage.

10.2 Quantitative evaluation

The quantitative study of the device has as main goal the validation of the model. This includes the characterization of the device parameters and components as well as its behaviour. The first relation that was to assessed is the one between θ, the independent variable of the linear pouch motor model, and the strain ϵ. As a reminder, θ is the tangential angle of the pouch curved surface with the middle line (figure 8.4.A), and is a state variable of the geometry of the pouch. Following the geometric models, θ impacts the band volume. This is the second parameter that was measured. The last test conducted for the quantitative evaluation served for the characterization of the relation *pressure-force-elongation* of the prototype's bands. This longitudinal analysis aimed to assess the performances of the device and to compare them to the expected results of the pouch model.

[1] The bands were inflated and deflated at high frequency for a long period of time. During one hour two bands underwent inflation during 3 seconds and deflation during 5 seconds. This protocol was configured with the same code that is used for SCT, by adjusting parameters.

10.2.1 Relation between the strain ϵ and θ

For different input pressures[2], the tangential angle was measured after an unconstrained contraction of the *StandardL* band. To assess θ, we used photography and a tracking software called *Tracker*. The input pressure is indicated using a post-it. A ruler positioned above the band serve as length reference on the image. The inflated pouch was captured using an Iphone 13 lens. The relevant information is the 2D projection of the pouch profile and it is supposed not to be distorted by the camera lens. To ensure the correct positioning of the camera regarding the pouch, we ensured that the back side of the pouch joint was at the same level as the front side on the image and that the iPhone lens was parallel to the long side of the band, thanks to a table and the structure of the iPhone (figure 10.1).

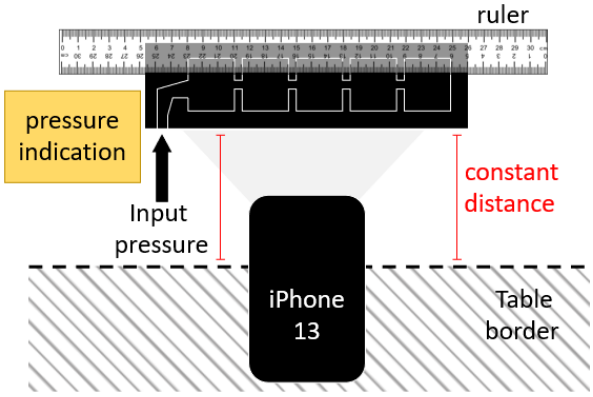

Figure 10.1: Schematics of the method used to obtain the pictures of the band under inflation. Additional tape was used after inflation to align the band with the setup.

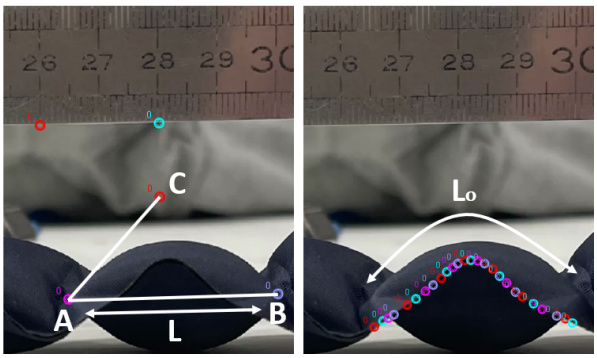

Figure 10.2: Tracking method used to asses the retraction ϵ and the tangential angle θ of the pouches of the *StandardL* band for different pressures inputs. **Left:** A reference length of 2[cm] is defined on the ladder. Three points (A, B and C) are placed and used to evaluate the retracted length L and the tangential angle $\theta = B\hat{A}C$. **Right:** The profile of the deformation of the joint is assessed to get the initial length of the pouch L_0.

Once the images are acquired, *Tracker* is used to assess the pixel lengths of the pouch before and after contraction (figure 10.2, left and right). The initial length is extracted from the length of the joint of the pouch. The angle θ and the strain ϵ are then computed from the pixel coordinates using a python script:

$$\theta = \arccos\left(\frac{\vec{AB}\cdot\vec{AC}}{\|\vec{AB}\|\cdot\|\vec{AC}\|}\right) \text{ and } \epsilon = 1 - \frac{L^{px}}{L_0^{px}}$$

10.2.2 Volume

In order to review the relation between the volume and θ according to the geometrical models of the *StandardL* band, the relation between the strain ϵ of a pouch and the volume

[2] 100, 250, 350, 400 and 450 [mbar].

of the band was experimentally verified. To do so, bands where filled with water with a syringe of 100[mL] capacity. Water was added progressively until reaching a high pressure in the pouches, the water could not be inserted anymore. The band was hold vertically and the plunger was released to let the pressure decrease inside the band, to the atmospheric pressure. The bands were weighted before the swelling with a clamp in a recipient. Then after filling them with water. The difference in weight corresponds then the the quantity of water inserted and thus the volume available in the band. These mass measurements have been made with a precision of 1[mg]. When the band was filled at maximum capacity, we clamped the entry of the band and detached the syringe, and weighted the band. Then we measured θ of the band filled with water, to later compare the volume expected by the model for this angle and the measured volume.

10.2.3 Longitudinal analysis

To characterize the behaviour of bands, we conducted a longitudinal analysis. The goal was to obtain states of the inner pouch pressures, the retraction force and the retraction length. The testing protocol was repeated on two bands of standard dimensions with the same characteristics, set apart that one had been fatigued. To do so, we imposed pressure levels while attaching loads to the hanging band and measured the retraction.

As visible on figure 10.4, a band was attached to a piece of rigid wood fixed using clamps to a table. We used a whole punch and twine then made knots to create the attaches in the band. Three equidistant holes were pierced on either extremities of the bands to distribute the force on multiple points instead of one and reducing stress and potential tear. The twine on one side served to attach the band to the wood piece so that the strap hung vertically, on the other side the twine was used to attach loads to the band.

Retraction force In order to quantify the retraction force developed at different input pressures, a weight was attached to the band when deflated and placed on a scale. The load was attached with the twine at a height that allowed that almost[3] no weight was lifted by the band when it was deflated (it could be checked with the scale) but the twine was on the verge of taking tension whenever the band would retract. The cords had to be just tensed enough so that even the slightest retraction would decrease the mass displayed on the scale and the force yielded could be calculated. The scale had a precision of 0.1[g]. We used loads of 10[g], 20[g], 50[g], 78.5[g], 100[g], 200[g], 500[g], 1[kg], 2[kg]. Measures with no load attached were also taken.

Pouch pressure The pouch pressure was imposed during the testing. A pressure reducer was connected to an air output of 8[bar]. The reducer had a button that allowed to control the output pressure from 0 to 0.6[bar]. The circuit was connected to a manometer at the output of the reducer to measure pressure. A pressure sensor, that converts the air pressure into a current signal bounded between 4 and 20[mA], was also connected to the pneumatic circuit. It provided a more precise measure of the pressure in the band. The sensor was chosen with a range from 0 to 500[$mbar$], since the treatment should reach maximum 400[$mbar$]. For each weights we imposed pressures from 0 to 450[$mbar$]. We fixed a load, or none, and increased the pressure gradually by 50[$mbar$] steps.

[3] Maximum 3.75[%] of the mass in the worst case, for the 80[g] load.

Retraction length To measure the retraction of the band we used photography and the tracking software *Tracker*. An iPad Pro camera was placed at the level of the band, at about 1.5[m] of the setup. Markers were drawn using chalk at each pouch intersection on the bands to facilitate the identification of the important tracking points. A ruler of 1 meter long was placed on the side of the band, at the same distance to the camera, to keep a length reference on the picture. The band was placed in front of a white background that contrasts, see figure 10.4. For each weight and pressure level, when the weight measurement stabilized, a picture of the hanging band was taken. After the testing process, for each specific load, the related pictures has been assembled into short films of 9 images, in order to import them into *Tracker*. As visible on figure 10.3, the heat-points were hand-tracked, and the pixel distances where converted in [mm] using the ruler as reference or in [%] regarding the first state (input pressure of 0[bar]). Finally, a python script takes the exported coordinates as input to convert them in a list of coordinate tuples easier to process.

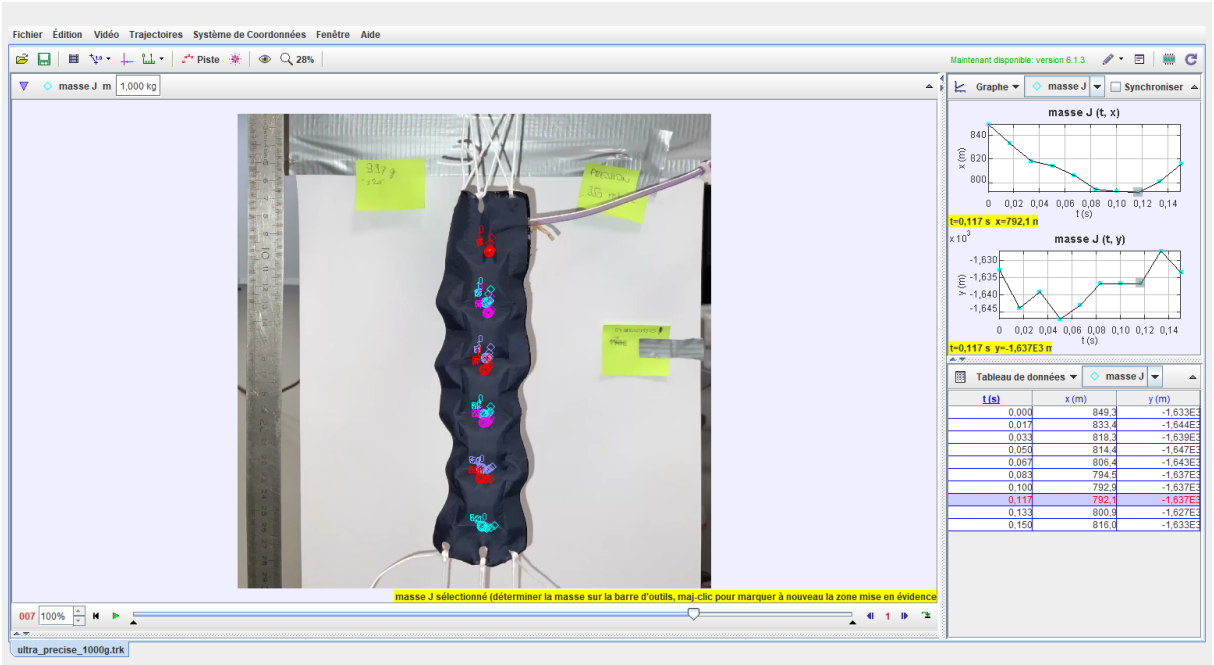

Figure 10.3: Strain tracking method using the software *Tracker*. The tracked points define the pouches longitudinal length, taking care to consider pouch intersections for further analysis.

To simplify the treatment of the data, pieces of paper with indications about the current state were placed on the frame before taking each picture. One paper indicated the pressure of the pouches, one indicated the weight lifted by the band and a last one had the reference of the band that was tested, as seen of figure 10.4. All the pressure and mass data were manually imported from the pictures to a python script to be analysed with the *Tracker* length outputs.

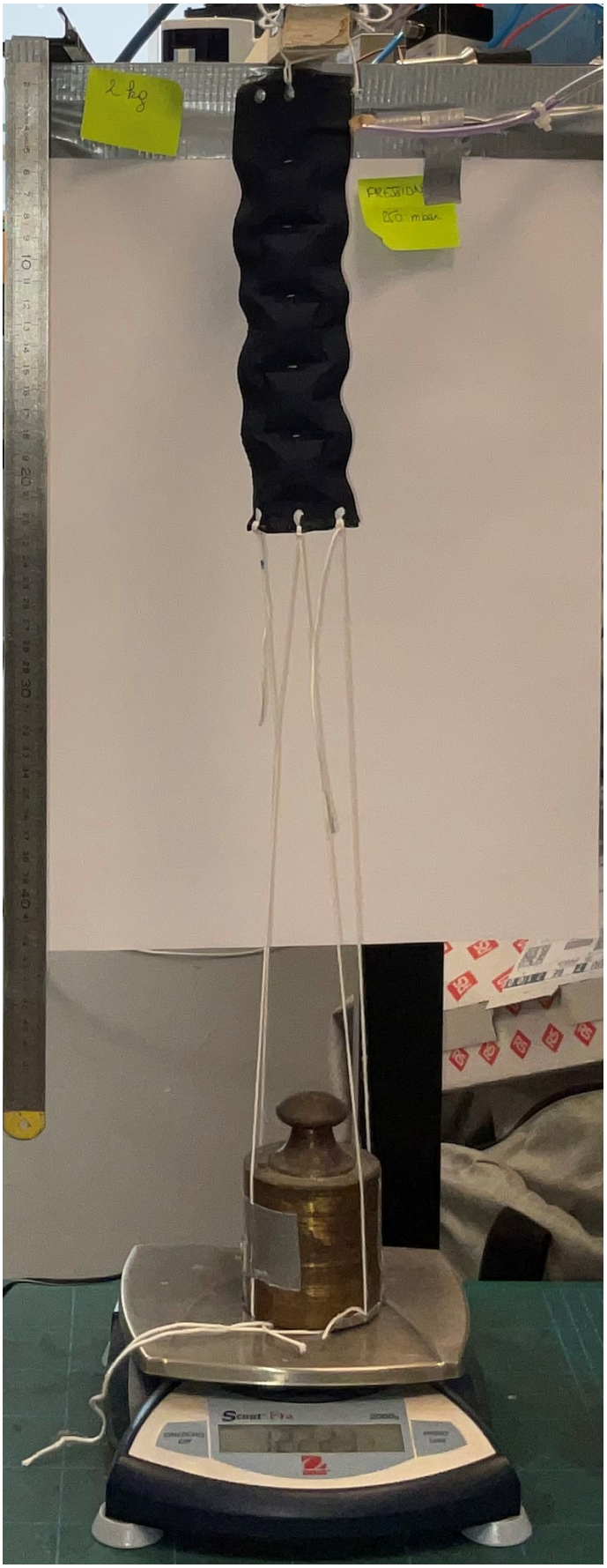

Figure 10.4: Picture of the experimental set-up for the longitudinal analysis.

Chapter 11

Results and discussion

11.1 Evaluation of air tightness

11.1.1 Effect of sealing protocol

Observations of the leaks on the three individual pouches fabricated with different sealing protocols revealed the following results. The pouch pressed at 170[°C] for 45[s] showed two small leak on the side sealing, see figure 11.1. The pouch heat-pressed at 200[°C] for 45[s] shown showed one small leak on the side sealing, as visible on figure 11.2. For the sealing at 230[°C] for 15[s], two small leaks appeared on the side sealing. The leaks were located in the folds that form during swelling. However, on this last pouch we observed that the layers of fabric were badly superposed. This provoked a thinner joint on the side of the air chamber and may cause more leakage.

Figure 11.1: Leak detector bubbles on both sides of a pouch sealed at 170°C for 45s.

The tests at 200[°C] for 60[s] did not produce usable pouches. The TPU-coated textile melted too much, was damaged and brittle when cooled, see figure 11.4. It could not create an air chamber. We did not test the pouch with the leak detector and excluded these sealing parameters.

The process of sealing the layers at 200[°C] for 45[s] was selected based on our observations. The pouch created at 230[°C] had poorer results but this was probably related to the bad overlapping of the layers. However heat-pressing for only 15[s] is not practical: it is too short and a delay rapidly has a bigger impact since it represents a high proportion of sealing time. After this test we decided to create bands with larger borders for the next

tests to try to minimize leakage on the sides of the pouches and see the impact. Originally the bands were designed with borders of 5[mm] (*StandardS*) and we created one with 15[mm] of side borders (*StandardL* band). A larger border minimizes the consequences of a shift between layer and so minimize the presence of side leaks.

Figure 11.2: Leak detector bubbles on a pouch sealed at 200°C for 45s.

Figure 11.3: Leak detector bubbles on a pouch sealed at 230°C for 15s.

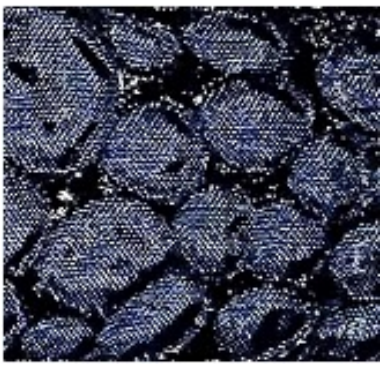

Figure 11.4: TPU sealed at 230°C for 45s.

11.1.2 Effect of borders and intersections dimensions

The results of the spray on the *StandardS* band showed leaks on the sides of the band. On the *StandardL* band, that observation disappeared. The bigger borders effectively prevent the side leaks. On both bands we observed similar bubbles in the intersections between pouches. No difference of leaks appeared with the bands that had intersection lengths of 2[mm] and 15[*mm*] and the *StandardL*. Same conclusion for the band with intersections of 8[mm]. The larger border prevented side leaks, but may have provoked more loss from the intersection leaks. However this was not visible.

11.1.3 Effect of fatigue

No difference was observed between the fatigued and not-fatigued bands. Both showed minor leaks on the folds at the intersections between pouches. The bands present thus leaks even at their first inflation. These leaks were so small that the band pressure should not be affected during SCT, considering the air flow that the pump provides. However

this observations remain qualitative and should be studied in a quantitative way to be confirmed.

11.2 Relation between the strain ϵ and θ

For different input pressures, the relation between the strain of a inflated pouch and its tangential angle was measured for the *StandardL* band. Figure 11.5 compares these measurements to the pouch model and to the truncated pyramidal model. The truncated pyramidal model is closer to the measurements that the pouch model. However, the reader can observe that the profile of ϵ_{pyr} (eq. 8.6) still underestimates the strain of the pouch for low angles. This underestimation for lower pressures may come from the presence of the intersections that could bias the measurements of the tangential angle. Further analysis could use only a simple pouch to obtain potentially better data.

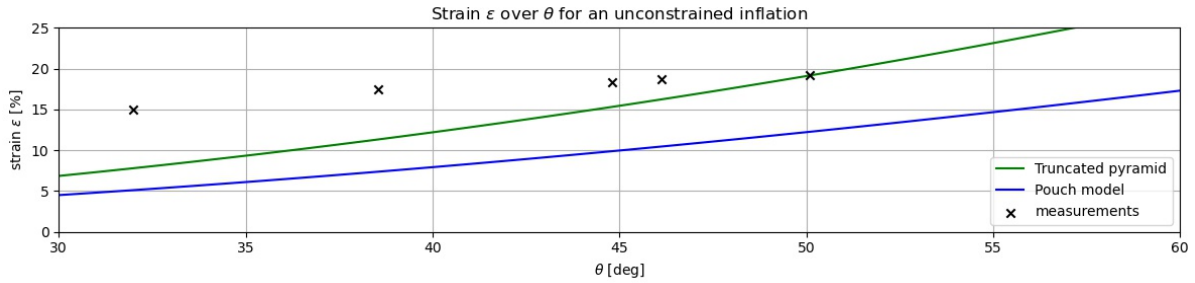

Figure 11.5: Mean measurements of the *StandardL* band pouches strains under known pressures compared to the pouch model and truncated pyramid model strain estimation for $\theta = \theta_{max}$. For each inflation state, four measurements were made. The standard deviations on ϵ and θ are respectively 2.37[%] and 0.14°.

The advantage of the truncated pyramid model is that the constraint on the inflation height $h(\theta)$ (eq. 8.2) could be modified after experimentation, and is not intrinsic, such as the pouch model.

Since the measured values are assessed for known pressures, they characterise the mechanical properties of the TPU-textile used. Figure 11.6 defines the linear approximation that relates the the tangential angle of the pouches of the band with the input pressures for an unconstrained contraction.

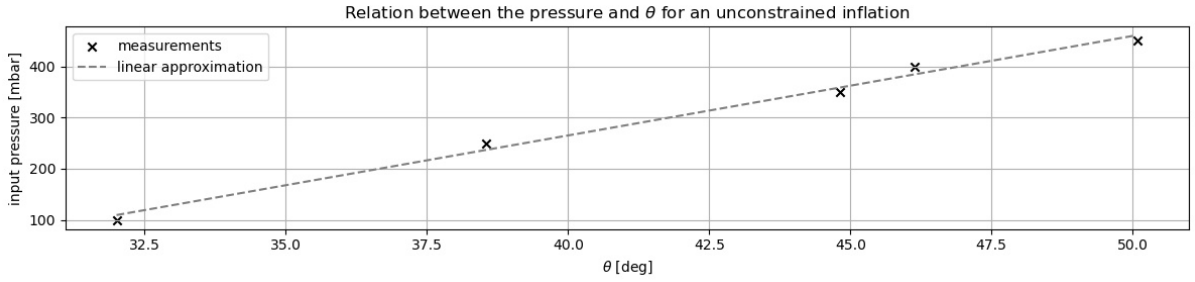

Figure 11.6: Mean measurements of the tangential angle θ for fixed input pressures after an unconstrained retraction of the *StandardL* band. The linear approximation is given (eq. 11.1).

That linear approximation is expressed as follow:

$$\hat{p}_{band}(\theta) = 19.5 \times \theta - 512 \mid \text{with } \theta \text{ expressed in degrees.} \tag{11.1}$$

Despite this characterization, the results raise the question of a new variable to characterize the state of inflation of a pouch and other constraints. The advantage of the truncated pyramidal model with θ as state variable is that it could stay compatible with the pouch model of Niiyama et al., allowing to use the force-to-pressure relation built on θ. Otherwise, other geometric variables such as the height of inflation h could be used in future models, in order to be easily measurable for the given pouch motor application.

11.3 Volume

Based on the three repeated measurements, the mean volume of the *StandartL* pneumatic band was determined to be 20706.666[mm^3] with a standard deviation of 1086.442[mm^3]. Regarding figure 11.7, where the models are used to approximate the total volume of a *StandardL* band, the measurements appear to invalidate both the Niiyama et al. model and the truncated pyramid model developed in section 8.1.

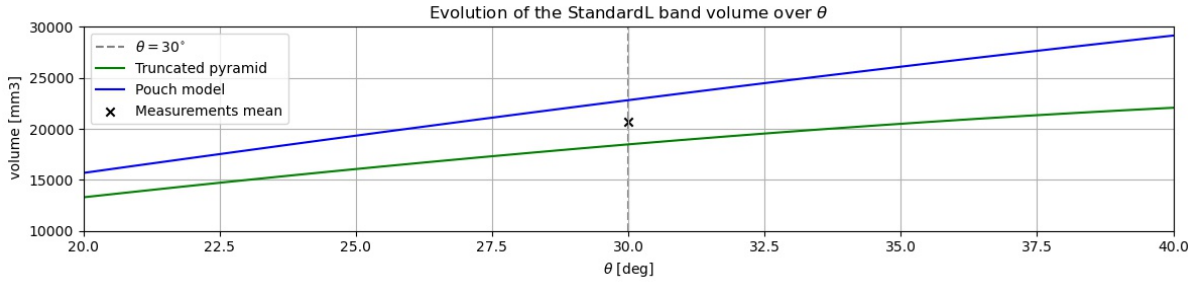

Figure 11.7: Comparison between the *StandardL* band volume estimations using the Niiyama model and the truncated pyramidal model. The physical maximal volume of the band at p_{atm} was measured at $\theta = 30°$ (experimentally). The mean experimental measurement of the maximal volume of the band is denoted by the black cross.

The difference between the measurements and the truncated pyramidal model possibly comes from an incorrect constraint on h (figure 8.5) and/or the fabric distortion.

11.4 Longitudinal analysis

The longitudinal analysis had for objective to characterize the pneumatic band and compare our results to the ones of the article we based our work on and validate the reproducibility of the results. The pouch motors are also known as *Peano motors* or *flat pneumatic artificial muscles*. Since the article of Niiyama et al., other studies where conducted to analyze their behaviour and create dynamic models [143, 144, 145, 146]. They all show similar relations between the retraction force F_{strap}, the strain ϵ and the input pressure of the pouch motors. The relation between F_{strap} and ϵ is similar to an hyperbole, the curves having different slopes depending on the pressure level. On the other hand, force and pressure are linked by a linear relation for a constant strain. This is visible on the results

of Schara et al.'s experiment, at figure 7.2. Their slope is related to the strain level they experience.

Figure 11.8 shows measured forces over the measured strains for different input pressures. On the same graph, we plotted the relation as described by the pouch motor model of Niiyama et al. but for pressures 75% smaller than our inputs pressures. We observe a drop in the measured force of the band compared to the theoretical F_{strap} predicted by the pouch motor model. Yet, the experimental results of Schara et al. fitted the model well, as seen on figure 7.2. The tube providing input pressure was not correctly sealed with the entrance of the pouch. The inner diameters of the bands inputs were designed to be tight to the tubes[1] and they were deeply introduced into the elbow of the bands. It was hypothesised that the pressure loss would be relatively negligible. Nonetheless, there was a leak of air at the interface between the band and its air supply for the tests. We were expecting that the high air debit of the pressure source would counteract the pressure loss caused by the leak. However, it was not the case and the leak must have skewed the pressure in the band. The pressure p_{band} is not equal to the input pressure in this experimental set-up. The impact of the leakage should be increasingly important as the input pressure is high. The higher the input pressure, the more p_{band} differs from the input pressure and F_{strap} is lower than it should be with an hermetic sealing. Furthermore we hypothesize that the the pressure level used to draw the curves are not isobaric inside the band and the force deployed could probably have been higher.

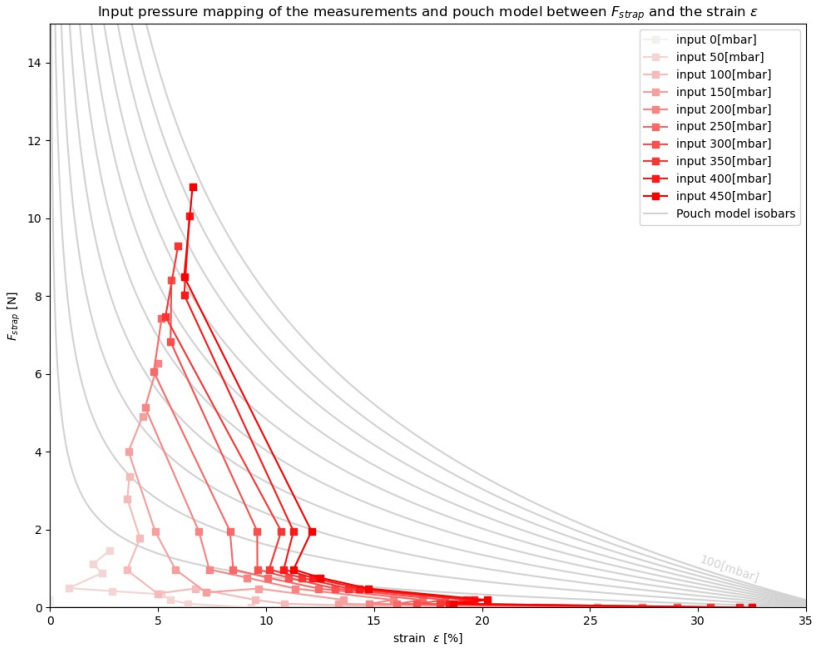

Figure 11.8: In red, the isobaric relations between F_{strap} and ϵ obtained experimentally using a input pressure ranging from 0 to 450[mbar] into the *StandardL* band. In grey, the isobaric curves of the pouch model for input pressures ranging from 0 to 100[mbar] with increments of 10[mbar] in an unsuccessful attempt to match the data.

[1] For a tube outer-diameter of 4[mm], an inner diameter of the band input of 4[mm] was designed, playing with the elasticity of the TPU-coated textile for a better sealing.

Figure 11.9 also illustrates the measured force of the band over its measured strain. It takes into account the total strain of the band, including intersections between pouches. For this graph, one colored line corresponds to an attached weight, and the dots or crosses corresponds to different bands that were tested. As the pressures was increased, the mass displayed on the scale (placed under the hanging band with the weight on top) decreased. Although, the scale never indicate a mass of 0[g] for either the 1[kg] or 2[kg] loads because the weight was never lifted up entirely. The strain ϵ should logically stay very close to zero in these conditions. Yet, the graph shows a rise in strain as the force increases. Our hypothesis is that this is also due to the testing set-up. The nods of the twine around the band could tighten up progressively as the force imposed increased over the tests. This allowed retraction of the band and no lifting of the weight. Due to this observation we can not study the behaviour of the band at constant strain as we hoped for high loads.

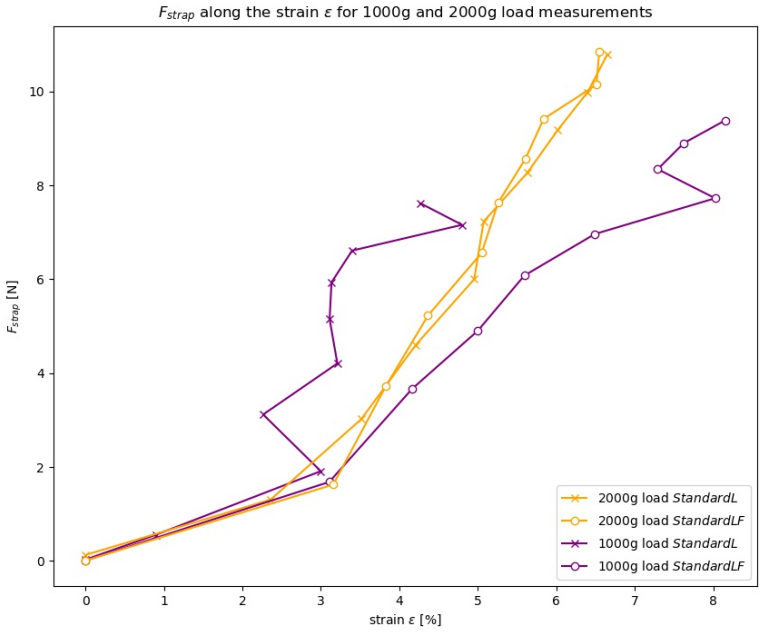

Figure 11.9: The of experimental results of F_{strap} over ϵ for the 1[kg] and 2[kg] loads attached to each band. The yellow lines indicate the 2000[g] loads attached and the purple lines indicates the 1000[g] load. Crosses are related to the tests on one a fatigued standard band and dots to a classic standard band.

The next graph, figure 11.10, show the mean measurements of the strain of the band over the input pressure at constant force levels, specifically at 0.01[N] and 0.02[N]. These force levels correspond to the loads of 10[g] and 20[g]. The force is considered constant because the load was immediately completely lifted since the first pressure level. The same weight acted on the strap during the entire inflation process. The results present smaller strains than expected by the pouch model at the given input pressure levels (dotted lines). They also have a reduced curvature. Once again, the leak must have had on impact on these observations, since we think that the band inner pressure was lower than the input pressure.

In a trial to evaluate the leak hypothesis we used the pouch model to find the theoretical

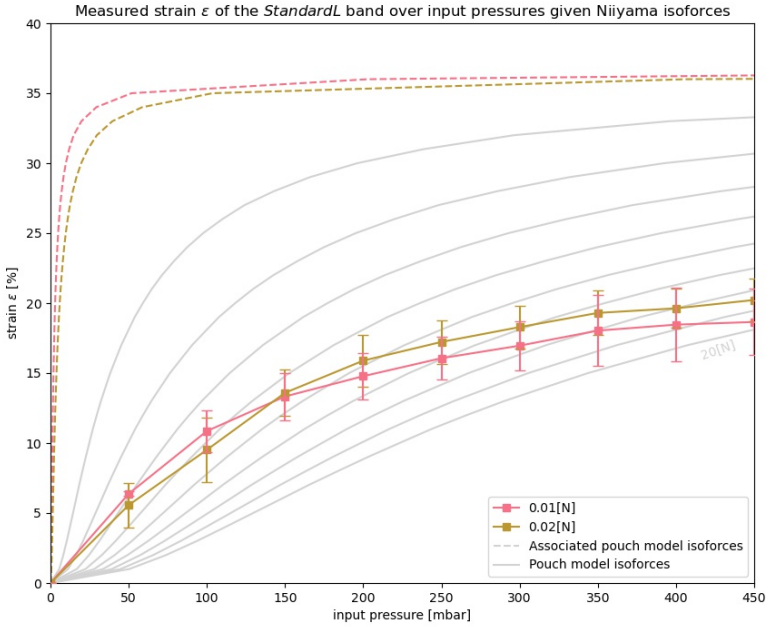

Figure 11.10: Mean measured strain over the input pressures for 0.01[N] or 0.02[N] forces imposed on the straps. The error bars corresponds to the maximum and the minimum value of strain at each pressure level. The dotted lines correspond to the relation predicted by the pouch model for the specific level of forces 0.01[N] and 0.02[N]. The grey lines are curves predicted by the pouch model for isoforce conditions with F_strap between 2[N] and 20[N] (by increments of 2[N]).

inner pressure of the pouch corresponding to observed retraction. We based our calculation only on the retraction of the pouches, not the entire band and the intersections between pouches. Then we computed the error of pressure $Error_p$ between the input pressure p_{in} and the theoretical pressure in the band, p_{band}, as $Error_p = \frac{p_{in} - p_{band}}{p_{in}}$. Figure 11.11 shows this error plotted over the input pressure for all the assessed loads. For the lighter loads, that imposed a constant force on the strap, this percentage of error is the highest and is constant over the pressure range. This implies that as the input pressure increases, the inner pressure increases as well and proportionally. However, the difference in input and inner pressures grows. The error is very high and this behaviour could be explained by the leak. For the most heavy loads, the profile of the curve is different. As the input pressure increases, the error decreases. The inner and input pressure are getting closer as the input pressure rises. For those loads, the force is increased at each pressure level because more weight was lifted by the band. Therefore, since for constant forces the error remained constant, it gives the impression the determining factor is more the force that the pressure and that lines for constant forces could all by horizontal. It also seems that lines for constant forces would just be approximately parallel but at lower errors as the force is greater. We formulate two hypothesis on this observed behaviour. The first one is that the leak could get closed as the tension on the material grows. The other one, not exclusive of the other, is a *valve effect*. The top intersections, closed to the input of air, could block the air return to the leak due to a progressive section narrowing allowed by the elasticity of the band material.

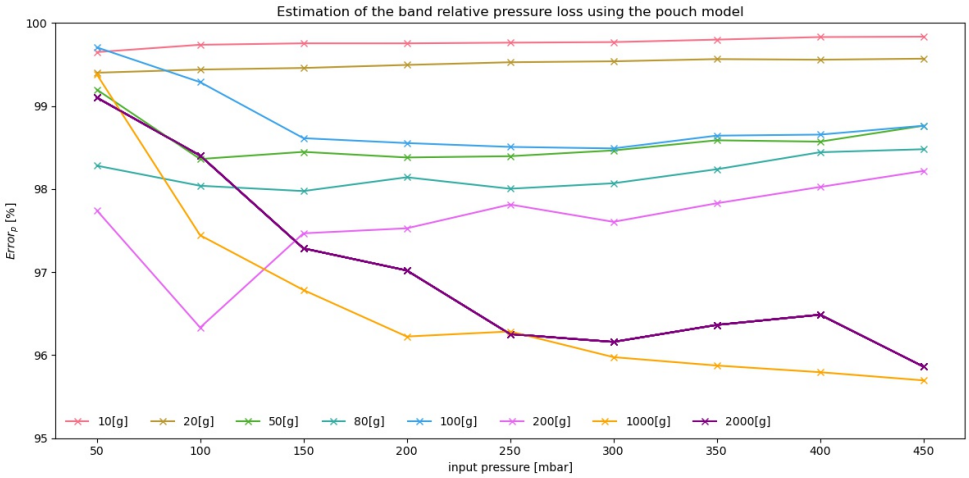

Figure 11.11: Estimation of the band relative pressure loss over the input pressure, using the pouch model. All curves correspond to a specific load.

We then wanted to evaluate the behaviour of the different pouches in a band. Therefore, the strain over the input pressure with regard to each pouch was plotted on figure 11.12 for the 10[g], 200[g] and 2000[g] loads. The pouches are numbered from the less distal to the most distal of the pressure source. Over the input pressure levels, the strain has an increasing trends: As expected, the band and individual pouches retract more when the pressure is higher. The thing to observe here is the difference of profile in strain at one pressure level for the different pouches. The first pouch is less inflated at most pressure levels and for all loads. This can be related to the air leak discussed from the start. The impact would be higher for the closest pouches. The internal pressure in the pouches would be reduced more in the nearest pouch to the leak. The inner pressure is more different to the input pressure for those pouches than for the pouches further away. Since the pressure is lower, the strain should be lower also. In addition, the strain of the first pouch is equal to zero for the 2000[g] load at all pressures. This seems to indicate that the tension is particularly high on the top of the band and the first pouch and could confirm that the leak is blocked by the textile that is tensed.

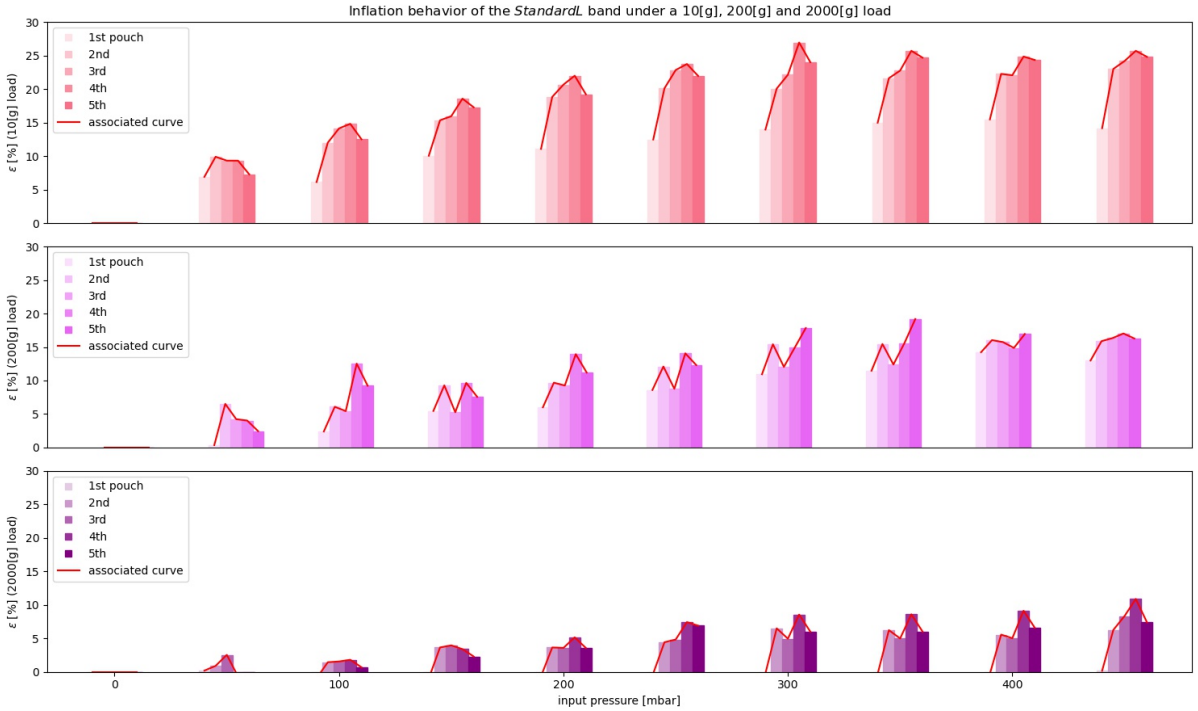

Figure 11.12: The inflation behaviour of a standard band under 10[g], 200[g] and 2000[g] loads. The strain over the input pressure for each pouch of the band is plotted. The pouches are numbered from top to bottom when the band was hanging. The strain is the mean value for a pouch over an input pressure level for all loads. The "1st" pouch is the closest to the air input.

To summarize

The testing phase led to select a sealing protocol of 45[s] at 200[°C] for the TPU textile in regards with the observed leaks. The dimensions of intersection do not seem to impact the leaks between pouches but a larger size of border helps to mitigate the leaks on that part of the bands. The fatigue test did not show differences on the tightness between a fatigued or not fatigued band.

For estimation of the relation between ϵ and θ the truncated pyramid model predictions are closer to the measurements that the ones of the pouch model. However the strain seems to be underestimated for angles under 50° by both models.

The measured volume of a band was found to be overestimated by the pouch model, as expected due to the geometry of a real pouch, and underestimated by the truncated pyramid model.

The longitudinal analysis showed that the testing set-up should be reviewed. The nods of twine tightened progressively as weight was added on the band and is skewed the measurements. More importantly, the air supply was not sealed to the band and the leak of air had a big impact on the results. The internal pressure band was not as high as the input pressure and this distorted the curves that should have been observed. An estimation of the pressure error was calculated and showed a proportionate impact to the input pressure. Thus a higher difference between input pressure and inner pressure as the

supplied pressure was more important. Furthermore the effect decreased for higher loads but stayed high: above 95% of error. This could be explained by a rising tension in the material that would block the leak of air around the tube. The evaluation of the strain on each pouch showed no retraction on the closest pouch to air supply for high loads, and leads to the same conclusion.

Chapter 12

Future prospects

This thesis comes to an end but the work on the prototype is destined to be brought further. We thought of a number of prospects that could be investigated concerning the fabrication process, the features of the device and the study of its performances, until the day it is officially ready for use.

12.1 Fabrication of the prototype

Stamping technique To enhance the efficiency and reliability of the stacking and sealing of the bands, a solution is to develop a metallic patron that could press the layers together directly in the shape needed (figure 12.1). This technique was proposed by Niiyama et al. and referred to as stamping. The metallic patron is heated and placed on the two TPU-coated layers for a determined amount of time. The heat only melts the TPU at the desired zones, and there is no more need for a non-stick layer inside the band. Be aware that TPU is a highly heat-sensitive material. To avoid any heat diffusion under the bands, the support can be made of fiberglass, a insulative material whose melting point is above 200[°C]. The fabric can be cut before the heating, requiring a frame to guarantee the alignment, or after the process, hence easing the layers alignment. Instabilities of the initial process are resolved and reproducibility becomes easier. Design files for the given setup are automatically generated while designing a band using the automation script (appendix B).

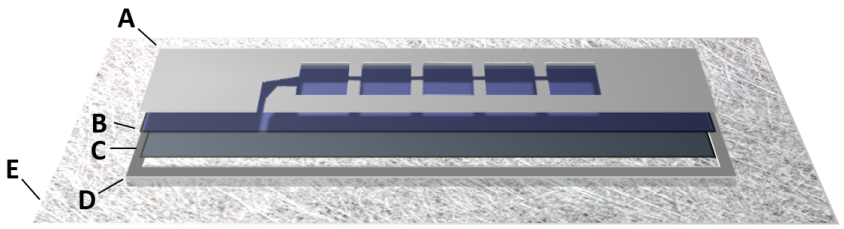

Figure 12.1: Schematic of the pressing using a metallic stamp on a fiberglass support, with the metallic patron (A), the two rectangles of one-side TPU-coated textile (B and C), to frame to guarantee their alignment (D) and the fiberglass support (E) to minimize the heat diffusion during heating.

Integration of the luer-locks If Schara et al. used of luer-locks to connect the tubes to the pneumatic bands, there is no certainty about the tightness of the connection.

Additional measures such as using proper sealing techniques[1] or adhesive materials may be necessary. However, luer-locks should be integrated to the pneumatic circuit to improve the modularity of the device. They allow to dismantle the device between the electronic components, the tubes and the bands. The device specification could thus easily be changed and adapted to the patient specific needs (length of the tubes, design of the bands). We had trouble finding medical tubes with luer-locks or barbed adaptors and ran out of time to integrate them.

Color code A color code could be added to the luer-lock connectors system, to the bands, tubes, and to the corresponding knobs. It would ease the calibration and connections. For the moment, the bands all have the same dimensions but if they were individually adapted to the leg diameter, the color code would make connection more simple and reduce the risks of misuse of the device.

Closed-loop circuit Another feature that could be added to the prototype is a closed-loop control, using pressure sensor(s) into the pneumatic circuit. If anything happens during the therapy that impact the received pressure, suach a leakage or the detachment of a band, the controller will detect it and respond according to the therapy protocol.

Intermittent Pneumatic Compression The device we produced is suited for SCT protocols, however it could updated to provide intermittent pneumatic compression (IPC) therapy. As a reminder, the IPC Device refers to a peristaltic compression,(figure 6.2). To implement this feature, the Arduino code should be modified and the valves changed. The chosen valve needs to be able to block the air from exiting the band.

Pressure profile For the moment, the pressure increase over time in a band depends on the performance curve of the selected pump and the duty-cycle of the associated valve, that allow a fixed pressure release. It could be of interest to control the profile of that pressure increase, by progressively modifying the duty-cycle value to its desired final value.

Pressure control Added to the pressure profile challenge, the valve oscillations used to regulate the pressure create a lot of noise and vibrations. For the comfort of the users, it is necessary to minimize these aspect, by changing the technology or by isolating these components.

One controller - two legs The controller only allows to provide the therapy to one leg at a time. Updating the device to two legs will require an upgrade of the microcontroller used, since the maximum of connectable bands is of 5 for the Arduino nano IOT33 pins. Since two homologous bands inflates together, the performances of the pump have to be adapted to a doubled work volume. The SCT protocol code has also to receive minor changes to control multiples bands at a time.

Medical device certification A lot of work still needs to be done until the medical device certification of the OS-SCT. Despite the fact we had the *ISO14971* standard in mind while designing the upgrade, a rigorous risk management based on a SCT device life-cycle will be necessary. Risk evaluation should be done before and after every iteration

[1] For exemple, using Teflon into the connector

of the prototype to ensure that the final design will not have to be re-thinked to be certified later.

12.2 Analysis of the prototype

Truncated pyramid model study For the selected height $h(\theta)$ constraint, the truncated pouch model seems closer to the reality but is not conclusive yet. As for the pouch model, this model does not take the physical characteristics into account, meaning that for any pressure build-up in the pouch, it could not fit every material. However, the advantage of the truncated pyramid model is that the constraint on the inflation height $h(\theta)$ (eq. 8.2) could be modified after experimentation, and is not intrinsic, such as the pouch model. Modifying the constraint should allow to obtain a empirically plausible evolution profile for the volume of the truncated pyramid (eq. 8.8). Moreover, the state variable θ could be revised to define a new variable easier to measure. A last perspective could be to work using spheres instead of cylinder like the work of Niiyama, discarding the truncated pyramidal model.

Quantitative evaluation of the leaks A quantitative evaluation of the leaks could be done by inflating a band at a given pressure, block the air exiting the band with an appropriate valve and measuring how much time the band takes to completely deflate. It would allow to define the potential pressure loss of the band during inflation, since it can impact the performance of the SCT.

Longitudinal analysis The longitudinal analysis should be reproduced in better conditions. First of all the band should be sealed to its air supply during testing to allow no leak at the input. Secondly the testing method could be modified to suppress the hanging loads and the twine that served to attached them. One could use a Universal testing machine as in the article of Schara et al. or a dynamometer for the force measurement.

Radial analysis Finally a radial analysis should be conducted. It will evaluate the model of pressure on the leg over the input pressure. This can be done with flat and flexible force sensors like the Flexiforce sensors. The sensors would be placed between a band and a leg or a PVC tube. Data will need to be acquired on different spots of the band to evaluate the mean force and pressure over the leg. We tried to conduct this experiment but had troubles calibrating the sensors and could not pursue the testing in the remaining time.

Fluid mechanics The design of the bands, upgraded from Schara et al., has not been studied from a fluid mechanics perspective. This design presents an elbow and many straight angles. It could be revelant to rethink the design to optimize the inflation and especially the deflation behavior of the bands, to avoid valve effects.

Flat muscles geometry The conception script developed for the bands design opens up a whole flied of analysis regarding the geometry chosen for the flat muscle motor, regarding the OS-SCT or not. This script can be easily adapted to allow non-rectangular pouches by modifying the `arc` function of *IPCdevice_designer_v2.py*.

Conclusion

This thesis has for goal to make a step forward towards open-source appropriable hospitals. The COVID-19 pandemic triggered the effort of scientists around the world to develop new technologies and highlighted the importance of open-source resources, notably for clinical matters. To participate, the students had to identify the stakes of the medical devices that would fit that frame, develop a selection protocol of devices and develop or elaborate an open-source appropriable version.

The completed work allowed the authors to meet the following objectives :

- Present the stakes and meaning of an open-source appropriable medical device.
- Identify the needs for an open-source appropriable medical device.
- Develop a selection method to choose an appropriate medical device.
- Expand on the sequential compression device principles and on the existing devices on the market.
- Develop a functioning prototype, including modeling and fabrication, by improving an open-source proposition of Schara et al.. Enhancements regarding the open-source appropriable aspect were brought and all the material for future update is open-source available to all public.
- Test the prototype, compare the results to those expected by the pouch model[140] and discuss them.
- Suggest future prospects for additional research.

The first part (part I) of this works allowed a better understanding of the open-source appropriable hospital background. The open-source status encompasses an entire mindset that aims for openness of knowledge and material. OS resources should provide as much information as possible and tools for understanding, reproduction and improvement. They should be designed to be affordable on both price and methods. The appropriable medical device was defined in the frame of this thesis as easily fabricated, minimally expensive, rigorously documented and with facilitated protocol and interface. The need for such device was identified mostly in surgical, emergency and intensive care units. Diagnostic tools and devices related to cardiovascular diseases also deserve special attention as well as remote wearable devices.

All this information allowed to develop a selection method for devices that are of interest towards an open-source appropriable hospital. The criteria include sector of use, exclusion of consumable items, the various type of use, among others. The protocol led to

choose the sequential compression device for fabrication and study. This medical device provides compression to the legs in order to facilitate blood flow and is an essential device of intensive care unit which makes it adapted to the needs of an open-source appropriable device. Part II included the selection methodology, the presentation of the SCD and a overview of the existing devices on today's market.

In part III, the only[2] currently existing OS device for SCT was presented. This prototype was published by Schara et al. and is composed of pouch bands that retract when inflated, creating compression when wrapped around the leg. This type of technology is a *pouch motor*. The models, methods, results and material of Schara et al. were reviewed and the *openness* of their work was discussed. Then, an alternative geometry modelling, the truncated pyramid model[3], was developed and compared to the pouch model used in the initial device. The dimensioning of the pneumatic circuit and the fabrication of the prototype were designed to fit the OS appropriable frame. This was achieved by complete referencing and justification of all the steps of the process. Furthermore, the SCT operation script was updated to a software, more modular and easily adaptable. The pneumatic bands design was changed to become reproducible, economic and adaptive, and a script was produced to facilitate modifications of the design. The fabricated prototype has a total cost of 71.20€ which is significantly less than devices on the market. Some risks were mitigated with the addition of new functionalities (risk of incorrect therapy, usage misuse, poor manufacturing). Additionally, all the resources produced will be made available on a GitLab hosted by UCLouvain[4].

The last part (part IV) relates to the study of the prototype. The tightness of the device was qualitatively evaluated with a leak detector spray. As a results, the sealing protocol to avoid leaks as much as possible was fixed to $200[°C]$ for $45[s]$. The borders of the bands where made larger and fatigue was concluded to have no noticeable impact on tightness. The relations between the tangential angle θ, the strain ϵ of the pouches and the volume of the bands were measured and compared to two geometric models: the pouch model of Niiyama and the proposed truncated pyramid model. The truncated pyramid model estimates of strain for different values of θ were closer to reality than for the initial pouch model. Then, the volume for $\theta = 30°$ was measured and once again compared to the estimations of both models. Here, both models where discarded. Finally, the relations between strain, pressure and force were evaluated and compared to the results expected with the pouch model. It clearly appeared that the results did not fit the models correctly. The main hypothesis is that a leak at the air input affected the behaviour of the band. It majorly dropped the inner pressure and the forces deployed. The effect of this leaks seems to be smaller for higher weights. This could be because high weights create a lot of tension in the textile and could block the space between the air supply tube and the band. Study of the distribution of pressure inside the pouches of a band was also conducted and seems to confirm that hypothesis. However, the testing method were not optimal and should be modified to conduct a more rigorous evaluation of the device for future research. Other future prospects include simplification of the fabrica-

[2] To the best of the authors knowledge.

[3] The truncated pyramid model is aiming to improve the future dimensioning of the flat motor technology.

[4] All material and resources useful to the prototype production and testing has been made available freely, on Forge UCLouvain in the OpenMedTech group: `https://forge.uclouvain.be/openmedtech/sequential-compression-device.git`.

tion process by stamping, addition of Luerlocks for tightness and modularity. Further medical features that could also be brought: closed-loop control, IPC therapy, treatment of two legs simultaneously. Enhancements regarding the prototype analysis are necessary. Among others, quantitative evaluation of leaks, more rigorous longitudinal analysis and radial analysis could be conducted to later lead to a potential certification of the device.

In conclusion, the work is thought to be rigorously documented, modular, economic and (re)produced or updated with ease. This shapes the produced SCD prototype towards the equipment park of an open-source appropriable hospital.

List of Figures

List of Tables

Appendix A

Specification sheets

The following appendix contains precise specifications about the prototype.

1. *StandardL* detailed dimensions;
2. OS-SCD prototype components specifications overview;
3. Skocoom pump specification sheet;
4. ZR320-02PM-4.5V pump specifiation sheet.

Band ID:5-4-30-30-60-5-5-50-50

Date:2023/04/27

Precise dimensions of the StandardL pneumatic band
(for informative purpose only)
Length unit : [mm]

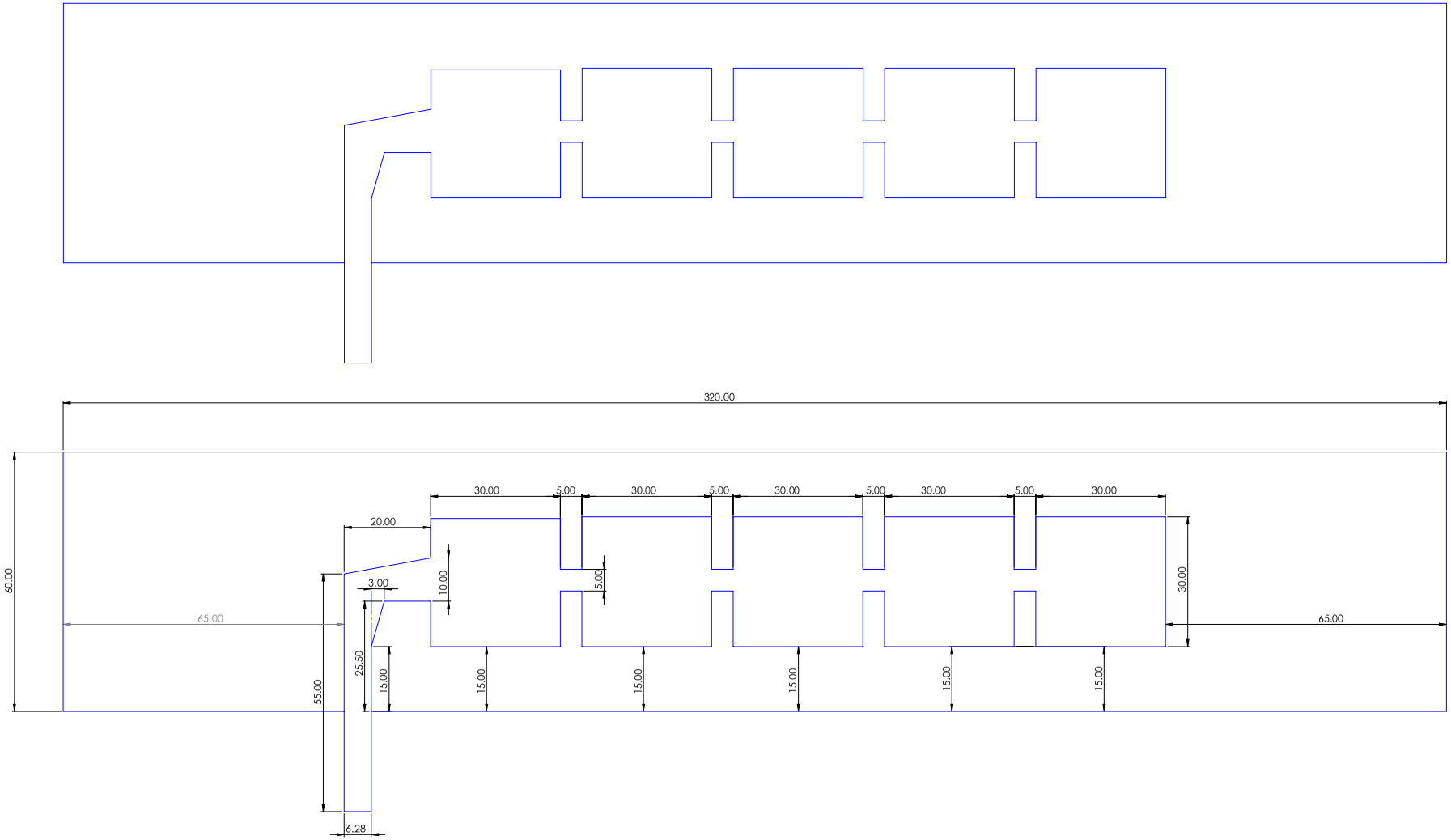

Components - precise description

Drive links may be deprecated or not up-to-date, please refer to the Forge GitLab linked to this project

The susmentionned GitLab contains every details of the project.

All the specifications sheets we found are stored here
https://drive.google.com/drive/folders/1-vRpSUxZW-rc5TYF7eE5loehlPPyNJy3?usp=sharing

Here are some useful links to find electromechanical components :
- https://www.digikey.be/fr/
- RS | Distributeur de composants électroniques et solutions industrielles (rs-online.com)
- https://www.mouser.fr/

The following elements are enhanced descriptions of the components used to build the OS-SCD prototype. With added mechanical and electronical specifications. Price are given without value added taxes.

Microcontroller

Complete name	*Arduino Nano IOT 33with headers (SKU: ABX00032)*
Dimensions	48mm x 18mm
Weight	5 grams
Operating voltage	3.3V
Connections	Two 15-pin connectors (one on each side)
Comment	The integrated DC-DC power supply allows you to power the board up to 21V while maintaining high efficiency and providing a significant amount of current to external devices without overheating. 1 piece for 1 device.
Where to buy it	https://store.arduino.cc/products/arduino-nano-33-iot-with-headers
Price	23.40€/pc.

Battery (from the initial prototype, not implemented in the device yet)

Complete name	*Galaxy 2S (7.4V) 120 mAh Lipoly Battery Pack*
Dimensions	19 x 25 x 15.5mm
Weight	11 grams
Tension de sortie	7.4V
Connexions	Mating connector : JST
Comment	12V Power Supply are a great charging solution.

Where to buy it	https://www.fingertechrobotics.com/proddetail.php?prod=G-2S-mAh
Price	8.54€/pc.

LCD-screen

Complete name	*ASunFounder IIC I2C TWI Serial 2004 20x4 LCD Module Shield)*
Dimensions	60 x 99 x 22mm
Weight	/
Operating voltage	5V
Connections	Two I/O ports : SDA and SCL
Comment	http://wiki.sunfounder.cc/index.php?title=I2C_LCD2004
Where to buy it	https://www.amazon.fr/SunFounder-Serial-Module-Arduino-Mega2560/dp/B01GPUMP9C/ref=sr_1_1
Price	12.99€/pc.

Micro-pump

Complete name	*Micro Air Pump ZR320-02PM-4.5V*
Dimensions	37.7 x 18 x 8mm
Weight	NaN
Operating voltage	4.5V (load current < 580 mA)
Air flow	> 0.3L/min (flow rate of 205ml/min from our article)
Maximum pressure	<= -55kPa
Noise	<60dB (30cm away)
Lifetime	30,000 cycles (10s on + 5s off) – drop in 15 pressure
Comment	To use between 5-45°C with a maximum 30-80% relative humidity. 1 piece for 1 device.
Where to buy it	https://www.adafruit.com/product/4700#description
Price	6.5€/pc.

Solenoid valve

Complete name	*6V Air Valve (2-positions 3-way solenoid valve)*
Dimensions	14.5 x 36.02 x 12.5mm
Weight	NaN
Operating voltage	6V
Operating current	240mA
Resistance	NaN

Comment	Warning, valves has not been tested over 300mmHg air pressure. Better valves should be selected for further iterations of the prototype. Remark: Electrovannes and solenoid valves refer to the same technologies. 3 pieces are required for one device.
Where to buy it	https://shop.mchobby.be/fr/air-pneumatic/2229-plastic-air-valve-6v-3232100022294.html
Price	3.81€/pc.

Pneumatic tube (2mm)

Complete name	*PU Tube*
Dimensions	ID : 2.5mm OD : 4mm (standard compatible with the solenoid valves output)
Weight	/
Material	Polyurethane (=PU)
Comment	One device requires 3m
Where to buy it	https://be.farnell.com/en-BE/smc/tu0425c-20/tubing-4mm-clear-20m/dp/3640784
Price	13.6€/20m

Pneumatic tube (4mm)

Complete name	*PU Tube*
Dimensions	ID : 4mm OD : 6mm (standard compatible with the pump output and valves input)
Weight	/
Material	Polyurethane (=PU)
Comment	One device requires 0.4m
Where to buy it	https://be.farnell.com/en-BE/smc/tu0604c-20/tubing-6mm-clear-20m/dp/3630006
Price	28.74€/20m

Four way connector

Complete name	*Four way connector*
Dimensions	OD: 4mm
Weight	/
Material	1 piece is required for one device.
Comment	Ours were ordered on amazon. The delivering cost of Qosina were too expensive.
Where to buy it	https://www.qosina.com/cross-connector-barbed-97357
Price	11.35€/10pcs.

Needles (Luer-lock females)

Complete name	*16 Gauge 1" length Blunt Tip Stainless Steel Dispense Needles*
Dimensions (needle)	Gauge : 25.4mm - Inner : 1.35mm - Outer : 1.65mm Chart of needle using different in-out diameters : NeedChart 32472.1645631065.jpg (1280×766) (bigcommerce.com)
Comment	Fits all standard Luer Lock or Luer Slip Syringes. 1-in blunt-tip. Dimensions of Luer-fittings are defined in ISO 594-2. 3 pieces are required for one device.
Where to buy it	https://www.amazon.fr/sourcing-map-aiguilles-distribution-transparent/dp/B0B3RW4YJZ/
Price	14.75€/20pcs.

Luer-lock (not implemented in the device yet)

Complete name	*Male Luer Lock to Barb Connector*
Dimensions	Fits 3/32 inch ID Tubing (0.093inch, 2.38mm)
Luer fitting	ISO 594-2
Comment	The delivering cost of Qosina were too expensive. Used to handle the connection of the bands to the system. 3 pieces are required for one device.
Where to buy it	https://www.qosina.com/male-luer-lock-to-barb-connector-11559 (female equivalent in case we need it) https://www.qosina.com/female-luer-lock-to-barb-connector-11558
Price	$0.33/pc.

TPU Coated Nylon

Complete name	*Nylon, 70den, TPU-coated one side, 170g/sqm, heat-sealable*
Dimensions	One band requires 320x125mm of textile
Fabric	TPU Coated Nylon 70d.
Comment	Taffeta fabric type. 1m is enough to produce 9 bands, 3 bands are required in one device.
Where to buy it	https://www.extremtextil.de/en/nylon-70den-tpu-coated-one-side-170g-sqm-heat-sealable.html
Price	12,61€/m

Parchment paper

Complete name	*Parchment paper*

Dimensions	One band requires 190x70mm
Comment	Can produce at least 20 bands, 3 bands are required in one device.
Where to buy it	Any supermarket.
Price	2€

Hook-and-loop fasteners

Complete name	*Hook-and-loops fasteners*
Dimensions	2000 mm x 30 mm
Comment	Loops were hand-designed and laser-cutted in 6mm wood chips. 1 meter is required for 1 device.
Where to buy it	VERITAS, 163 Louvain-la-Neuve, Place de l'accueil 10/37.
Price	11.00€/2m

Electronic components

Potentiometers	10 kΩ
Resistors	330 kΩ
Transistors	NPN (TIP28B, PN2222A)
Diode	/
Wires	/

型号Model:SC0801XPM

旧版型号: SC3101PM

气泵 Air Pump

Application

Beauty equipment/Gas sampling/
Sphygmomanometer, etc

产品尺寸 Dimension:

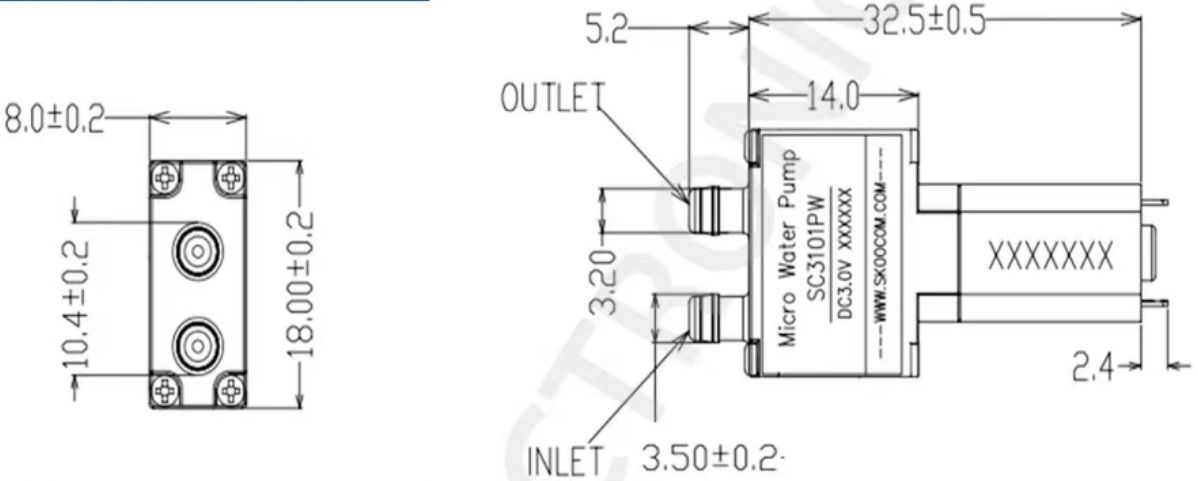

性能曲线图 Performance curve:

性能曲线图 Performance curve:流量和噪音变化

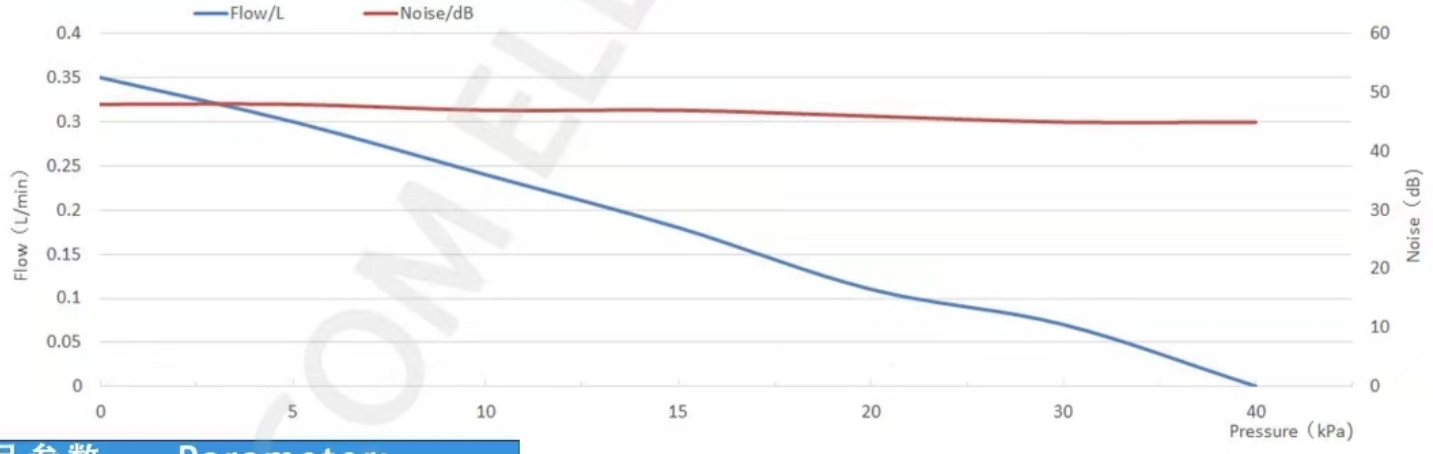

产品参数 Parameter:

Specification 产品规格			
额定电压 Rated voltage	DC3.0V	DC6.0V
额定电流 Rated current	<350mA	<150mA
气 流 量 Air flow	>0.3L/min	
压 力 Pressure	>40kPa	
噪 音 Noise	<55dB (30 cm away)	
使用流体 Medium	Air	
寿命试验 Lifetime test	100,000 cycle(5s on, 5s off)	
使用环境 Working environment	0~50 ℃, 75% RH	

Tel:+86-755-81461051 Fax:+86-755-81461030 Email:sales@skoocom.com www.skoocom.com

Micro Air Pump ZR320-02PM Specification

1. Scope of application

This specification is suitable for miniature air pump ZR320-2PM DC:3.0V DC:4.5V DC:6V DC:12V.

2. Test conditions:

2-1 Test environment temperature and humidity:

ambient temperature 20℃, relative humidity 65%RH is the standard

Test in the following environment: ambient temperature 5-45 ℃, relative humidity 30-80% RH

2-2 Test orientation: horizontal

2-3 load: air

3. Performance:

3-1	Rated voltage	DC:3.0V	DC:4.5V	DC:6V	DC:12V
3-2	Use voltage	DC2.2V~3.7V	DC3.0V~4.5V	DC5.2V~6.5V	DC10.8V~13.2V
3-3	Load current	＜ 650mA	＜ 580mA	＜ 500mA	＜ 280mA

Note: The above load current refers to the current value when the rated voltage supply air pump is used to inflate to the highest pressure in a 100ml container.

3-4 Noise: Put a 5cm thick sponge under the pump body and place it 30cm away from noise meter

The suction pressure is measured from 0 to -40kpa under rated voltage.

Less than 60dB

3-5 Flow: ≥1.8LPM

3-6 Maximum pressure: The maximum pressure value when the suction pressure is increased from 0 to stop when the rated voltage is used ≤ -55kpa

3-7 Operating temperature range:

The air pump works well between temperature 5℃ to 50℃ and humidity 30%RH to 80%RH.

3-8 Storage temperature range:

Keep the air pump in good condition between temperature -20℃ to 60℃

and humidity 30%RH to 85%RH.

4. Reliability test:

4-1 Low temperature characteristics:

After placing it at -20° C for 72 hours, take it out and place it at room temperature (20° C±5° C) for 2 hours. Re-test checks 3-3 3-4 3-5 3-6

The test results are normal.

4-2 High temperature characteristics:

After being placed at 60° C for 72 hours, take it out and place it at room temperature (20° C±5° C) for 2 hours. Re-test checks 3-3 3-4 3-5 3-6

The test results are normal.

4-3 High temperature and high humidity:

Leave out for 72 hours in an environment with a temperature of 60° C and a humidity of 80-85% and place it at room temperature (20° C±5° C) for 2 hours. Re-test checks 3-3 3-4 3-5 3-6

The test results are normal.

4-4 Low-temperature environment test:

After 5 hours at 5℃, there is no abnormality in the test at this temperature.

4-5 High temperature environment test:

There is no abnormality in the test at this temperature after 5 hours at 50℃.

4-6 Life test:

In a 500ml container, open for 10 seconds and stop for 5 seconds as a cycle test.

After 30,000, follow the test requirements of 3-3 3-4 3-5 3-6

Pressure within the attenuation range of 15%.

5. Other

5-1 Drop test: Use standard packaging methods and place them on the concrete floor from the front, side, and corners from a height of 50cm.

Its performance and structure are not abnormal in free fall.

5-2 Abnormal test:

There is no burning or smoke after continuous power-on for 8 hours at the maximum voltage.

5-3 Motor terminal:

There is no abnormality with 0.3 kg weight and terminal load. The terminal must be soldered at a soldering iron temperature of 380℃, and the operation must be completed within 2S

5-4 Appearance: The product must not be damaged or dirty.

Appendix B

Automated band design and files

Here follows the description of the automated design and referencing of the bands.

Step 1 : design your band

Using main.py, defind the desired parameters:

```
#######################################################
#                                                     #
# * Run this file to generate your pneumatic band * #
#                                                     #
#######################################################
# imports
from IPCdevice_designer_v2 import draw_svg
from IPCdevice_designer_v2 import write_info
from IPCdevice_designer_v2 import gauge_value_chart
```

```
# specifications (to fill by hand)
n = 5 # pouch number [mm]
ID = 4 # inner diameter [mm]
l = 30 # pouch width [mm]
g = 30 # pouch length [mm]
L = 60 # global width [mm]
ll= 5 # interconnection width [mm]
gg= 5 # interconnexions length [mm]
Gplus = 60 # additionnal length [mm] (end)
Gminus = 60 # additionnal length [mm] (beginning)
temperature = 200 # heating temperature [Celsius]
duration = 45 # heating time [s]
```

With the geometrical paramters defined on the figure below. Duration and temperature depends on the desired fusion protocol for the given band and do not influence the design files generation.

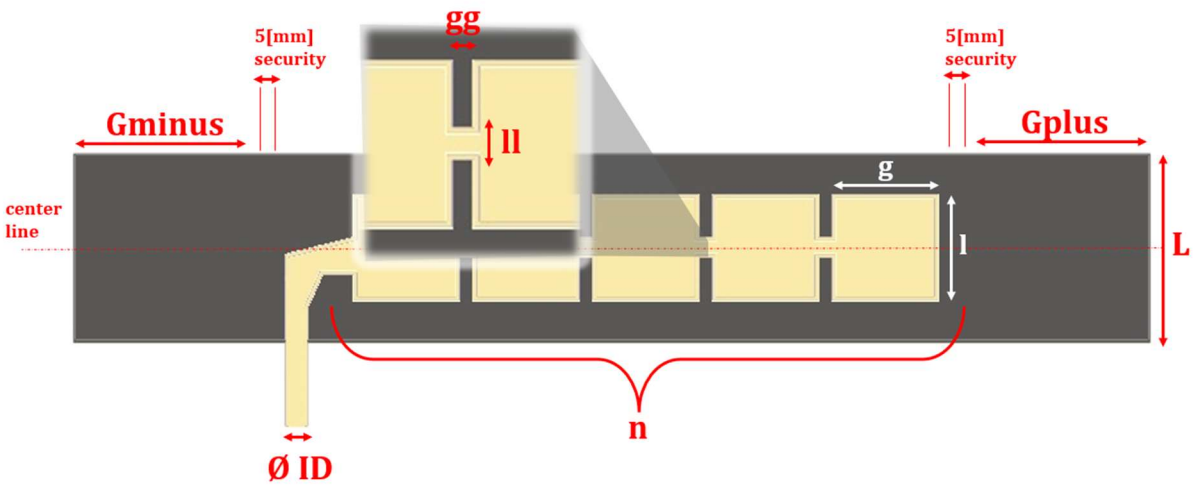

Step 2 : give it a nickname

The name of your band will be automatically defined. To ease the identification of the band during discussions, a tag can be chosen before generating the files :

[n - ID - l - g - L - ll - gg - Gplus - Gminus]_tag

```
tag = '_'+'StandardL'
```

Step 3 : generate your files

Run the main script to create your files.

Step 4 : find your files

After the run, a folder with the name of your band +"_FOLDER" is automatically created in the same repertory as the main.py script.

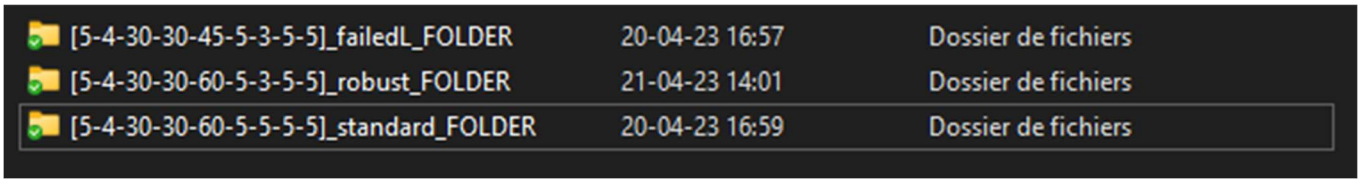

In the folder, all the needed files are labeled by the name of the band in case they need to be exported out of their initial folder.

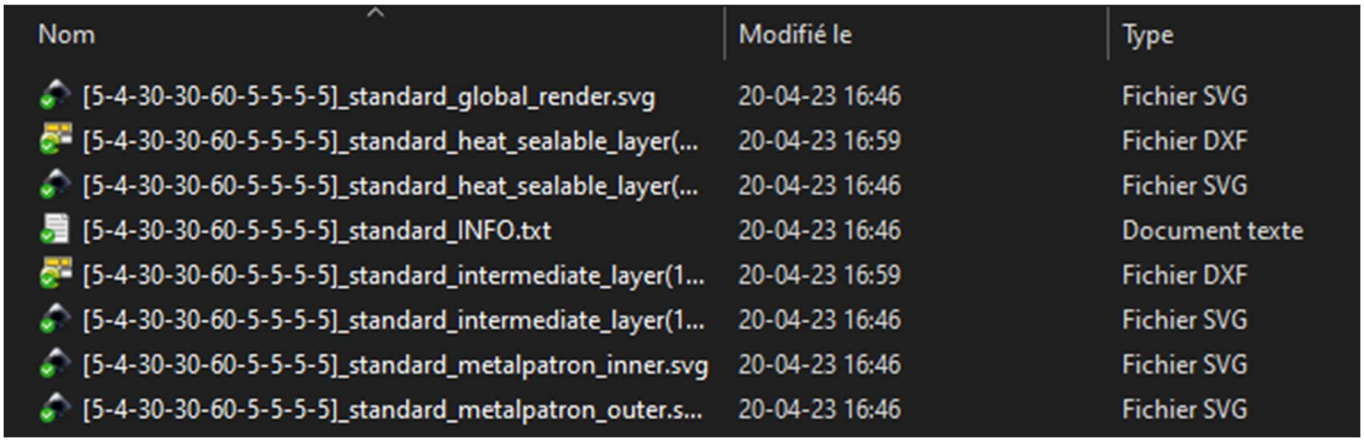

Among the different files, you will find :

A global render of the band

To verify that the design is correct at first sight. The file is of .svg format.

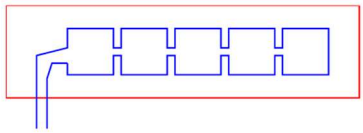

The distinct cutting files for the heat-sealable layers and the intermediate layer

WARNING: You will need to convert the .svg files to .RXF in order to use them with a laser-cutter.

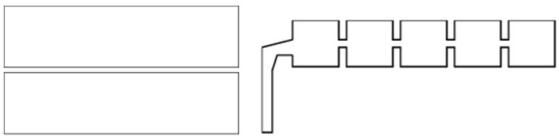

A first design of a metal-stamp: metal_patron files

They were never tested, but they aim to create a metal stamp to remove the ned of a non-stick layer inside the band.

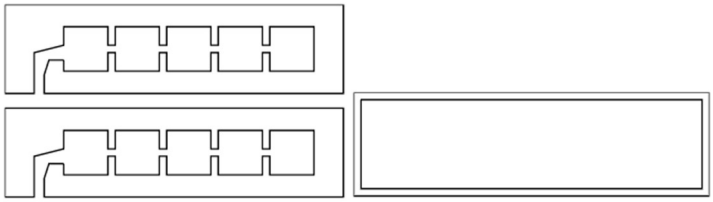

An info file that resume all the information about the band

The INFO.txt file is the key of the band identification system. It contains everything that is needed to accelerate the fabrication process and to use the band for testing.

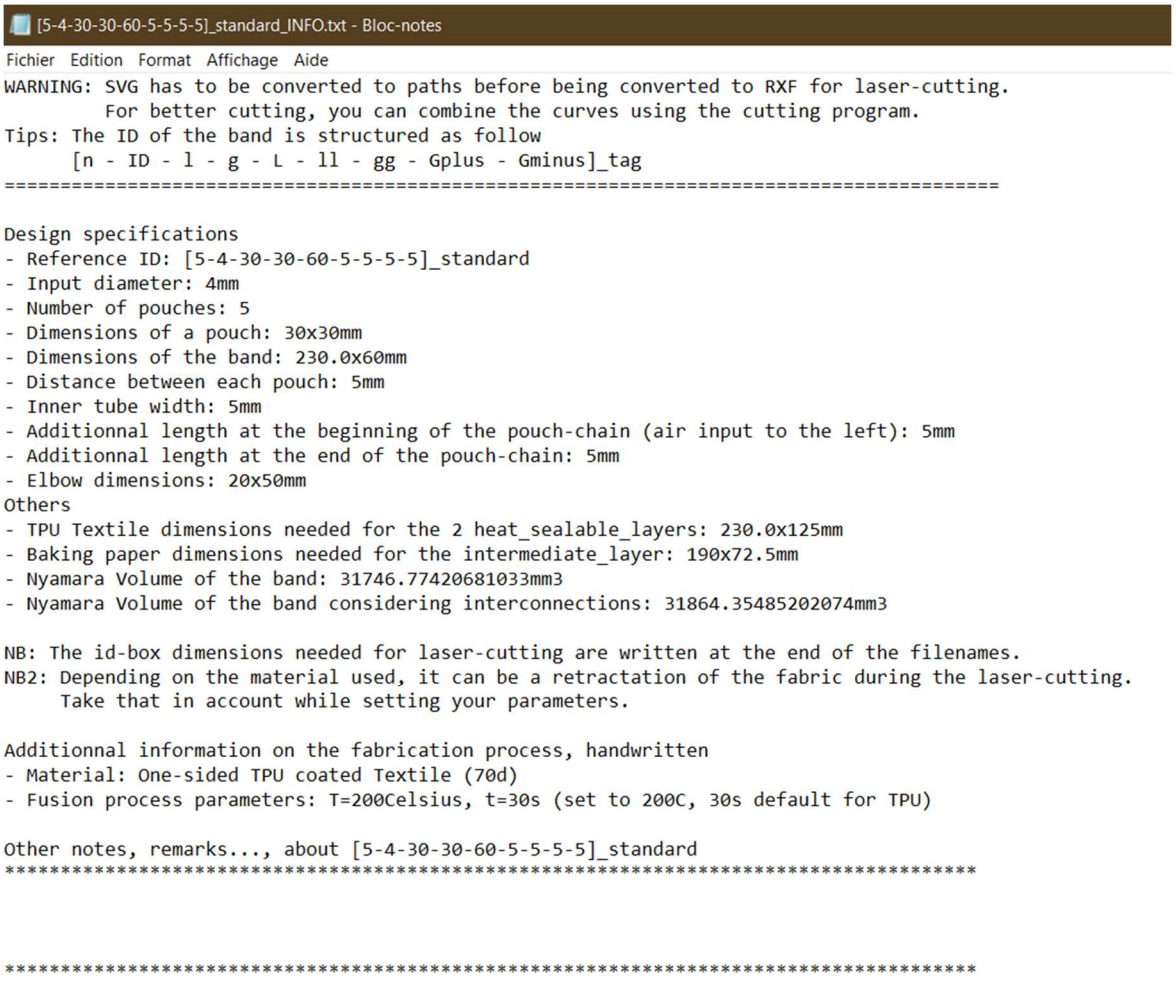

```
[5-4-30-30-60-5-5-5-5]_standard_INFO.txt - Bloc-notes
Fichier  Edition  Format  Affichage  Aide
WARNING: SVG has to be converted to paths before being converted to RXF for laser-cutting.
         For better cutting, you can combine the curves using the cutting program.
Tips: The ID of the band is structured as follow
      [n - ID - l - g - L - ll - gg - Gplus - Gminus]_tag
================================================================================

Design specifications
- Reference ID: [5-4-30-30-60-5-5-5-5]_standard
- Input diameter: 4mm
- Number of pouches: 5
- Dimensions of a pouch: 30x30mm
- Dimensions of the band: 230.0x60mm
- Distance between each pouch: 5mm
- Inner tube width: 5mm
- Additionnal length at the beginning of the pouch-chain (air input to the left): 5mm
- Additionnal length at the end of the pouch-chain: 5mm
- Elbow dimensions: 20x50mm
Others
- TPU Textile dimensions needed for the 2 heat_sealable_layers: 230.0x125mm
- Baking paper dimensions needed for the intermediate_layer: 190x72.5mm
- Nyamara Volume of the band: 31746.77420681033mm3
- Nyamara Volume of the band considering interconnections: 31864.35485202074mm3

NB: The id-box dimensions needed for laser-cutting are written at the end of the filenames.
NB2: Depending on the material used, it can be a retractation of the fabric during the laser-cutting.
     Take that in account while setting your parameters.

Additionnal information on the fabrication process, handwritten
- Material: One-sided TPU coated Textile (70d)
- Fusion process parameters: T=200Celsius, t=30s (set to 200C, 30s default for TPU)

Other notes, remarks..., about [5-4-30-30-60-5-5-5-5]_standard
********************************************************************************



********************************************************************************
```

This file contains :

- A detailed listing of the band design and fusion
- The pre-cutting dimensions needed for the materials to be put in the laser-cutter, ensuring a 5mm security and therefore minimizing material and time loss.
- Estimation of the band volume for a 45 tangential angle using the pouch model of Niiyama et al.
- Other information such as the fusion protocol wanted that can be customized in the code before generation.

Appendix C

SCT protocol code

Here is a paper version of the .ino code developed for our upgrade of the OS-SCT device.

All material and ressources useful to the prototype production and testing has been made available freely, on Forge UCLouvain in the OpenMedTech group:

`https://forge.uclouvain.be/openmedtech/sequential-compression-device.git`

```
// Author : Arthur Van Geersdaele
// Date-time : 23-06-01, 09h03m17s
#include <LiquidCrystal_I2C.h>
#include <Wire.h>

// USER-ZONE

// Arduino connexion pins
// - for pump
int Pump1pin = 10;
// - for valves (from distal band to proximal)
int valvesPins[] = {9, 8, 7};
// - for potentiometers (ID - impulse duration control, DC - duty cycles control)
int PotIDpin = A0;
int PotDCPins[] = {A1, A2, A3};

// Specifications
const int n_bands  = sizeof(valvesPins) / sizeof(int);

// Therapy parameters
int impulse_duration; // [ms] (to set with the potentiometer or to force below)
float duty_cycles[n_bands]; // [%] (to set with the potentiometer or to force below)
[allows to regulate the inner-pressure]
float impulse_repartition[] = {33.33, 33.33, 33.33}; // [%] (to manually define: size
= n_bands, sum = 100)
int period = 1; // [ms] (to manually define) [period on which the duty cycle is
applied]
int end_waiting_time = 5000; // (to manually define) [ms]

// Using potentiometers (set to false override the potentiometers)
bool impulse_duration_pot = true;
bool duty_cycle_pot = true;

if (!impulse_duration_pot) {
  impulse_duration = 15000;
}
if (!duty_cycle_pot) {
  for (int i = 0; i < n_bands; i++) {
    duty_cycles[i] = 100.0;
  }
}

// NOT TO BE EDITED

// Time management
unsigned long start_time = 5*60*1000; // you got X seconds to set up the parameters to
the desired values before the SCT starts
unsigned long current_time;
unsigned long condition;
unsigned long remaining;
int counter = 1;

// Screen management
```

```
LiquidCrystal_I2C lcd(0x27, 2, 1, 0, 4, 5, 6, 7, 3, POSITIVE);
char buffer[10];

// Conversion management for potentiometers
float readValue1;
float readValue2;
float writeReadConversion=255./1023.;
float writeValue1;
float writeValue2;

// Useful functions for therapy
void contraction(int pin, float onTime, float offTime){
  digitalWrite(pin, HIGH);
  delay(onTime);
  digitalWrite(pin, LOW);
  delay(offTime);
};

void sequence(int i, int pin, float onTime, float offTime){
  digitalWrite(pin, HIGH);
  while (millis() -  start_time - round((float) (impulse_duration +
end_waiting_time)*(counter-1)) < impulse_repartition[i] * impulse_duration /100) {

    contraction(pin, onTime, offTime);
  }
  digitalWrite(pin, LOW);
};

// Useful structural function
void cumulative(float* tmp, int n_bands) {
  for (int i = 1; i < n_bands; i++) {
    tmp[i] = tmp[i] + tmp[i-1];
  }
}

// TODO : LCD function to light the code

void setup() {
  // Debug and feedbacks
  Serial.begin(9600);
  lcd.begin(20, 4);

  // PinModes
  pinMode(Pump1pin, OUTPUT);
  pinMode(PotIDpin, INPUT);
  for (int i = 0; i < n_bands; i++) {
    pinMode(valvesPins[i], OUTPUT);
    pinMode(PotDCPins[i], INPUT);
  }

  // Data conversion
  cumulative(impulse_repartition, n_bands);
```

```
// For Start confirmation
pinMode(LED_BUILTIN, OUTPUT);
digitalWrite(LED_BUILTIN, HIGH);delay(1000);digitalWrite(LED_BUILTIN, LOW);
delay(1000);
digitalWrite(LED_BUILTIN, HIGH);delay(1000);digitalWrite(LED_BUILTIN, LOW);
delay(1000);
digitalWrite(LED_BUILTIN, HIGH);delay(1000);digitalWrite(LED_BUILTIN, LOW);

// Settings phase
lcd.clear();
// Display setting title
lcd.setCursor(0, 0);
lcd.print("[SCT SETTINGS]");
// - display impulse duration label
lcd.setCursor(0, 1);
lcd.print("ID: ");
lcd.setCursor(17, 1);
lcd.print("[s]");
// - display duty cycles label
lcd.setCursor(0, 2);
lcd.print("DC: ");
lcd.setCursor(17, 2);
lcd.print("[%]");
while(millis() < start_time){
  // - display impulse duration
  lcd.setCursor(4, 1);
  dtostrf(impulse_duration/1000, 2, 0, buffer);
  lcd.print(buffer);
  // - display duty cycles
  for(int i = 0; i < n_bands; i++){
    lcd.setCursor(3+i*4, 2);
    dtostrf(duty_cycles[i], 3, 0, buffer);
    lcd.print(buffer);
    if(i != n_bands){
      lcd.print("/");
    }
  }
  // Potentiometers for period ~ needs selector implementation
if(impulse_duration_pot){
  readValue1=analogRead(PotIDpin);
  writeValue1=(writeReadConversion)*readValue1/5;
  impulse_duration = writeValue1 * 500;
}
// Potentiometers for duty_cycle ~ needs selector implementation
if(duty_cycle_pot){
  for(int i = 0; i < n_bands; i++){
      readValue2=analogRead(PotDCPins[i]);
      writeValue2= (readValue2/1023.);
      duty_cycles[i] = writeValue2 * 100;
  }
}
  // - display remaining time before SCT
  lcd.setCursor(0, 3);
```

```
    lcd.print("time left: ");
    lcd.setCursor(10, 3);
    current_time = millis();
    remaining = start_time - current_time;
    dtostrf(remaining/1000.0, 3, 0, buffer);
    lcd.print(buffer);
    lcd.setCursor(17, 3);
    lcd.print("[s]");
    delay(500);
  }

  // Display SCT running title
  lcd.setCursor(0, 0);
  lcd.print("[SCT RUNNING] ");
  // Display total SCT duration
  lcd.setCursor(0, 3);
  lcd.print("time:          ");
  lcd.setCursor(15, 3);
  lcd.print("[min]");
  // Handling time
  start_time = millis();
  // Pump start
  digitalWrite(Pump1pin, HIGH);
}

void loop() {
  // Display total SCT duration
  lcd.setCursor(5, 3);
  current_time = millis();
  remaining = current_time - start_time;
  dtostrf(remaining/60000.0, 3, 0, buffer); // current time - 5 minutes setting - 5
seconds blink
  lcd.print(buffer);
  // Straps inflation
  for (int i = 0; i < n_bands; i++) {
    // Duty Cycle
    float onTime = (duty_cycles[i] / 100.0) * period;
    float offTime = period - onTime;
    // Impulse sequence
    sequence(i, valvesPins[i], onTime, offTime);
  }
  delay(end_waiting_time);
  counter = counter+1;
}
```

Appendix D

List of the acronyms

ASF Apache Software Foundation

CD Cardiovascular Disease 43

CERN European Organization for Nuclear Research

CLI Critical Limb Ischemia 33

DC Duty Cycle 46

DIY Do It Yourself

DVT Deep Vein Thrombosis 32

EMA European Medical Agency

EU European Union 35

FDA U.S. Food and Drug Administration 11

FDM Fused Deposition Modeling 13

FH Free Hardware Foundation 6

FOSH Free and Open-Source Hardware 6

Bibliography

[1] Alessandro Santini, Antonio Messina, Elena Costantini, Alessandro Protti, and Maurizio Cecconi. COVID-19: dealing with ventilator shortage. *Current Opinion in Critical Care*, 28:652–659, December 2022. URL https://www.ncbi.nlm.nih.gov/pmc/articles/PMC9612413/.

[2] Center for Devices and Radiological Health. Medical Device Shortages During the COVID-19 Public Health Emergency. *FDA*, December 2022. URL https://www.fda.gov/medical-devices/coronavirus-covid-19-and-medical-devices/medical-device-shortages-during-covid-19-public-health-emergency.

[3] Laurent Meyer, director of the biomedical service at Cliniques Universitaires Saint-Luc. Meeting discussion with Laurent Meyer, February 2023.

[4] Simone Mora, Fábio Duarte, and Carlo Ratti. Can Open Source Hardware Mechanical Ventilator (OSH-MVs) initiatives help cope with the COVID-19 health crisis? Taxonomy and state of the art. *HardwareX*, 8:e00150, October 2020. URL https://www.sciencedirect.com/science/article/pii/S2468067220300596.

[5] Science, technology and innovation efforts to address COVID19 | UNCTAD, . URL https://unctad.org/topic/commission-on-science-and-technology-for-development/covid-19.

[6] Breath4life, March 2023. URL https://breath4life.odoo.com/. publisher: Breath4Life.

[7] Mark Schara, Mingde Zeng, Barclay Jumet, and Daniel J. Preston. A low-cost wearable device for portable sequential compression therapy. *Frontiers in Robotics and AI*, 9, 2022. URL https://www.frontiersin.org/articles/10.3389/frobt.2022.1012862.

[8] Bruce Perens. Perens Open Source Definition LG #26. *Linux Gazette*, January 1998.

[9] Robert Viseur. From open source software to open source hardware. In Imed Hammouda, Björn Lundell, Tommi Mikkonen, and Walt Scacchi, editors, *Open Source Systems: Long-Term Sustainability*, IFIP Advances in Information and Communication Technology, pages 286–291. Springer, 2012.

[10] Free software is a matter of liberty, not price — free software foundation — working together for free software, 2022. URL https://www.fsf.org/about/.

[11] Open Source Hardware (OSHW) Definition 1.0, May 2012. URL https://www.oshwa.org/definition/.

[12] CHRISTINA Raasch. PRODUCT DEVELOPMENT IN OPEN DESIGN COMMUNITIES: A PROCESS PERSPECTIVE. *International Journal of Innovation and Technology Management*, April 2012. URL https://www.worldscientific.com/doi/epdf/10.1142/S021987701100260X.

[13] Commercialising intellectual Property: Licence Agreements, 2021. URL https://op.europa.eu/en/publication-detail/-/publication/e510929d-f015-11eb-a71c-01aa75ed71a1/language-en/format-PDF/source-227478787.

[14] Arnoud Engelfriet. Choosing an open source license. *IEEE Software*, 27, 2010.

[15] Josh Lerner and Jean Tirole. The Scope of Open Source Licensing. *The Journal of Law, Economics, and Organization*, 21(1):20–56, 04 2005. URL https://doi.org/10.1093/jleo/ewi002.

[16] Best Practices for Open Source Hardware 1.0, November 2012. URL https://www.oshwa.org/sharing-best-practices/.

[17] Open Source Licenses by Category | Open Source Initiative. URL https://opensource.org/licenses/category.

[18] Daniel K. Fisher and Peter J. Gould. Open-Source Hardware Is a Low-Cost Alternative for Scientific Instrumentation and Research. *Modern Instrumentation*, 1(2):8–20, April 2012. URL http://www.scirp.org/Journal/Paperabs.aspx?paperid=18950.

[19] Joshua M. Pearce. Quantifying the Value of Open Source Hardware Development, December 2014. URL https://papers.ssrn.com/abstract=3331131.

[20] Roberto Acosta. *Open source hardware*. Thesis, Massachusetts Institute of Technology, 2009. URL https://dspace.mit.edu/handle/1721.1/55201.

[21] Lorraine Morgan and Patrick Finnegan. Benefits and drawbacks of open source software: An exploratory study of secondary software firms. In Joseph Feller, Brian Fitzgerald, Walt Scacchi, and Alberto Sillitti, editors, *Open Source Development, Adoption and Innovation*, pages 307–312, Boston, MA, 2007. Springer US. ISBN 978-0-387-72486-7.

[22] Gerrit Niezen, Parisa Eslambolchilar, and Harold Thimbleby. Open-source hardware for medical devices. *BMJ innovations*, 2(2):78–83, April 2016.

[23] J.W. Paulson, G. Succi, and A. Eberlein. An empirical study of open-source and closed-source software products. *IEEE Transactions on Software Engineering*, 30(4):246–256, April 2004.

[24] Christof Ebert. Open source drives innovation. *IEEE Software*, 24(3):105–109, 2007.

[25] European Commission. Directorate General for Communications Networks, Content and Technology. *The impact of open source software and hardware on technological independence, competitiveness and innovation in the EU economy: final study report.* Publications Office, LU, 2021. URL https://data.europa.eu/doi/10.2759/430161.

[26] Joel West. Patterns of Open Innovation in Open Source Software.

[27] Combining Open Source with Open Standards. URL https://www.openstack.org/videos/sydney-2017/combining-open-source-with-open-standards.

[28] Standards and Open Source: Bringing them together, November 2017. URL https://openforumeurope.org/wp-content/uploads/2018/09/StandardsandOpenSourceBringingthemtogether-1.pdf.

[29] Jérémy Bonvoisin, Jenny Molloy, Martin Häuer, and Tobias Wenzel. Standardisation of Practices in Open Source Hardware. *Journal of Open Hardware*, 4(1):2, August 2020. URL http://openhardware.metajnl.com/articles/10.5334/joh.22/.

[30] Shaul Oreg and Oded Nov. Exploring motivations for contributing to open source initiatives: The roles of contribution context and personal values. *Computers in Human Behavior*, 24(5):2055–2073, September 2008. URL https://www.sciencedirect.com/science/article/pii/S0747563207001537.

[31] J. Piet Hausberg and Sebastian Spaeth. Why makers make what they make: motivations to contribute to open source hardware development. *R&D Management*, 50(1):75–95, 2020. URL https://onlinelibrary.wiley.com/doi/abs/10.1111/radm.12348.

[32] Jason Xinghang Dai, Jean-François Boujut, Franck Pourroy, and Philippe Marin. Issues and challenges of knowledge management in online open source hardware communities. *Design Science*, 6:e24, 2020.

[33] Ştefan Stănciulescu, Sandro Schulze, and Andrzej Wąsowski. Forked and integrated variants in an open-source firmware project. In *2015 IEEE International Conference on Software Maintenance and Evolution (ICSME)*, pages 151–160, 2015.

[34] Linus Nyman. *Understanding Code Forking in Open Source Software: An examination of code forking, its effect on open source software, and how it is viewed and practiced by developers*. Hanken School of Economics, February 2015. URL https://helda.helsinki.fi/handle/10138/153135.

[35] Jérémy Bonvoisin and Robert Mies. Measuring openness in open source hardware with the open-o-meter. *Procedia CIRP*, 78:388–393, 2018. URL https://www.sciencedirect.com/science/article/pii/S2212827118312095. 6th CIRP Global Web Conference – Envisaging the future manufacturing, design, technologies and systems in innovation era (CIRPe 2018).

[36] Georg von Krogh, Sebastian Spaeth, and Karim R Lakhani. Community, joining, and specialization in open source software innovation: a case study. *Research Policy*, 32(7):1217–1241, July 2003. URL https://www.sciencedirect.com/science/article/pii/S0048733303000507.

[37] Clay Shirky, Michael Cusumano, et al. *Perspectives on free and open source software*. MIT press, 2005.

[38] Official Journal of the European Union. REGULATION (EU) 2017/745 OF THE EUROPEAN PARLIAMENT AND OF THE COUNCIL of 5 April 2017 on medical devices, amending Directive 2001/83/EC, Regulation (EC) No 178/2002 and Regulation (EC) No 1223/2009 and repealing Council Directives 90/385/EEC and 93/42/EEC, May 2017.

[39] Elisabetta Biasin and Erik Kamenjasevic. Open Source Hardware and Healthcare Collaborative Platforms: Common Legal Challenges, December 2020. URL https://papers.ssrn.com/abstract=3741157.

[40] Joshua M. Pearce. Distributed Manufacturing of Open Source Medical Hardware for Pandemics. *Journal of Manufacturing and Materials Processing*, 4(2):49, June 2020. URL https://www.mdpi.com/2504-4494/4/2/49.

[41] Soufiane Belhouideg. Impact of 3D printed medical equipment on the management of the Covid19 pandemic. *The International Journal of Health Planning and Management*, 35(5):1014–1022, 2020. URL https://onlinelibrary.wiley.com/doi/abs/10.1002/hpm.3009.

[42] Andre Maia Chagas, Jennifer C. Molloy, Lucia L. Prieto-Godino, and Tom Baden. Leveraging open hardware to alleviate the burden of COVID-19 on global health systems. *PLoS Biology*, 18(4):e3000730, April 2020. URL https://www.ncbi.nlm.nih.gov/pmc/articles/PMC7182255/.

[43] Medical Devices: Managing the Mismatch : an Outcome of the Priority Medical ... - World Health Organization - Google Livres. URL https://books.google.be/books?hl=fr&lr=&id=p58xsysgif0C&oi=fnd&pg=PP2&dq=managing+the+mismatch&ots=aWNTaRo7-a&sig=41DxexJWRZs6d8-QA0lDt6ZRQeA#v=onepage&q=managing%20the%20mismatch&f=false.

[44] Patricia M. Danzon and Sean Nicholson. *The Oxford Handbook of the Economics of the Biopharmaceutical Industry*. Oxford University Press, April 2012. ISBN 9780199909261. Google-Books-ID: UMhpAgAAQBAJ.

[45] Guven Bektemur, Nedim Muzoglu, Mehmet Ali Arici, and Melike Kaya Karaaslan. Cost analysis of medical device spare parts. *Pakistan Journal of Medical Sciences*, 34(2):472–477, 2018. ISSN 1682-024X. doi: 10.12669/pjms.342.14245. URL https://www.ncbi.nlm.nih.gov/pmc/articles/PMC5954400/.

[46] Market surveillance and vigilance, April 2023. URL https://health.ec.europa.eu/medical-devices-sector/directives/market-surveillance-and-vigilance_en.

[47] James C. Robinson and Timothy T. Brown. Quantifying Opportunities for Hospital Cost Control: Medical Device Purchasing and Patient Discharge Planning. September 2014. URL https://escholarship.org/uc/item/8kw7q49k.

[48] Current health expenditure (CHE) per capita in US$, . URL https://www.who.int/data/gho/data/indicators/indicator-details/GHO/current-health-expenditure-(che)-per-capita-in-us$.

[49] Electrification of health-care facilities: Percentage of health-care facilities with reliable electricity supply(%), . URL https://www.who.int/data/gho/data/indicators/indicator-details/GHO/hcf-electricity--percentage-of-health-care-facilities-with-access-to\-reliable-electricity-(-).

[50] Emergency medical condition - Glossary, . URL https://www.healthcare.gov/glossary/emergency-medical-condition.

[51] Hannah Ritchie, Fiona Spooner, and Max Roser. Causes of death. *Our World in Data*, February 2018. URL https://ourworldindata.org/causes-of-death.

[52] A Comprehensive Guide | Patient Monitoring Devices, . URL https://soteradigitalhealth.com/blog/a-comprehensive-guide-patient-monitoring-devices.

[53] Top 10 Most Used Medical Diagnostic Test Equipments, June 2022. URL https://isnmedical.com/medical-diagnostic-test-equipment/.

[54] 6 Common Types of Diagnostic Medical Equipment, . URL https://www.verywellhealth.com/common-types-of-diagnostic-medical-equipment-2318211.

[55] labcompare. Diagnostic Medical Imaging Equipment. URL https://www.labcompare.com/Clinical-Diagnostics/6082-Diagnostic-Medical-Imaging-Equipment/.

[56] Mental Health Treatments, . URL https://mhanational.org/mental-health-treatments.

[57] familydoctor org editorial staff. Different Types of Mental Health Treatment, February 2018. URL https://familydoctor.org/different-types-mental-health-treatment/.

[58] Lisa D. Mills and Trevor J. Mills. Natural Disasters. In Judith E. Tintinalli, J. Stephan Stapczynski, O. John Ma, Donald M. Yealy, Garth D. Meckler, and David M. Cline, editors, *Tintinalli's Emergency Medicine: A Comprehensive Study Guide*. McGraw-Hill Education, New York, NY, 8 edition, 2016. URL https://accessmedicine.mhmedical.com/content.aspx?bookid=1658&sectionid=109384453.

[59] Joe Dawson. The Physical and Emotional Effects of Bad Car Accidents, November 2019. URL https://dawsonlawfirm.com/the-physical-and-emotional-effects-of-bad-car-accidents/.

[60] World Health Organization. *INJURIES and VIOLENCE THE FACTS 2014*. Geneva, 2014. ISBN ISBN 978 92 4 150801 8. URL https://apps.who.int/iris/bitstream/handle/10665/149798/9789241508018_eng.pdf.

[61] Traumatic Injury, December 2012. URL https://ufhealth.org/traumatic-injury.

[62] Weinstein Legal. Know the Risks & Types of Injuries During a Natural Disaster, November 2017. URL https://medium.com/@weinsteininjurylawyer/know-the-risks-types-of-injuries-during-a-natural-disaster-13b4425f5d0d.

[63] Sam D. Say. 4 Types of Natural Disasters and Their Specific Injuries. URL https://blog.sscor.com/4-types-of-natural-disasters-and-their-specific-injuries.

[64] What is a traumatic injury?, . URL https://www.topdoctors.co.uk/medical-dictionary/traumatic-injury.

[65] Alyssa Jordan. How to Treat Traumatic Injury Emergencies, December 2020. URL https://www.unitekemt.com/blog/traumatic-injury-emergencies/.

[66] Kiran Kumar Patnaik, Sudeepa Das, Sachidananda Mohanty, and Hemanta Panigrahi. Pattern of Isolated Fatal Mechanical Injury in Homicidal Deaths: A Cross-Sectional Study. *Journal of Clinical and Diagnostic Research : JCDR*, 11(9):HC01–HC04, September 2017. ISSN 2249-782X. doi: 10.7860/JCDR/2017/26344.10598. URL https://www.ncbi.nlm.nih.gov/pmc/articles/PMC5713757/.

[67] Mass casualty incident, April 2023. URL https://en.wikipedia.org/w/index.php?title=Mass_casualty_incident&oldid=1149600844. Page Version ID: 1149600844.

[68] Forensic Identification in Mass Disasters, October 2022. URL https://www.azolifesciences.com/article/Forensic-Identification-in-Mass-Disasters.aspx.

[69] Intensive Care NSW. Equipment in the intensive care unit, May 2017. URL https://aci.health.nsw.gov.au/networks/icnsw/patients-and-families/equipment.

[70] Medical Equipment for the ICU - Essential Checklist, . URL https://www.portea.com/nursing/list-icu-equipment/.

[71] Critical Care Equipment Checklist, . URL https://avantehs.com/learn/equipment-checklists/critical-care-equipment-checklist.

[72] Median age, . URL https://ourworldindata.org/grapher/median-age.

[73] Ageing and health, . URL https://www.who.int/news-room/fact-sheets/detail/ageing-and-health.

[74] Aging: What to expect, . URL https://www.mayoclinic.org/healthy-lifestyle/healthy-aging/in-depth/aging/art-20046070.

[75] Jane A. Driver, Luc Djoussé, Giancarlo Logroscino, J. Michael Gaziano, and Tobias Kurth. Incidence of cardiovascular disease and cancer in advanced age: prospective cohort study. *BMJ*, 337:a2467, December 2008. ISSN 0959-8138, 1468-5833. doi: 10.1136/bmj.a2467. URL https://www.bmj.com/content/337/bmj.a2467.

[76] Jennifer L. Rodgers, Jarrod Jones, Samuel I. Bolleddu, Sahit Vanthenapalli, Lydia E. Rodgers, Kinjal Shah, Krishna Karia, and Siva K. Panguluri. Cardiovascular Risks Associated with Gender and Aging. *Journal of Cardiovascular Development and*

Disease, 6(2):19, April 2019. ISSN 2308-3425. doi: 10.3390/jcdd6020019. URL https://www.ncbi.nlm.nih.gov/pmc/articles/PMC6616540/.

[77] What does the hospital of the future look like?, . URL https://www.vlerick.com/en/insights/what-does-the-hospital-of-the-future-look-like/.

[78] 5 Trends That Will Determine The Hospital From The Future, September 2022. URL https://medicalfuturist.com/5-trends-that-will-determine-the-hospital-from-the-future/.

[79] Bernard Marr. The Top 5 Healthcare Trends In 2023. URL https://www.forbes.com/sites/bernardmarr/2022/12/06/the-top-5-healthcare-trends-in-2023/.

[80] MEDEVIS, . URL https://medevis.who-healthtechnologies.org/about.

[81] World Health Assembly (WHA) Resolution 60.1: Smallpox Eradication: Destruction of Variola Virus Stocks, . URL https://biosecuritycentral.org/resource/requirements-and-protocols/wha60.1/.

[82] Prioritizing medical devices, . URL https://www.who.int/activities/prioritizing-medical-devices.

[83] Interagency List of Priority Medical Devices for Essential Interventions for Reproductive, Maternal, Newborn and Child Health, . URL https://www.who.int/publications-detail-redirect/9789241565028.

[84] WHO list of priority medical devices for cancer management, . URL https://www.who.int/publications-detail-redirect/9789241565462.

[85] WHO list of priority medical devices for management of cardiovascular diseases and diabetes, . URL https://www.who.int/publications-detail-redirect/9789240027978.

[86] Priority medical devices list for the COVID-19 response and associated technical specifications, . URL https://www.who.int/publications-detail-redirect/WHO-2019-nCoV-MedDev-TS-02T.V2.

[87] Package of eye care interventions, . URL https://www.who.int/publications-detail-redirect/9789240048959.

[88] Trauma and Emergency Surgery Kit (TESK) 2019, . URL https://www.who.int/emergencies/emergency-health-kits/trauma-emergency-surgery-kit-who-tesk-2019.

[89] Koleno Intermittant Flowtron DVT Pumps, . URL hhttps://th.bing.com/th/id/R.e428d73c10ea0665417631902455484c?rik=JqR1QMy8aFZykg&pid=ImgRaw&r=0.

[90] William Calawerts and Kari Mader. Do sequential compression devices reduce morbidity and mortality in patients admitted to the hospital? *Evidence-Based Practice*, Publish Ahead of Print, January 2023. ISSN 1095-4120, 2473-3717. doi: 10.1097/EBP.0000000000001756. URL https://journals.lww.com/10.1097/EBP.0000000000001756.

[91] Dee Unglaub Silverthorn and Joan Frederic Brun. *Physiologie humaine: une approche intégrée*. Pearson, Paris, 2018. ISBN 9782326002203.

[92] Carl C. Arnoldi. The Venous Return from the Lower Leg in Health and in Chronic Venous Insufficiency: A Synthesis. *Acta Orthopaedica Scandinavica*, 35(sup64): 3–75, January 1964. ISSN 0001-6470. doi: 10.3109/ort.1964.35.suppl-64.01. URL http://www.tandfonline.com/doi/full/10.3109/ort.1964.35.suppl-64.01.

[93] CDC. What is Venous Thromboembolism? | CDC, February 2020. URL https://www.cdc.gov/ncbddd/dvt/facts.html.

[94] Lymphedema: Symptoms, Causes & Treatment, . URL https://my.clevelandclinic.org/health/diseases/8353-lymphedema.

[95] Critical Limb Ischemia | Vascular Center | UC Davis Health, . URL https://health.ucdavis.edu/vascular/diseases/cli.html#:~:text=Critical20limb20ischemia20(CLI)20is,but20less20common20than20claudication.

[96] Department of Surgery - Critical Limb Ischemia, . URL https://surgery.ucsf.edu/conditions--procedures/critical-limb-ischemia.aspx.

[97] Arteriosclerosis / atherosclerosis - Symptoms and causes, . URL https://www.mayoclinic.org/diseases-conditions/arteriosclerosis-atherosclerosis/symptoms-causes/syc-20350569.

[98] Critical Limb Ischemia: Causes, Symptoms and Treatment, . URL https://my.clevelandclinic.org/health/diseases/23120-critical-limb-ischemia.

[99] Sherif Sultan, Nader Hamada, Esraa Soylu, Anne Fahy, Niamh Hynes, and Wael Tawfick. Sequential compression biomechanical device in patients with critical limb ischemia and nonreconstructible peripheral vascular disease. *Journal of Vascular Surgery*, 54(2):440–447, August 2011. ISSN 0741-5214. doi: 10.1016/j.jvs.2011.02.057. URL https://www.sciencedirect.com/science/article/pii/S074152141100423X.

[100] Wael A. Tawfick, Nader Hamada, Esraa Soylu, Anne Fahy, Niamh Hynes, and Sherif Sultan. Sequential Compression Biomechanical Device Versus Primary Amputation in Patients With Critical Limb Ischemia. *Vascular and Endovascular Surgery*, 47(7): 532–539, October 2013. ISSN 1538-5744, 1938-9116. doi: 10.1177/1538574413499413. URL http://journals.sagepub.com/doi/10.1177/1538574413499413.

[101] Marzanna T. Zaleska and Waldemar L. Olszewski. The Effectiveness of Intermittent Pneumatic Compression in Therapy of Lymphedema of Lower Limbs: Methods of Evaluation and Results. *Lymphatic Research and Biology*, 17(1):60–69, February 2019. ISSN 1539-6851. doi: 10.1089/lrb.2018.0005. URL https://www.liebertpub.com/doi/abs/10.1089/lrb.2018.0005.

[102] admin. Enhancing patient outcomes with sequential compression device therapy, August 2013. URL https://www.myamericannurse.com/enhancing-patient-outcomes-with-sequential-compression-device-therapy/.

[103] DVT Prevention: Intermittent Pneumatic Compression Devices, November 2019. URL https://www.hopkinsmedicine.org/health/treatment-tests-and-therapies/dvt-prevention-intermittent-pneumatic-compression-devices.

[104] Pennsylvania Patient Safety Authority. Unexpected Risk from a Beneficial Device: Sequential Compression Devices and Patient Falls | Advisory. URL http://patientsafety.pa.gov:80/ADVISORIES/Pages/200509_13.aspx.

[105] Licorn Publishing and Guiboles. Risks and contraindications of medical compression treatment, June 2021. URL https://www.phlebolymphology.org/risks-and-contraindications-of-medical-compression-treatment/.

[106] Anticoagulant medicines, February 2018. URL https://www.nhs.uk/conditions/anticoagulants/.

[107] EUDAMED. URL https://ec.europa.eu/tools/eudamed/eudamed.

[108] AccessGUDID - ("Sequential compression"). URL https://accessgudid.nlm.nih.gov/devices/search?query=Sequential+compression.

[109] Abeer Yamany and Bassant Hamdy. Effect of sequential pneumatic compression therapy on venous blood velocity, refilling time, pain and quality of life in women with varicose veins: a randomized control study. *Journal of Physical Therapy Science*, 28(7):1981–1987, July 2016. ISSN 0915-5287. doi: 10.1589/jpts.28.1981. URL https://www.ncbi.nlm.nih.gov/pmc/articles/PMC4968489/.

[110] Mireille van Beekvelt, W.N. Asten, and Maria Hopman. The effect of electrical stimulation on leg muscle pump activity in spinal cord-injured and able-bodied individuals. *European journal of applied physiology*, 82:510–6, September 2000. doi: 10.1007/s004210000211.

[111] LLC Rapid Reboot Recovery Products. 510(k) Summary, September 2018. URL https://www.accessdata.fda.gov/cdrh_docs/pdf18/K182668.pdf#:~:text=The%20Rapid%20Reboot%20Compression%20Therapy%20System%20is%20indicated,stroking%20of%20tissues%20by%20using%20an%20inflatable%20garment.

[112] Lymphedema Pump - CircuFlow™ 5150 Preparation & Use - Bing video, . URL https://youtu.be/w1QBk8YkZIg.

[113] Venowave – Designed to improve circulation, . URL https://www.venowave.com/.

[114] K. T. Delis, Z. A. Azizi, R. J. Stevens, J. H. Wolfe, and A. N. Nicolaides. Optimum intermittent pneumatic compression stimulus for lower-limb venous emptying. *European Journal of Vascular and Endovascular Surgery: The Official Journal of the European Society for Vascular Surgery*, 19(3):261–269, March 2000. ISSN 1078-5884. doi: 10.1053/ejvs.1999.1047.

[115] Normatec 3 Legs | Hyperice. URL https://hyperice.com/products/normatec-3-legs/.

[116] Kendall SCD™ 700 Series Controller | Cardinal Health, . URL https://www.cardinalhealth.com/en/product-solutions/medical/compression/kendall-scd-compression-system/kendall-scd-700-series-controller.html.

[117] Francois Vermeulen. FW: Compressietoedtellen, May 2023.

[118] (PDF) Kendall SCD™ 700 Series Controller Error Key Guide, . URL https://www.premiermpi.com/Images/700%20Series%20Controller%20Error%20Key.pdf.

[119] Aura Healthcare. CircuFlow 5150. URL http://www.aurahc.com/wound-care/devon-medical-circuflow-5150.

[120] Devon CircuFlow 5150 One Leg Sleeve Included, Sequential Lymphedema Pump., . URL https://www.compressionmedical.com/lymphedema-pumps/devon-circuflow-5150-one-leg-sleeve-included-sequential-lymphedema-pump/.

[121] DAESUNG MAREF MK300L User Manual (Page 8 of 68) | ManualsLib. URL https://www.manualslib.com/manual/2221328/Daesung-Maref-Mk300l.html?page=8#manual.

[122] DAESUNG MAREF DVT-2600 USER MANUAL Pdf Download | ManualsLib, . URL https://www.manualslib.com/manual/1300912/Daesung-Maref-Dvt-2600.html.

[123] Buy DS MAref & DVT-2600 Intermittent Pneumatic Compression Device (DVT Pump) at best price from Hospitalsstore.com, . URL https://www.biomedsuppliers.com/ds-maref-dvt-2600-ipc-medical-pump-intermittent-pneumatic-compression\-pump-for-dvt/.

[124] AIROS 6 Sequential Compression Device - OPERATING INSTRUCTIONS FOR USE GUIDE, . URL https://airosmedical.com/wp-content/uploads/2023/03/A6IFU-0001-REV-E.pdf.

[125] AIROS 6 Sequential Compression Device, . URL https://airosmedical.com/compression-therapy-products/airos-6/.

[126] AIROS 6 Sequential Compression Device and Garments, . URL https://www.rehabmart.com/product/airos-6-sequential-compression-device-47963.html.

[127] K211283 - FDA Administration, August 2021. URL https://www.accessdata.fda.gov/cdrh_docs/pdf21/K211283.pdf.

[128] Compare Control Units » Rapid Reboot. URL https://rapidreboot.com/leg-compression-pump-therapy/.

[129] Lympha Press Optimal Plus, . URL https://lymphapress.com/products/lympha-press-optimal-plus/.

[130] Optimal Plus Lymphedema Pump, . URL https://ebraceshop.com/Optimal-Plus-Lymphedema-Pump.html.

[131] (88) PlasmaFlow™ Application Video - YouTube. URL https://www.youtube.com/watch?v=-Rp9L2h5wCs&ab_channel=Breg%2CInc.

[132] Sequential Circulators. URL https://3vg.af5.myftpupload.com/products/pneumatic-compression/sequential-circulators/.

[133] Bio Compression Sequential Pneumatic Circulator Lymphedema Pump Device, Select Your Sleeve Below., . URL https://www.compressionmedical.com/lymphedema-pumps/bio-compression-sequential-pneumatic-circulator-lymphedema-pump-device\-select-your-sleeve-below/.

[134] VenaPro System (Pair), . URL https://www.breg.com/products/dvt-prophylaxis/venapro/venapro-system-pair/.

[135] AirRelax LGT-2200DVT - Guangzhou Longest Science & Technology - PDF Catalogs | Technical Documentation, . URL https://pdf.medicalexpo.com/pdf/guangzhou-longest-science-technology/airrelax-lgt-2200dvt/78556-172285.html.

[136] LegFit – LegFit. URL https://legfit.ch/.

[137] Instructions for use, May 2022. URL https://legfit.ch/wp/wp-content/uploads/2023/04/C2118-LegF-IFU-en.pdf.

[138] The Huntleigh AC550 Flowtron Excel System | Biomedix Medical, Inc, . URL https://www.biomedixmedical.com/product/the-huntleigh-ac550-flowtron-excel-system/.

[139] Instruction For Use FLOWTRON EXCEL, December 2020. URL https://qbank.arjo.com/productdocumentation/247933EN_10.pdf.

[140] Ryuma Niiyama, Xu Sun, Cynthia Sung, Byoungkwon An, Daniela Rus, and Sangbae Kim. Pouch Motors: Printable Soft Actuators Integrated with Computational Design. *Mary Ann Liebert*, May 2015. ISSN 2169-5172. URL https://dspace.mit.edu/handle/1721.1/107946.

[141] T. Wingate Todd and Anna Lindala. Dimensions of the body: Whites and American negroes of both sexes. *American Journal of Physical Anthropology*, 12(1):35–119, 1928. ISSN 1096-8644. doi: 10.1002/ajpa.1330120104. URL https://onlinelibrary.wiley.com/doi/abs/10.1002/ajpa.1330120104.

[142] Thermoplastic Polyurethane (TPU) Product range Typical values, 2021. URL https://www.albis.com/dam/jcr:adc2e781-ce0a-412a-83a0-8cfc3404ae01/Desmopan%20Product%20Range.pdf.

[143] Characterizing the Peano fluidic muscle and the effects of its geometry properties on its behavior - IOPscience. URL https://iopscience.iop.org/article/10.1088/0964-1726/25/6/065013.

[144] Allan Joshua Veale, Sheng Quan Xie, and Iain Alexander Anderson. Modeling the Peano fluidic muscle and the effects of its material properties on its static and

dynamic behavior. *Smart Materials and Structures*, 25(6):065014, May 2016. ISSN 0964-1726. doi: 10.1088/0964-1726/25/6/065014. URL https://dx.doi.org/10.1088/0964-1726/25/6/065014.

[145] Jackson Wirekoh and Yong-Lae Park. Design of flat pneumatic artificial muscles. *Smart Materials and Structures*, 26(3):035009, February 2017. ISSN 0964-1726. doi: 10.1088/1361-665X/aa5496. URL https://dx.doi.org/10.1088/1361-665X/aa5496.

[146] A novel flat modular pneumatic artificial muscle - IOPscience. URL https://iopscience.iop.org/article/10.1088/1361-665X/ab84b9.

UNIVERSITÉ CATHOLIQUE DE LOUVAIN
École polytechnique de Louvain
Rue Archimède, 1 bte L6.11.01, 1348 Louvain-la-Neuve, Belgique | **www.uclouvain.be/epl**